SOLID-STATE NMR INVESTIGATION FOR UNDERSTANDING SUBLIMATION BEHAVIOR OF AN ENCAPSULATED DRUG IN POLYMORPHIC FORMS OF A CYCLODEXTRIN-BASED POLYPSEUDOROTAXANE COMPLEX

SUDESHNA KUNDU

A DISSERTATION SUBMITTED IN PARTIAL FULFILLMENT OF THE REQUIREMENT FOR THE DEGREE OF

DOCTOR OF PHILOSOPHY

(PHARMACEUTICAL SCIENCES)

LABORATORY OF PHARMACEUTICAL TECHNOLOGY

GRADUATE SCHOOL OF PHARMACEUTICAL SCIENCES

CHIBA UNIVERSITY

JAPAN

CONTENTS

ABSTRACT	1
INTRODUCTION	4
EXPERIMENTAL SECTION	11
RESULTS AND DISCUSSION	16
Part I Evaluation of sealed-heating preparation conditions to obtain	
HC form complex	16
Characterizations of PEG/γ-CD-PPRX	16
Preliminary investigation of sealed-heating conditions to prepare the HC	
form complex	18
Encapsulation behavior of other guest drugs in the HC form complex	33
Determination of encapsulation efficiency of guest drugs by solution-state	
¹ H NMR	36
Discussion on the correlation between encapsulation efficiency and guest	
drug properties	41
Part II Evaluation of drug's sublimation rate and molecular mobility	
in three polymorphic complexes	45
Preparation of three polymorphic complexes with SA as the model drug	45
Thermal stability of the three polymorphic complexes	47
Sublimation rate of SA from the polymorphic complexes	50
Molecular dynamics evaluation of the polymorphic complexes by ¹³ C MAS	
measurements	55
Temperature-dependent molecular dynamics of the polymorphic	
complexes	63
Molecular dynamics evaluation of the complexes by ¹ H MAS measurement	66

Quantitative assessment of molecular dynamics of SA and PEG in the	
polymorphic complexes by ${}^{13}\text{C-}T_1$ measurement	68
Discussion on the correlation between molecular mobility of SA and its	
sublimation rate	72
Discussion on the influence of SA dynamics on the molecular motion of γ -	
CD and PEG in the complexes	74
CONCLUSIONS	79
FUTURE PERSPECTIVES	81
REFERENCES	82
ACKNOWLEDGEMENTS	91
LIST OF PUBLICATIONS	92
THESIS COMMITTEE	93

ABSTRACT

The encapsulation of active pharmaceutical ingredients (APIs) in macrocyclic host compounds is a widely investigated formulation strategy to enhance the physicochemical properties of APIs. Cyclodextrins (CDs) are widely utilized as supramolecular hosts in pharmaceuticals to form inclusion complexes that enhance drug solubility, stability, etc. The formation of CD-based inclusion complexes typically involves the incorporation of drugs into the hydrophobic cavity of CD. In addition to the CD cavity, intermolecular spaces in a CD crystal structure can be exploited to form new CD-based complexes. CDs can also form supramolecular complexes with linear polymers, such as polyethylene glycol (PEG), known as CD-polypseudorotaxane (CD-PPRX). The supramolecular structure of CD-PPRX consists of stacked columns of CD-polymer inclusion complexes arranged in a parallel manner with intermolecular spaces between the columns. Previous studies have established that drugs can be incorporated into the intermolecular spaces of PEG/γ-CD-PPRX by sealed-heating technique, yielding a unique multicomponent supramolecular complex, drug/(PEG/γ-CD-PPRX). Such complexes improved the dissolution and stability of the encapsulated drug. Furthermore, the host structure of PEG/γ-CD-PPRX can exist in three polymorphic forms, which are monoclinic columnar (MC), hexagonal columnar (HC), and tetragonal columnar (TC). The effect of a polymorphic supramolecular structure of the drug/(PEG/γ-CD-PPRX) complex on its physical properties has not been investigated yet. Thus, the present study aimed to prepare the three polymorphic forms of the drug/(PEG/y-CD-PPRX) complex, and investigate the difference in the physical properties of encapsulated drugs at the molecular level.

Upon reviewing the established preparation conditions for the drug/(PEG/ γ -CD-PPRX) complex, it was found that the reported preparation conditions resulted in either MC or TC

form complex. Thus, in the first part of the study, the sealed-heating preparation conditions to obtain the HC form of the drug/(PEG/ γ -CD-PPRX) complex were investigated. In the second part of the study, three polymorphic forms of the drug/(PEG/ γ -CD-PPRX) complex were prepared, and the sublimation rate of the guest drug was evaluated as the physical property. Several solid-state NMR techniques were used to assess the molecular state of the complexes, and the correlation between the sublimation rate and molecular dynamics of the guest drug was established.

In this study, γ-CD and PEG of molecular weight 2000 were used to prepare the PEG/γ-CD-PPRX. The screening for the various sealed-heating conditions to obtain the HC form of the drug/(PEG/γ-CD-PPRX) complex was conducted with six different guest drugs, namely, salicylic acid (SA), salicylamide (SAM), paracetamol (PCT), 2-naphthoic acid (2-NA), phenothiazine (PTZ), and naproxen (NPX). In the screening experiments, the changes in the crystal structure of PEG/γ-CD-PPRX and the guest encapsulation were examined by powder X-ray diffraction. It revealed that a low sealed-heating temperature with a small amount of water was the optimal preparation condition for obtaining the HC form complex. The stoichiometry and the encapsulation efficiency of each guest drug in the HC form complex were measured by solution-state ¹H NMR. Guest drugs, SA, SAM, and 2-NA were encapsulated in a stoichiometric ratio in the HC form complex, whereas complete encapsulation of PCT, PTZ, and NPX could not be achieved. Furthermore, the stoichiometric complexation was determined by the cross-sectional area of the guest drug, and the encapsulation efficiency was governed by the guest drug properties, such as vapor pressure and molecular size.

In the second part of the study, SA was selected as the model drug to prepare the three polymorphic forms of the SA/(PEG/ γ -CD-PPRX) complex. The sublimation tendency of SA encapsulated in three polymorphic forms, MC, HC, and TC form of the SA/(PEG/ γ -CD-

PPRX) complex was evaluated by isothermal thermogravimetry. The sublimation rate of SA was significantly reduced by complexation. Moreover, the sublimation rate of SA differed among the complexes and decreased in the order of MC form > HC form > TC form. The molecular state of the complexes was then evaluated by magic-angle spinning (MAS) based ¹³C and ¹H solid-state NMR techniques. The NMR observables (chemical shift, linewidths) in ¹³C, ¹H MAS solid-state NMR spectra indicated that the encapsulated SA molecules existed as the monomeric form and molecular mobility of SA and PEG increased in the order of MC form > HC form > TC form complex. The 13 C spin-lattice relaxation time (T_1) measurement quantitatively confirmed the molecular mobility of SA and PEG in the order of MC form > HC form > TC form complex. From the ¹³C NMR line shapes, the molecular mobility of γ -CD was deduced to be in the order of MC form > HC form > TC form complex. The temperature-dependent ¹³C line shapes of SA peaks in the complexes revealed a rapid chemical exchange between two dynamic states of SA (free and bound) with varying adsorption/desorption rates, which resulted in different molecular mobility. The ¹H MAS spectra and temperature dependency of the ¹³C carbonyl chemical shift indicated that the adsorption/desorption process was influenced by proton exchange at the interaction site and interaction strength of SA in the complexes. The sublimation rate of SA was found to be correlated with its molecular mobility. Moreover, the molecular mobility order of γ-CD and PEG in the complexes also coincided with the mobility of SA, revealing fast guest-driven dynamics. The molecular-level insights obtained in this study will aid in the rational design of drug delivery systems to further improve the physicochemical properties of drugs.

INTRODUCTION

A large percentage of commercially available active pharmaceutical ingredients (APIs) possess poor physicochemical properties such as solubility, dissolution, stability, hygroscopicity, bioavailability, etc. These poor physicochemical properties of the APIs impact their therapeutic efficacy and are usually addressed by various formulation approaches. Encapsulation of APIs in macrocyclic host molecules or ordered porous materials, for example, cyclodextrins (CDs), cucurbit[n]urils, mesoporous silica, metalorganic frameworks, organic nanotubes, have emerged as a promising approach to improve physicochemical properties and delivery of APIs. 1-5 The molecular state of the encapsulated guest APIs is significantly changed and undergoes unique molecular motion as compared to the bulk state, which directly alters and improves its physicochemical properties. Several reports have established the relationship between molecular dynamics and the physical property of the guest API. The molecular state and dynamics of the guest API can be affected by various parameters such as cavity size or pore diameter, binding geometry, porous matrix, and host/guest interaction. 6-10 Knapik et al. demonstrated that the stability of amorphous ezetimibe incorporated in porous materials with different pore sizes was influenced by its altered molecular mobility, immobilization effect, and pore size. 11 Dionísio and co-workers investigated the effect of the physical state, molecular mobility, and distribution of naproxen encapsulated in three hydrophilic mesoporous silica hosts (MCM-41) with similar pore sizes. 12 The three different mesoporous hosts, which were unmodified MCM-41, silylated by methyl capping MCM-41sil, and biphenylene-bridged silica matrix PMOBph, differed in architecture and surface composition. The release of naproxen from the unmodified and silylated MCM-41 matrix agreed well with its molecular mobility, as probed by dielectric relaxation spectroscopy.¹² Therefore, the molecular dynamics of encapsulated APIs and their influence on physical properties are important to investigate.

CDs are the most widely employed supramolecular hosts in drug delivery, food and flavors, separation process, catalysis, and so on, due to their capability to form inclusion complexes, negligible cytotoxic effects, and cost-effectiveness. 13-18 CDs are cyclic oligosaccharides composed of six or more D-glucopyranose units connected by α-1,4 glycosidic linkages. CDs display a truncated conical structure with a hydrophilic external surface and a hollow hydrophobic cavity. This structural characteristic is attributed to the presence of hydroxyl groups on the rims and ether moieties in the interior of the cavity. ¹⁹ Typically, natural CDs such as α , β , and γ -CDs are utilized as host molecules to encapsulate guest compounds in the hydrophobic cavity to form inclusion complexes through hydrophobic and van der Waals interactions. In the pharmaceutical field, the CD-inclusion complexes with APIs are utilized for enhancing solubility or stability, as well as in taste or odor masking. ²⁰⁻²³ In addition to low molecular weight compounds, CDs can also form inclusion complexes with linear polymers such as polyethylene glycol (PEG), polypropylene glycol, etc., to generate a supramolecular structure known as CD-polypseudorotaxane (CD-PPRX).²⁴ The CD-PPRX is formed by self-assembly in water, where a series of CDs are threaded onto a polymer chain generating a column-like structure. The CD-PPRX structure is stabilized by hydrophobic interactions between the polymer chain and CD cavity, and hydrogen bonding between the adjacent threaded CD units.^{25, 26} The unique structure and properties of CD-PPRX have garnered significant attention. CD-PPRX can form hydrogel and molecular tubes that have served as effective carriers for delivering a range of guest drugs, such as small molecules, peptides, and nucleic acids.²⁷⁻³⁰

The crystal packing structure of CD-inclusion complexes is broadly categorized into three forms, cage-type, layer-type, and columnar-type.³¹ The crystal packing structure varies with the type of CD and the guest compound involved. γ -CD adopts a cage-type structure in the absence of a guest compound, where the CD cavities are blocked by the adjacent CDs.^{32, 33}

However, the γ-CD inclusion complex adopts a columnar structure irrespective of the guest molecules except for water molecules. Similarly, the γ -CD units in the γ -CD-PPRX structure are stacked over one another on a polymer chain in head-to-head or, tail-to-tail arrangement.³² Harada et al. first reported the inclusion complexation of PEG and γ-CD, where two PEG chains were incorporated in the γ-CD columns.³⁴ Furthermore, Kawasaki et al. revealed that the crystalline structure of inclusion complexes of γ -CD with various polymers including PEG adopts different hydrated and anhydrous packing structures depending on the water content in the crystal lattice.³⁵ The native hydrated tetragonalcolumnar (TC) structure can be transformed into the other hydrated monoclinic-columnar (MC) structure and anhydrous hexagonal-columnar (HC) structure, by the gradual removal of water molecules from the crystal structure.³⁵ On viewing along the c-axis, the packing of such pseudopolymorphic and polymorphic γ -CD columnar structure shows the γ -CD positions at a = 23.7 Å, b = 23.7 Å, $y = 90^{\circ}$ in TC form, at a = 17.6 Å, b = 14.0 Å, $y = 110^{\circ}$ in MC form, and at a = 16.4 Å, b = 16.4 Å, $\gamma = 120^{\circ}$ in HC form. The chemical structures of γ-CD and PEG, along with a schematic representation of the different crystalline forms of PEG/ γ -CD-PPRX from the side and top view, are shown in Figure 1.

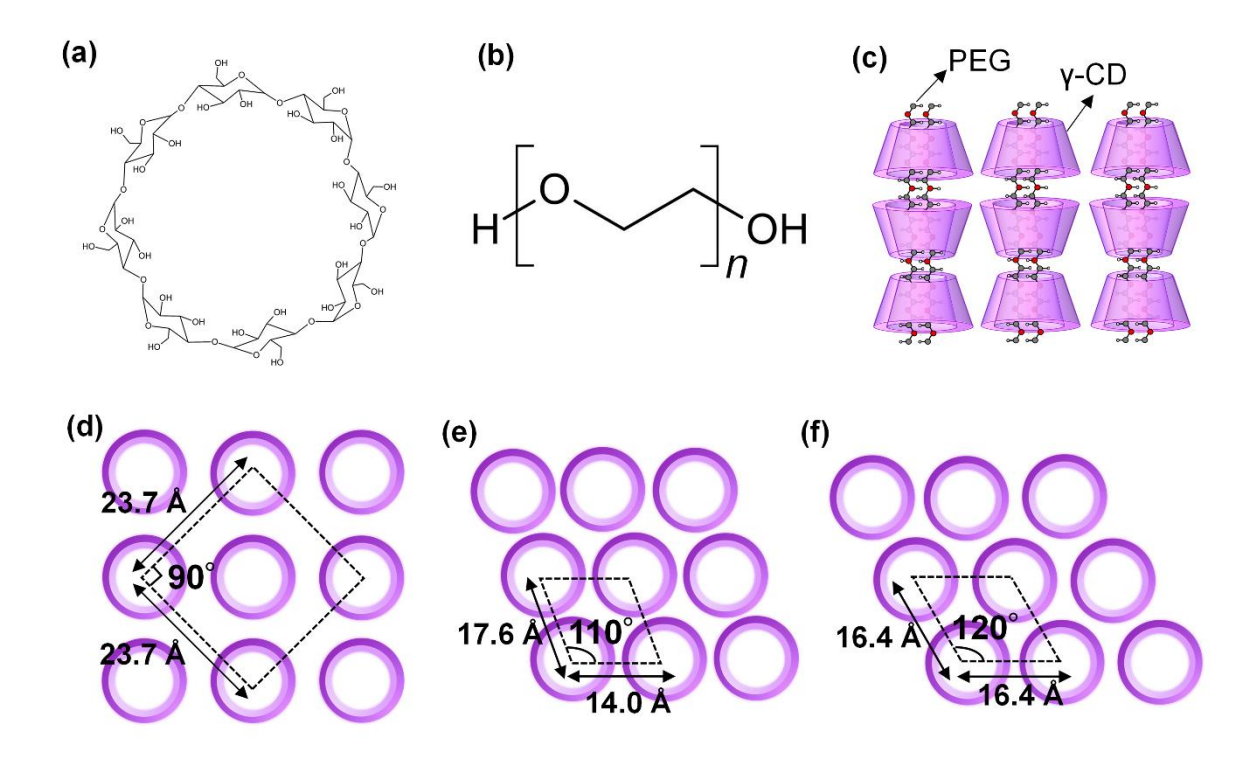


Figure 1. Chemical structures of (a) γ-cyclodextrin (γ-CD), (b) monomer of polyethylene glycol 2000 (PEG), and (c) schematic representation of PEG/γ-CD-PPRX from the side view and packing arrangements of different crystalline forms of PEG/γ-CD-PPRX from the top view of (d) tetragonal-columnar (TC) form, (e) monoclinic-columnar (MC) form, (f) hexagonal-columnar (HC) form. In the top view, the purple circle represents γ-CD and the polymers in the γ-CD cavity have been removed for clarity.

In most instances, the guest compounds are typically incorporated only in the CD cavity, however, a few exceptions have been reported. For instance, in the columnar structure of α -CD inclusion complexes with *m*-nitrophenol and *m*-bromophenol, the guest compounds were found to coexist within both the CD cavity and the intermolecular spaces between the columns.^{36, 37} Prior research has demonstrated that guest compounds such as APIs, metal ions, or surfactants can inhabit the intermolecular spaces of a γ -CD inclusion complex structure. 38-40 These findings motivated us to investigate the intermolecular spaces within a CD-PPRX columnar structure as potential sites for incorporating guest compounds and develop novel CD-based complexes. Previous studies have reported that APIs can be incorporated in the intermolecular spaces between the CD columns of PEG/γ-CD-PPRX by sealed-heating techniques to form a multicomponent supramolecular complex involving three components (y-CD, PEG, and guest drug/API), and are referred to as drug/(PEG/y-CD-PPRX) complexes. 38, 41, 42 To date, drug/(PEG/y-CD-PPRX) complexes have been reported with 17 different guest compounds including APIs. 38, 41, 42 These complexes have shown promising results in improving the physicochemical properties of the guest API such as dissolution and stability. However, all the reported drug/(PEG/γ-CD-PPRX) complexes exhibited MC form structure.^{38, 41} It was proposed that the incorporation of the guest molecule changed the initial HC form to the MC form structure. Additionally, water adsorption by humidification changes the crystalline structure of the MC form complex to the TC form structure, which is maintained even after water desorption by subsequent drying instead of reverting to the MC/HC form structure.³⁸ Thus, the preparation of the HC form of the drug/(PEG/ γ -CD-PPRX) complex was assumed to be difficult.

Polymorphism must be taken into consideration in pharmaceuticals, as changes in crystal packing and/or conformation of the same molecule can alter physicochemical properties such as solubility, bioavailability, and so on.⁴³ Polymorphism is extensively studied in low

molecular weight compounds. In contrast, there are few reports on polymorphism in supramolecular structures of rotaxanes or pseudorotaxanes. 44, 45 To the best of my knowledge, research works on polymorphism in multicomponent polypseudorotaxane structures have not been reported. Moreover, only a handful of studies have reported the difference in the physical properties contributed by the different crystal structures of the γ -CD inclusion complex. Toropainen et al. described that the dissolution profile of budesonide from the TC and HC form structure of budesonide/γ-CD inclusion complexes was dependent on the host crystal structure. 46 In addition, Hirotsu et al. reported a sustained and controlled release of insulin from PEGylated insulin/PPRX structure prepared with α-CD as compared to γ-CD.⁴⁷ This was facilitated by the tightly packed HC form structure in the former rather than the loosely packed TC form structure in the latter. Based on these reports, it is evident that pharmaceutical properties can be further controlled by the polymorphic crystal structure of the multicomponent supramolecular drug(PEG/γ-CD-PPRX) complex and needs to be explored. Reported studies have focused on how the host structure influences the dissolution of the encapsulated drug. However, there is a lack of research on the molecular dynamics of the encapsulated drug and its relationship with physical properties. Particularly, there are no molecular-level studies concerning encapsulated drugs in CD-based PPRX structures, although numerous studies have been reported for mesoporous silica. Such local molecular level investigations for multicomponent CD-based PPRX complexes remain challenging due to their complexity level. However, this can be enabled by utilizing solid-state NMR spectroscopy owing to its sensitivity in detecting molecular level differences. The overall purpose of this study is to prepare the three polymorphic forms of the drug/(PEG/ γ -CD-PPRX) complex and investigate the difference in the physical properties of encapsulated drugs at the molecular level.

The first part of this study focused on investigating sealed-heating conditions to prepare the HC form of drug/(PEG/ γ -CD-PPRX) complex. A screening study with six different guest drugs was conducted to rationalize the sealed-heating condition for the HC form complex preparation. The crystalline structure of the complex, stoichiometry/encapsulated amount, and molecular state of the guest drug in the obtained complexes were characterized using powder X-ray diffraction (PXRD), solution-state 1 H NMR, and Fourier transform infrared (FTIR) spectroscopy. Furthermore, the effects of guest drug properties such as vapor pressure, molecular size, and sealed-heating conditions, on the encapsulation behavior such as stoichiometry and encapsulation efficiency were investigated.

In the second part of this study, the physical property of the encapsulated drug in the three polymorphic forms of the drug/(PEG/ γ -CD-PPRX) complex was examined. For this purpose, salicylic acid (SA) was selected as the model drug. SA is typically used in topical formulations to treat chronic skin diseases for its keratolytic, anti-inflammatory, and bacteriostatic properties. 48, 49 A recent study by Murthy and co-workers demonstrated that SA suffers significant weight loss at skin temperature (32 °C) by sublimation due to its high vapor pressure from its crystalline state as well as topical formulations.⁵⁰ The physical stability issues related to the high vapor pressure of APIs have been addressed by cocrystal/salt formation or complexation with CDs. 51-53 Thus, the sublimation rate of SA from the three polymorphic forms of the SA/(PEG/γ-CD-PPRX) complex was determined by isothermal thermogravimetry. The MC and TC form of SA/(PEG/γ-CD-PPRX) complex was prepared by the previously reported method,³⁸ and the HC form complex was prepared by the newly established method. The molecular dynamics of the complexes were evaluated by variable temperature ¹³C cross-polarization (CP), ¹³C pulse saturation transfer (PST) with magic angle spinning (MAS) based solid-state NMR techniques, ¹H MAS, and ¹³C spinlattice relaxation time (T_1) measurement using ¹³C isotopically labeled SA.

EXPERIMENTAL SECTION

Materials

γ-cyclodextrin (γ-CD) was kindly provided by Cyclochem Co., Ltd. (Japan). Polyethylene glycol (PEG) with a molecular weight of 2000, salicylic acid (SA), and 2-naphthoic acid (2-NA) were procured from Wako Pure Chemical Industries, Ltd. (Japan). Salicylamide (SAM), paracetamol (PCT), (*S*)-(+)-naproxen (NPX), and phenothiazine (PTZ) were purchased from Nacalai Tesque, Inc. (Japan). SA with ¹³C isotopically labeled at the carboxylic acid carbon (¹³C-labeled SA) was purchased from Isotec (USA). All materials were of reagent grade and used without any additional purification.

Methods

Preparation of PEG/γ-CD-PPRX

PEG/ γ -CD-PPRX was prepared by the co-precipitation method. 300 mg of PEG was dissolved in 1 mL of water and added to 10 mL of a saturated γ -CD aqueous solution (232 mg/mL). The resulting solution showed immediate precipitation, which was then ultrasonically agitated at 25 °C for 1 h and stored at 25 °C for one day. The precipitate was collected by filtration, washed with water, and then dried in vacuo at 70 °C for 3 h to obtain the TC form of PEG/ γ -CD-PPRX. The dried precipitate was ground manually with a mortar and pestle and sieved through a 100-mesh sieve to obtain a particle size of less than 150 μm. The HC form of PEG/ γ -CD-PPRX was obtained by drying the initial TC form of PEG/ γ -CD-PPRX at 100 °C for 16 h in vacuo.

Preparation of HC form of drug/(PEG/ γ -CD-PPRX) complex by sealed-heating method

Preliminarily, the HC form of PEG/γ-CD-PPRX was converted to a highly crystalline form and used as the starting material for preparing the HC form of the drug/(PEG/ γ -CD-PPRX) complex. A 2 mL glass ampule with 500 mg of PEG/γ-CD-PPRX was connected to another 2 mL glass ampule containing 15 μL water by a silicon rubber plug. The connected ampules were then heated at 140 °C for 30 min and further dried at 100 °C for 3 h in vacuo, to obtain the high crystalline HC form of PEG/ γ -CD-PPRX. The high crystalline HC form of PEG/ γ -CD-PPRX and the guest drug molecule (SA, SAM, PCT, 2-NA, PTZ, and NPX) were mixed in a fixed molar ratio using a vortex mixer for 5 min to prepare a physical mixture (PM). Based on the stoichiometry obtained for each drug/γ-CD molar ratio in its MC form complex⁴¹, the molar ratio of 2:1 was used for guest drugs, SA, SAM, and PCT, and a molar ratio of 1:1 was used for guest drugs, 2-NA, PTZ, and NPX to prepare the PM. In the case of preparing samples with an excess amount of drug, a molar ratio of 3:1 was used for PCT, and a molar ratio of 2:1 was used for 2-NA, PTZ, and NPX to prepare the PM. 200 mg of the PM was added in a 2 mL glass ampule without or with an additional 2–25 µL water. The glass ampule was sealed and heated at 80–145 °C in an incubator (AS-ONE, OF-300V). In this study, such heating is referred to as 'sealed-heating'.

Preparation of the MC, HC, and TC form of SA(PEG/γ-CD-PPRX) complex

A physical mixture (PM) of SA and PEG/ γ -CD-PPRX (HC form) in a molar ratio of 2:1 was prepared. The MC form of the SA/(PEG/ γ -CD-PPRX) complex was obtained by sealed-heating the PM at 145 °C for 3 h. The HC form complex was prepared by sealed-heating the PM with 8 μ L of water at 80 °C for 3 h. The TC form complex was obtained by subjecting the MC form complex to a humidifying condition of 40 °C, 75% relative humidity (RH) for

7 days. The HC form and TC form complex were further dried at 40 °C in vacuo for 8 and 12 h, respectively, to reduce the water content to 2–3%. Additionally, the MC, HC, and TC form complex were prepared with ¹³C-labeled SA in a manner similar to as described above. For this, a mixture of SA with naturally abundant ¹³C and isotopically enriched ¹³C in a weight percent ratio of 85:15 was used to prepare the PM.

Quantitative determination of encapsulated guest drug in the HC form of drug/(PEG/ γ -CD-PPRX) complex

200 mg of the sealed-heated samples (SH samples) was suspended in 10 mL of diethyl ether or acetone and filtered to remove the non-encapsulated/free guest drug in the SH sample. The filtered SH sample was then dried at 40 °C in vacuo for 1 h. The dried SH sample (15 mg) was dissolved in 1 mL of dimethyl sulfoxide-d₆ (DMSO- d_6) and the solution-state ¹H NMR was measured. The relative ratio of the encapsulated guest drug to the γ -CD in each HC form of drug/(PEG/ γ -CD-PPRX) complex was evaluated by integrating the respective ¹H peaks of each guest drug with respect to the ¹H peak of γ -CD.^{54,55}

Powder X-ray diffraction (PXRD) measurement

The PXRD patterns were measured by a Rigaku MiniFlex II diffractometer (Japan) using the following conditions; radiation source: Cu K α , filter: Ni, voltage: 30 kV, current: 15 mA, scanning speed: 4°/min, scanning angle: 3–35°.

Variable temperature (VT) PXRD measurement

The VT-PXRD patterns were measured by a D8 ADVANCE diffractometer (Bruker, Germany) using the following conditions; radiation source: Cu Kα, filter: Ni, voltage: 40 kV, current: 40 mA, scanning angle: 3–35°, step size: 0.02°, counting per step: 0.2 s, heating range: 30–230 °C.

Solution-state ¹H NMR spectroscopy

¹H NMR experiments were performed using a JNM-ECZ600 NMR spectrometer (JEOL Resonance, Japan) operating at a magnetic field of 14.09 T. The following measurement conditions were used: method: ¹H single pulse (90°); relaxation delay: 8 s; scans: 8, and temperature: 27 °C. Tetramethylsilane (TMS, 0.0 ppm) was used as the internal standard.

Fourier transform infrared (FTIR) spectroscopy

Infrared measurements were performed using Alpha FTIR spectrometer (Bruker, Germany) using the KBr disk method. IR spectra were obtained in the scan range of 400–4000 cm⁻¹ at a resolution of 4 cm⁻¹ with 128 scans.

Thermogravimetric (TG) analysis

TG profiles of the prepared complexes were measured using EXSTAR TG/DTA-6200 instrument (Hitachi High-Tech Science Corporation, Tokyo, Japan). About 5 mg of the sample was heated at a temperature of 25–230 °C with a heating rate of 5 or 0.5 °C/min under a nitrogen gas flow rate of 200 mL/min. The water content of the prepared complexes was determined from the weight loss of water from 25–70 °C in the TG profiles. The sublimation rates of SA from its crystalline state, PM, and each complex were determined using TG under isothermal conditions. Approximately 5–6 mg of sample was uniformly filled in the sample pan to form a thin monolayer of particles. The samples were rapidly heated to 80 °C and then isothermally held for 200–720 min under a nitrogen gas flow rate of 200 mL/min during the measurement. The sublimation rate was estimated from the slope of the linear region of each isothermal thermogram by fitting a linear regression model. The isothermal TG measurement for each sample was conducted in triplicate, and the rate obtained is expressed as mean ± S.D.

Solid-state NMR spectroscopy

The 13 C and 1 H NMR spectra were acquired using a JNM-ECX400 NMR spectrometer (9.39 T, JEOL Resonance, Japan) equipped with a 4 mm H-X probe in the temperature range of 25–70 °C. 13 C CP/MAS NMR spectra were obtained with the following conditions: spin rate (ν), 5 and 15 kHz; decoupling method, two-pulse phase-modulation; contact time, 2–5 ms; recycle delay, 2–60 s. The 13 C PST/MAS NMR measurement conditions were as follows: ν , 5 and 15 kHz; decoupling method, two-pulse phase-modulation; recycle delay, 30 s. The 13 C spin-lattice relaxation time (13 C- T_1) of SA and PEG in each complex was measured using a saturation-recovery sequence. In the saturation recovery sequence, recovery time (τ) was altered from 0.1 s to the time needed to achieve equilibrium. The 13 C- T_1 values were calculated from the plot of integrated signal area against τ and the standard errors of fittings were estimated. For the 13 C- T_1 measurements, polymorphic complexes prepared with 13 C isotopically labeled SA at the carbonyl site were used. 14 H MAS NMR measurement conditions were as follows: ν , 15 kHz; recycle delay, 5 s; data points, 65536. The 13 C and 14 H spectra were externally referenced by setting the methyl carbon of hexamethyl benzene to 17.3 ppm and silicone rubber to 0.12 ppm, respectively.

RESULTS AND DISCUSSION

<u>Part I</u> Evaluation of sealed-heating preparation conditions to obtain the HC form complex

Characterization of PEG/y-CD-PPRX

The crystalline structure of the PEG/ γ -CD-PPRX was analyzed by PXRD and solution state 1 H NMR. The initial form of the obtained PEG/ γ -CD-PPRX was the TC form, confirmed by the presence of the characteristic diffraction peaks at $2\theta = 7.4^{\circ}$, 12.1° , and 16.5° of the TC form structure (Figure 2a). The HC form structure of PEG/ γ -CD-PPRX was obtained by drying the TC form at high temperature, as indicated by the characteristic diffraction peaks at $2\theta = 6.0^{\circ}$ and 15.9° (Figure 2c). This transformation agrees well with the previous reports. Figure 2d shows the schematic representation of the conversion of the TC, MC, and HC form of PEG/ γ -CD-PPRX by the gradual removal of water from the crystal lattice with the corresponding method. However, drying the TC form of PEG/ γ -CD-PPRX at room temperature could not yield the MC form, rather the MC and TC form (Figure 2b). The 1 H NMR spectrum of the PEG/ γ -CD-PPRX revealed that the stoichiometry of the monomer unit of PEG to γ -CD was 4:1 (Figure 3). This indicates the inclusion of two side-by-side PEG chains in each column of the PEG/ γ -CD-PPRX structure.

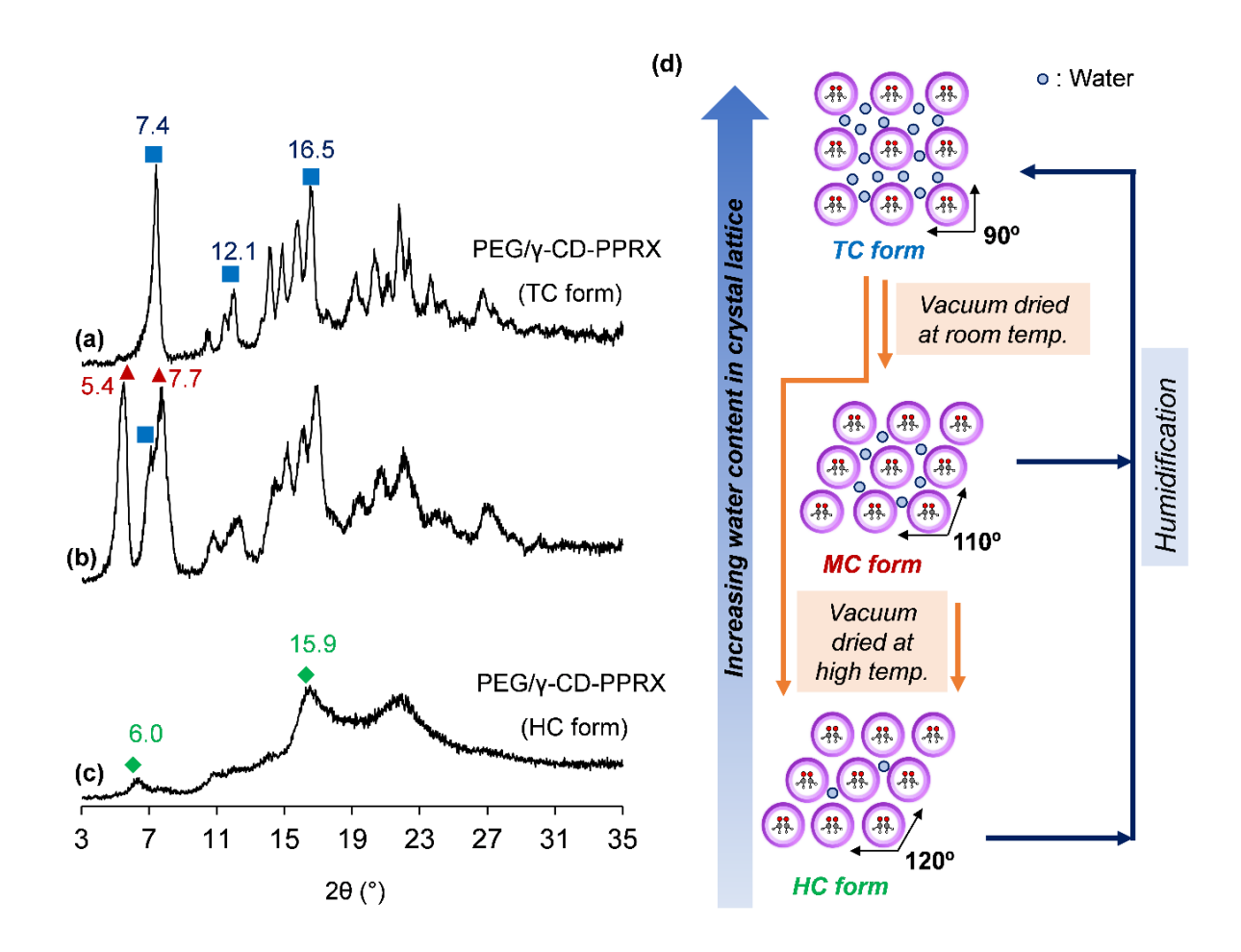


Figure 2. PXRD patterns of (a) tetragonal columnar (TC) form of PEG/ γ -CD-polypseudorotaxane (PEG/ γ -CD-PPRX), (b) dried sample of (a) at room temperature for 12 h, (c) hexagonal columnar (HC) form of PEG/ γ -CD-PPRX, and (d) schematic representation of conversion of the different polymorphic forms of PEG/ γ -CD-PPRX based on water content. The characteristic diffraction peaks are depicted by the following symbols, \blacksquare ; TC form, \blacktriangle ; MC form, and \blacklozenge ; HC form.

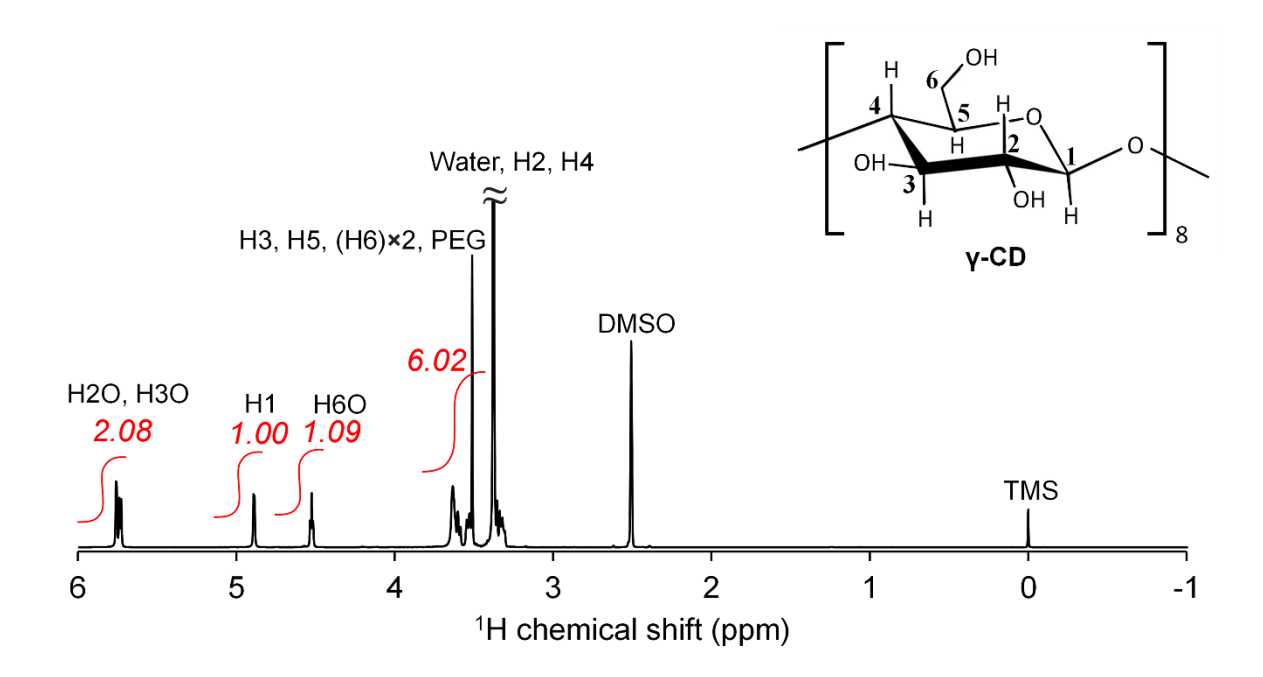


Figure 3. ¹H NMR spectrum of PEG/ γ -CD-PPRX in dimethyl sulfoxide- d_6 (DMSO- d_6) with area integrated with respect to H1 of γ -CD (containing 8 equivalent H1 per one molecule). The ¹H integration ratio of PEG to γ -CD was 2.0:1.0.

Preliminary investigation of sealed-heating conditions to prepare the HC form complex

For preparing the HC form complex, six different guest drugs were selected. The chemical structure of the six guest drugs with their vapor pressure and cross-sectional area (CSA) are listed in Table 1. So far, the MC form of drug/(PEG/ γ -CD-PPRX) complex with 17 different guest compounds has been reported.^{38, 41, 42} Irrespective of the guest compound, sealed-heating at a high temperature of above 110 °C yielded the MC form complex. Thus, a low sealed-heating temperature of 80–110 °C was primarily investigated to retain the initial HC form structure and incorporate the guest drug molecule in the intermolecular spaces, thereby forming the HC form of the drug/(PEG/ γ -CD-PPRX) complex.

Table 1 Chemical structure, vapor pressure, and cross-sectional area (CSA) of guest drugs used for screening.

		^a Vapor	^b Maximum	^b Minimum
Guest drug	Chemical structure	pressure (Pa)	$CSA (Å^2)$	$CSA (Å^2)$
Salicylic acid (SA)	ОН	7.57 (80 °C)	^c 45.4	^c 24.2
Salicylamide (SAM)	ONH ₂	1.32 (80 °C)	44.8	24.1
Paracetamol (PCT)	HONH	0.005 (80 °C) 0.014 (90 °C)	54.6	20.8
2-naphthoic acid (2-NA)	ОН	0.067 (80 °C) 0.571 (100 °C)	58.7	24.4
Phenothiazine (PTZ)	NH S	0.083 (80 °C) 0.596 (100 °C)	68.4	21.9
Naproxen (NPX)	ОН	0.0193 (80 °C) 0.062 (90 °C)	75.8	25.3

^aCalculated from the reported equation of temperature-vapor pressure relation⁵⁶⁻⁵⁹, or adopted from reference literatures.^{60, 61} Adopted from reference literature.⁴¹ Calculated by the three-dimensional molecular modeling method mentioned in the reference literature.⁴¹

SA:
$$\ln p = (34.5 \pm 0.3) - (11483 \pm 100)/T$$
, $r^2 = 0.9993$;

SAM:
$$\ln p = (36.4 \pm 0.3) - (12756 \pm 83)/T$$
, $r^2 = 0.999$;

PCT:
$$\ln p = (34.3 \pm 0.2) - (14010 \pm 86)/T, r^2 = 0.9998;$$

PTZ:
$$\ln p = (34.54) - (13076)/T$$
, $r^2 = 0.9988$;

NPX:
$$\ln p = (39.7 \pm 0.2) - (15431 \pm 65)/T$$
, $r^2 = 0.9998$,

where p is the vapor pressure in Pa and T is the temperature in K.

Initially, SA was chosen as the model drug to evaluate the sealed-heating conditions for preparing the HC form complex. As a pretreatment, the crystallinity of the HC form of PEG/ γ -CD-PPRX was enhanced by the annealing process as shown in Figure 4a. The PXRD pattern of the annealed HC form of PEG/γ-CD-PPRX showed increased peak intensity of the HC form, indicating high crystallinity (Figure 4b). The previous study by Kawasaki *et al.* demonstrated that the anhydrous HC form of PEG/γ-CD-PPRX obtained by the loss of water molecules from its TC form retained a crystalline order, but the degree of order was significantly reduced, indicating a low crystallinity.³⁵ Hence, it is noteworthy that the above-mentioned sealed-heating technique was able to obtain a high crystalline HC form of PEG/ γ -CD-PPRX for the first time. This high crystalline HC form of PEG/ γ -CD-PPRX was used as the initial form for further evaluation. A PM of PEG/γ-CD-PPRX (HC form) and SA mixed in a molar ratio of 2:1 was sealed-heated at 80-145 °C for 3 h and the corresponding PXRD patterns of the obtained SH samples are shown in Figure 5. The diffraction pattern of the SH sample prepared at 80 °C showed peaks corresponding to the HC and MC forms, with residual SA peaks (Figure 5c). The appearance of the MC form peak suggests the inclusion of SA in the intermolecular spaces and partial conversion to the MC form structure. The presence of residual SA peaks suggests incomplete encapsulation. Furthermore, the diffraction pattern of the SH sample prepared at 90 °C showed mainly MC form peaks along with some residual SA peaks (Figure 5d). On further increasing the sealedheating temperature to 100–110 °C, the diffraction pattern of the SH samples showed only MC form peaks without any residual SA peaks (Figure 5e-f). As demonstrated in our previous study, the MC form complex with SA as the guest drug was obtained at a sealedheating temperature of 145 °C, indicated by the diffraction pattern shown in Figure 5g.³⁸ These findings agree with previous findings that a higher sealed-heating temperature induces the conversion to the MC form complex.

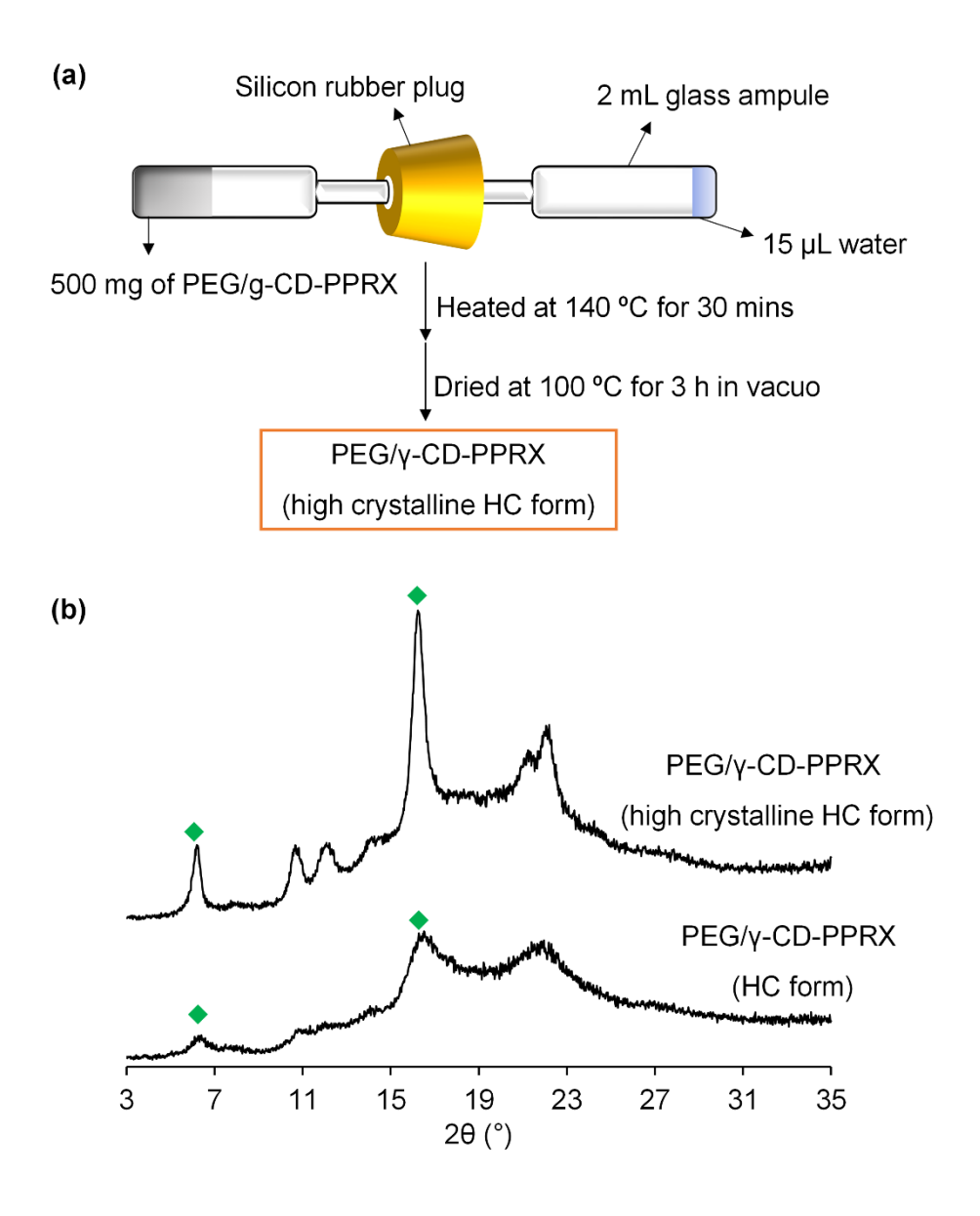


Figure 4. (a) Schematic representation of the sealed-heating method for preparation of high crystalline HC form of PEG/ γ -CD-PPRX, (b) PXRD patterns of high crystalline HC form of PEG/ γ -CD-PPRX (annealed), and HC form of PEG/ γ -CD-PPRX. The characteristic diffraction peaks are depicted by the symbol, •; HC form.

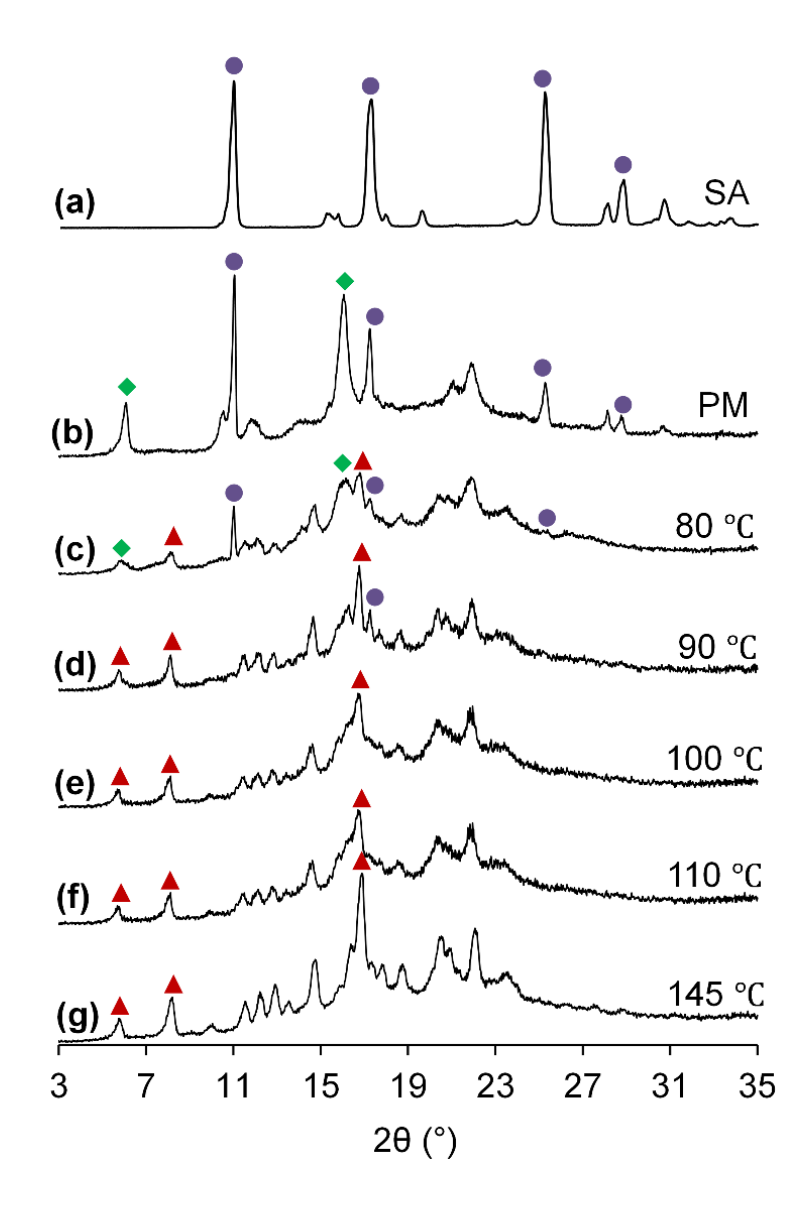


Figure 5. PXRD patterns of (a) SA, (b) PM of SA and HC form of PEG/γ-CD-PPRX, (c) SH sample of (b) prepared at (c) 80 °C (d) 90 °C (e) 100 °C (f) 110 °C, and (g) 145 °C for 3 h. The characteristic diffraction peaks are depicted by the following symbols, •; SA ▲; MC form, and •; HC form.

It was assumed that for incorporation of the guest drug into the intermolecular spaces in the HC form, the crystallinity of the columnar structure, that is, the stacking order of the γ -CDs in a column, as well as the lateral packing, needs to be maintained. Since water plays an important role in maintaining the crystalline order of these structures, ³⁵ additional water was added to the PM and further sealed-heated at 80 °C for 3 h to prepare the HC form complex. Figure 6 shows the PXRD patterns of the SH samples prepared at 80 °C for 3 h with a water content of 4–25 µL. In the PXRD patterns of SH samples with increasing water content from 4–8 μL (Figure 6c-e), the peak intensity of SA gradually decreased, and the peak intensity of the HC form increased. In addition, the MC form peaks that appeared in the SH sample with no water disappeared (Figure 6b). The PXRD pattern of the SH sample prepared at a sealed-heating condition of 80 °C for 3 h with 8 µL of water showed no residual peak of SA with the retention of HC form peaks (Figure 6e). Hence, the HC form of the SA/(PEG/γ-CD-PPRX) complex was successfully prepared at this sealed-heating condition. On the other hand, the PXRD pattern of the SH sample with a high water content (10–25 µL water) suggested the formation of the TC form of the SA/(PEG/ γ -CD-PPRX) complex, indicated by the gradual disappearance of the HC form peaks and the appearance of characteristic peaks of the TC form (Figure 6f-j). The TC form of the SA/(PEG/γ-CD-PPRX) complex was obtained at the low sealed-heating condition and high-water content (over 20 μL water), as reflected by the complete disappearance of the HC form peaks in the PXRD pattern.

For analyzing the role of guest drug and water in the conversion of the polymorphic structure (HC and TC), the HC form of PEG/ γ -CD-PPRX was sealed-heated without any guest drug at the same condition of 80 °C for 3 h with 0–25 μ L water. The PXRD pattern of this SH sample prepared with 8 μ L showed the characteristic peaks of HC form with increased intensity (Figure 7c). On the other hand, the PXRD pattern of the SH sample prepared with 25 μ L showed the characteristic peaks of TC form along with HC form peaks,

suggesting partial transformation (Figure 7d). However, complete transformation to the TC form was observed in the case of the SH sample prepared with SA at the same water content of 25 μ L (Figure 6j). This suggests that the additional water in the SH sample played a vital role in maintaining the HC form structure of PEG/ γ -CD-PPRX during the encapsulation. On the other hand, for the TC form complex formation, the guest drug (SA) and the additional water promoted the transformation of the HC form of the PEG/ γ -CD-PPRX structure to its TC form.

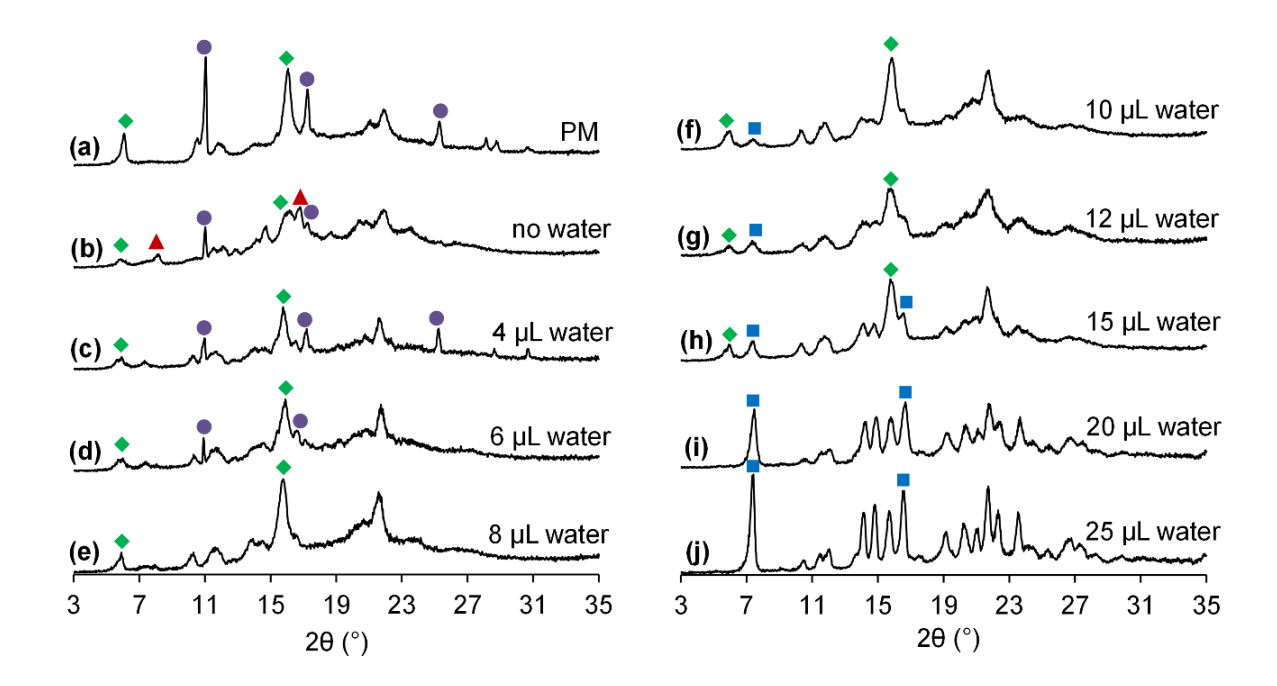


Figure 6. PXRD patterns of (a) PM of SA and HC form of PEG/ γ -CD-PPRX, SH sample of (a) prepared at 80 °C for 3 h with (b) no water, (c) 4 μ L water, (d) 6 μ L water, (e) 8 μ L water, (f) 10 μ L water, (g) 12 μ L water, (h) 15 μ L water, (i) 20 μ L water, and (j) 25 μ L water. The characteristic diffraction peaks are depicted by the following symbols, •; SA •; HC form •; TC form, and •; MC form.

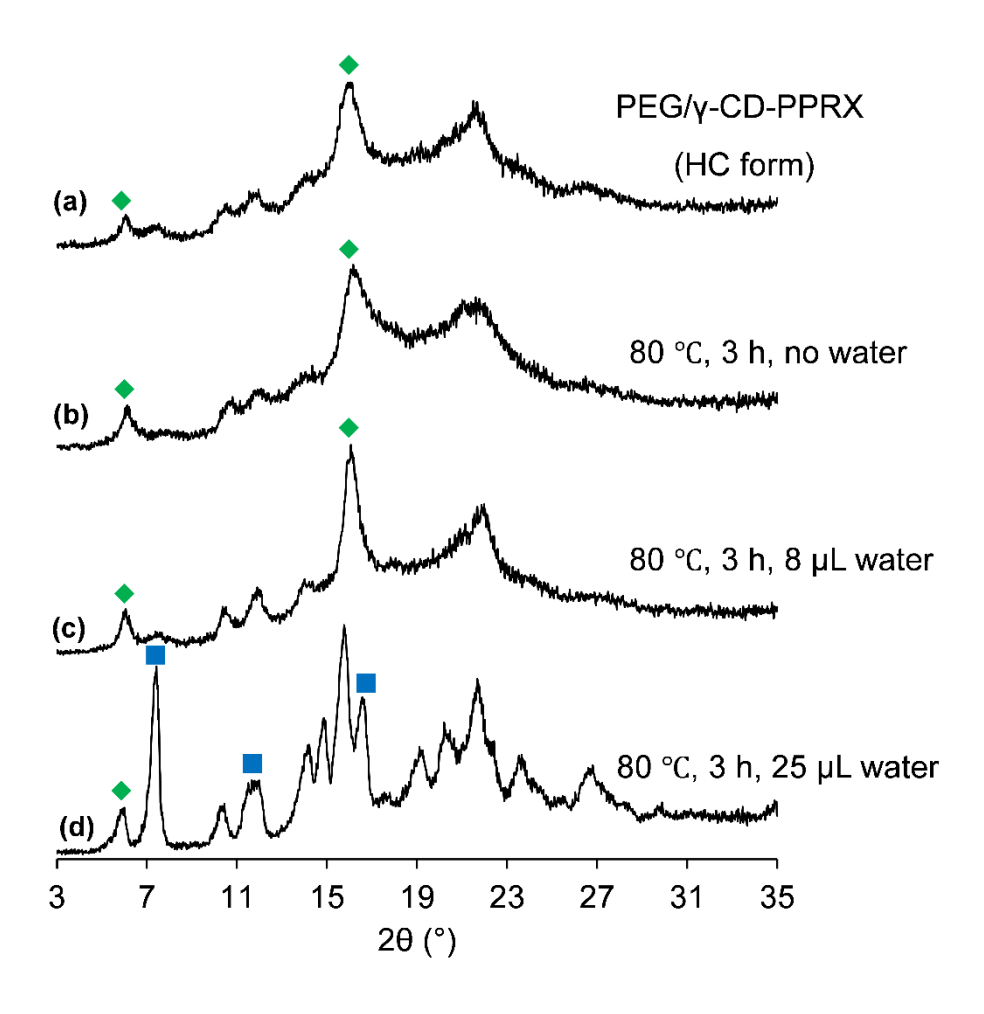


Figure 7. PXRD patterns of (a) HC form of PEG/ γ -CD-PPRX, the SH sample of (a) at 80 °C for 3 h with (b) no water, (c) 8 μ L water, and (d) 25 μ L water. The characteristic diffraction peaks are depicted by the following symbols, •; HC form, and •; TC form.

Furthermore, the encapsulated amount of SA in the HC form complex was determined by solution state ¹H NMR measurement. The ¹H NMR spectrum was measured after removing the non-encapsulated SA by washing it with diethyl ether. Figure 8a shows the ¹H NMR spectrum of the HC form of the SA/(PEG/ γ -CD-PPRX) complex. Relative to the integration value of the H1 peak of γ -CD (8.00, containing 8 equivalent protons), the integration value of the 'Ha' peak of SA was 1.87. This indicated that the encapsulated amount of SA to γ -CD in the HC form complex was almost in the molar ratio of 2:1, equivalent to the initial ratio of SA to γ-CD in the PM. Thus, stoichiometric complexation of SA at a molar ratio of 2:1 was suggested in the HC form complex. To confirm the complexation, the change in the molecular state of SA was further assessed by FTIR spectroscopy. The FTIR spectra of the HC form of the SA/(PEG/ γ -CD-PPRX) complex, along with the starting materials and PM, are presented in Figure 8b. The FTIR spectrum of the PM was a superimposition of the starting materials of SA and HC form of PEG/ γ -CD-PPRX. The carbonyl stretching band of the carboxylic group of SA⁶² shifted from 1657 cm⁻¹ to a higher wavenumber of 1673 cm⁻¹ in the HC form complex. In the MC form complex with SA as the guest drug, a similar higher wavenumber shift of the carbonyl stretching band of the carboxylic group of SA was observed.³⁸ This was attributed to the breaking of dimeric structure in the crystalline state of SA and new intermolecular interaction formation between SA and PEG/γ-CD-PPRX. The observed frequency shift in the IR spectrum can be associated with a similar change in the molecular state of SA and the formation of new intermolecular interactions in the HC form complex. Hence, the FTIR results confirmed the complexation of SA in the HC form.

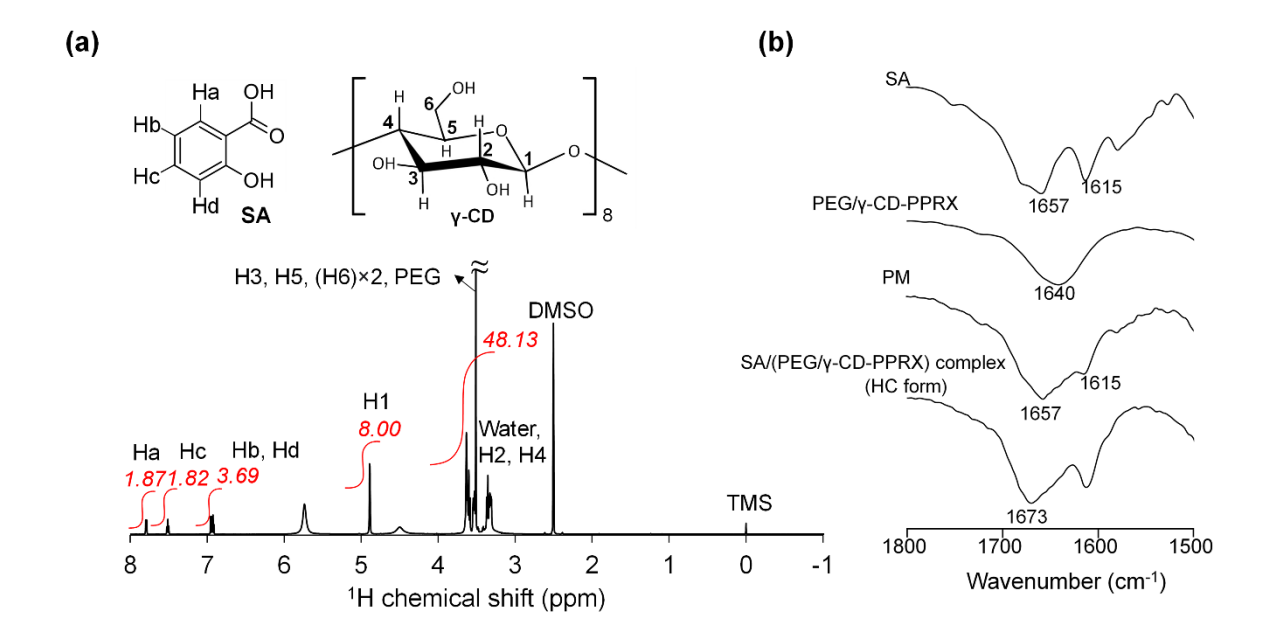


Figure 8. (a) ¹H NMR spectrum of the HC form of the SA/(PEG/ γ -CD-PPRX) complex in DMSO- d_6 and (b) FTIR spectra of the HC form of the SA/(PEG/ γ -CD-PPRX) complex with the respective starting materials.

Analogous observations were noted in the HC form complex preparation when SAM was used as the guest drug and sealed-heated at 80 °C for 3 h in the absence and presence of 2–25 μ L of water (Figure 9). The PXRD pattern of the SH sample prepared at the sealed-heating condition of 80 °C for 3 h with 8 μ L of water, showed the characteristic HC form peaks and no residual SAM peak (Figure 9f). Thus, the HC form of the SAM/(PEG/ γ -CD-PPRX) complex was successfully prepared at the same sealed-heating condition. Similarly, the TC form of SAM/(PEG/ γ -CD-PPRX) complex was obtained at a water content of 25 μ L (Figure 9g). The integration ratio of SAM to γ -CD in its HC form complex obtained from its 1 H NMR spectrum indicated that the SAM interacted stoichiometrically in the molar ratio of 2:1 (Figure 10a). Additionally, the carbonyl stretching band of the primary amide group of SAM (1675 cm⁻¹)⁶³ shifted to 1658 cm⁻¹ in its HC form complex (Figure 10b). Tozuka *et al.* reported a similar lower wavenumber shift of adsorbed SAM onto the micropores of folded sheets of mesoporous material (FSM-16), caused by the new hydrogen bond

formation between adsorbed SAM and the silanol groups of FSM-16.⁶⁴ This frequency shift of SAM in its HC form complex confirmed the complexation of SAM.

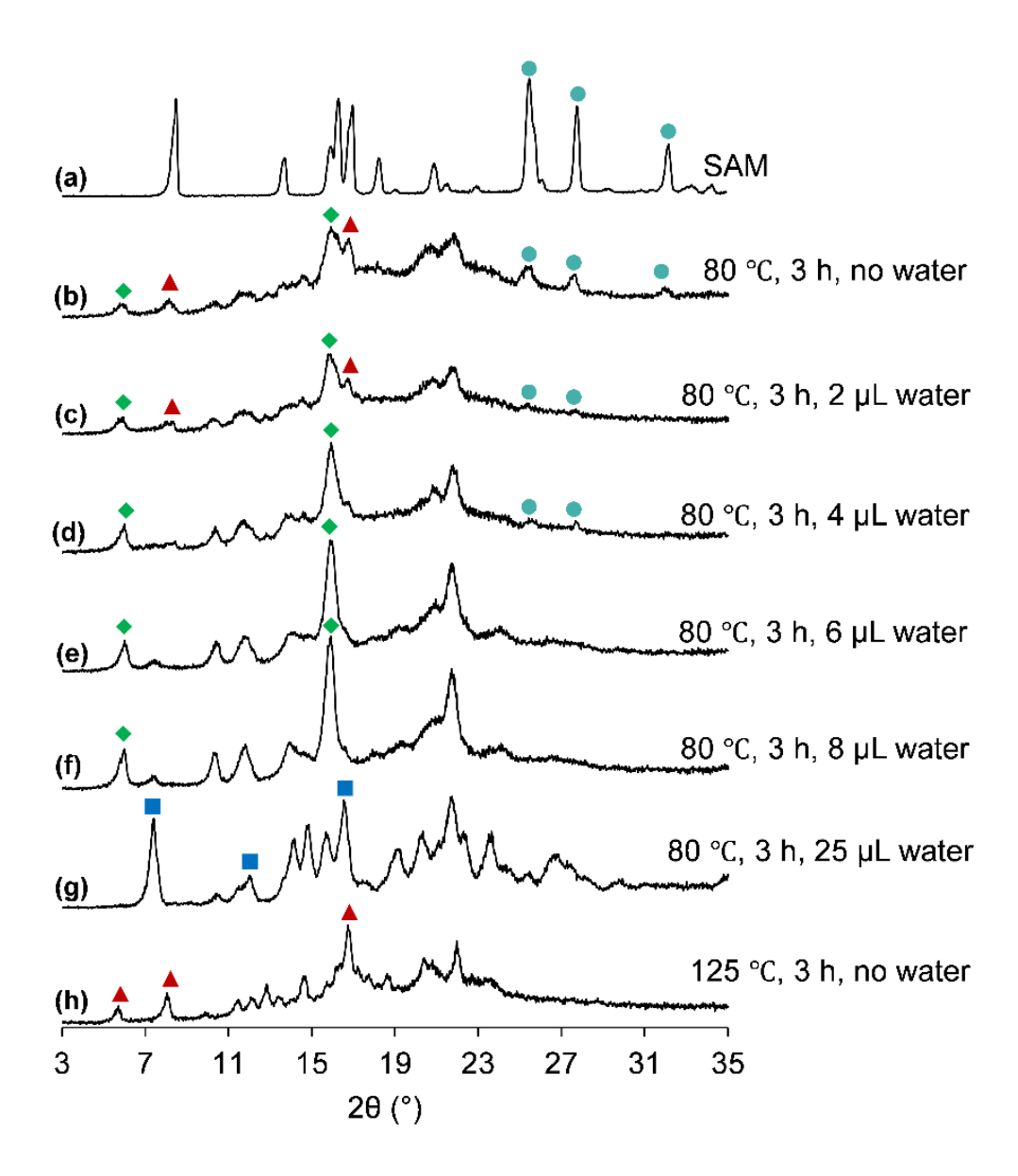


Figure 9. PXRD patterns of (a) SAM, (b) SH sample of SAM and HC form of PEG/γ-CD-PPRX prepared at 80 °C for 3 hours with, (b) no water, (c) 2 μL water, (d) 4 μL water, (e) 6 μL water, (f) 8 μL water, (g) 25 μL water, and (h) SH sample of SAM and HC form of PEG/γ-CD-PPRX prepared at 125 °C for 3 hours (MC form of SAM/(PEG/γ-CD-PPRX) complex). The characteristic diffraction peaks are depicted by the following symbols, •; SAM, •; HC form, •; TC form, and •; MC form.

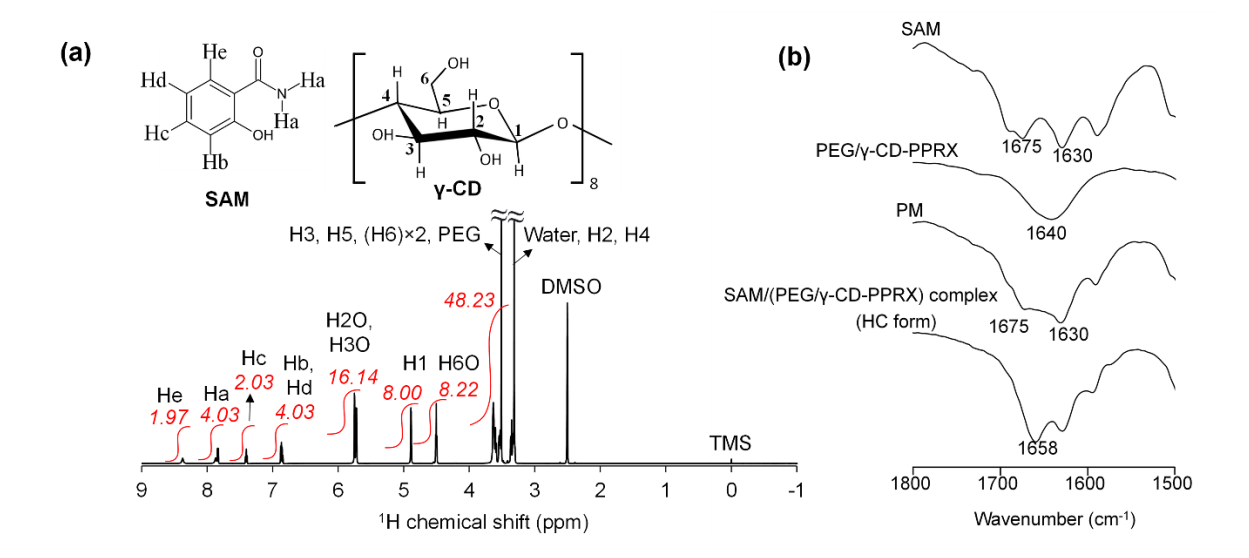


Figure 10. (a) ¹H NMR spectrum of HC form of SAM/(PEG/ γ -CD-PPRX) complex in DMSO- d_6 , and (b) FTIR spectra of HC form of SAM/(PEG/ γ -CD-PPRX) complex with the respective starting materials.

Furthermore, the stability of the polymorphic forms of the SA/(PEG/γ-CD-PPRX) complex was assessed. The changes in the PXRD patterns of the complexes after being subjected to humidification conditions of 75% relative humidity (RH) at 40 °C and drying in vacuo are presented in Figure 11. The HC form of the SA/(PEG/γ-CD-PPRX) complex was stable, even after drying and reducing the water content to 2–3%, which was determined by TG (data not shown) (Figure 11c). No significant change in the crystallinity was observed in the HC form complex after drying. The HC form complex transformed to the TC form complex upon water adsorption in a manner similar to that observed for the MC form complex in our previous study (Figure 11d-e).³⁸ The structure of the transformed TC form structure was maintained even after drying to a water content of 2–3% (Figure 11f).

The structural changes in the polymorphic complexes of SA/(PEG/ γ -CD-PPRX) with respect to sealed-heating conditions and water adsorption/desorption, as interpreted from the PXRD patterns, are summarized in Figure 12. These findings suggest that the formation

of polymorphic complexes of SA/(PEG/ γ -CD-PPRX) is determined by encapsulated SA, temperature, and water content. It is important to mention that all the prepared complexes of SA/(PEG/ γ -CD-PPRX) were stable with a low water content of 2–3%, indicating the formation of anhydrous polymorphs of the SA/(PEG/ γ -CD-PPRX) complex instead of the hydrated forms as exhibited by the host compound, PEG/ γ -CD-PPRX.

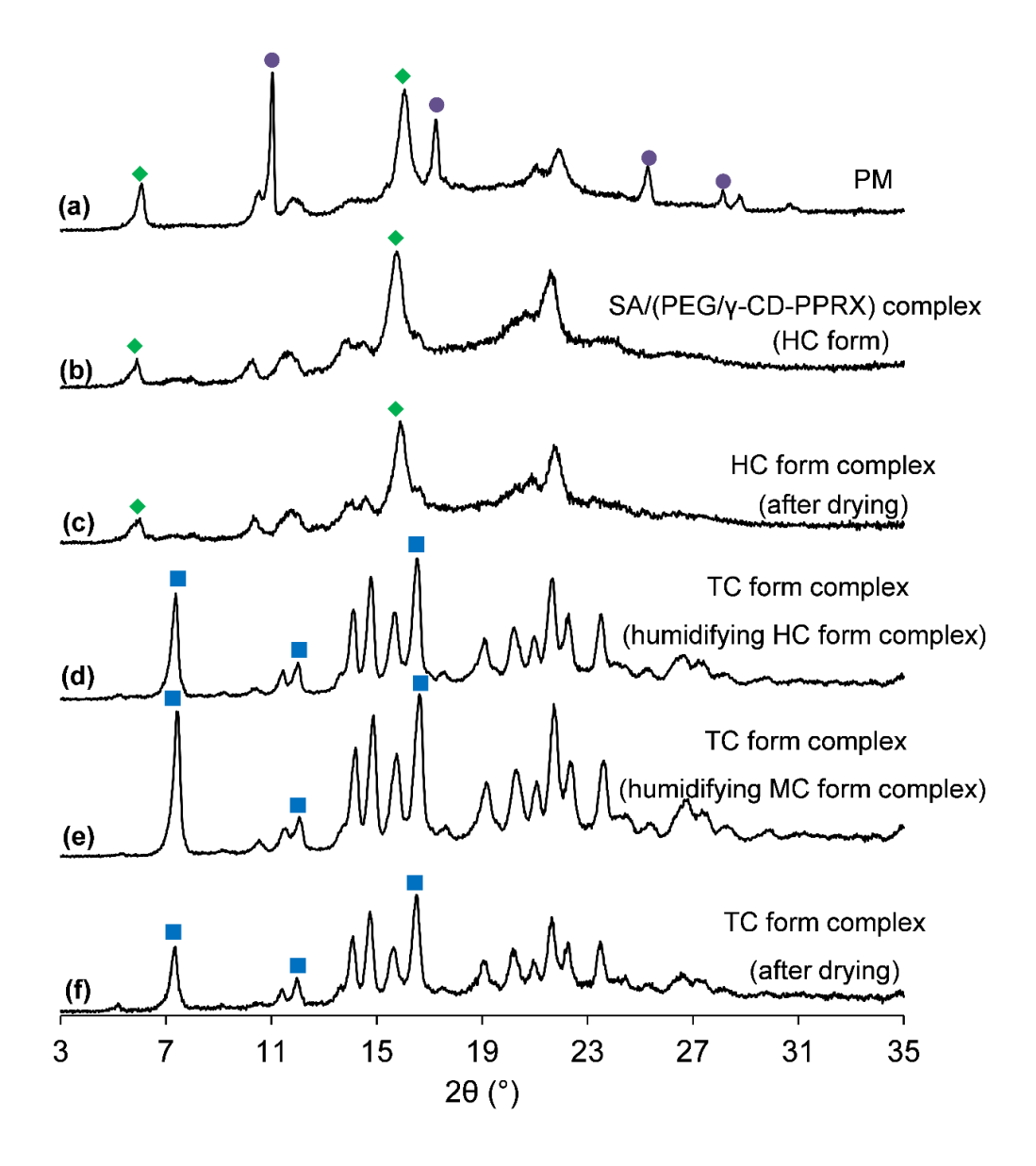


Figure 11. PXRD patterns of (a) PM of SA and HC form of PEG/γ-CD-PPRX, (b) HC form of SA/(PEG/γ-CD-PPRX) complex, (c) HC form of SA/(PEG/γ-CD-PPRX) complex after drying in vacuo at 40 °C for 8 hours, (d) TC form of SA/(PEG/γ-CD-PPRX) complex after humidifying the HC form complex for 3 days, (e) TC form of SA/(PEG/γ-CD-PPRX) complex after humidifying the MC form complex for 7 days, and (f) TC form of SA/(PEG/γ-CD-PPRX) complex after drying in vacuo at 40 °C for 12 hours. The humidifying condition used is 75% relative humidity at 40 °C. The characteristic diffraction peaks are depicted by the following symbols, •; SA, •; HC form, and •; TC form.

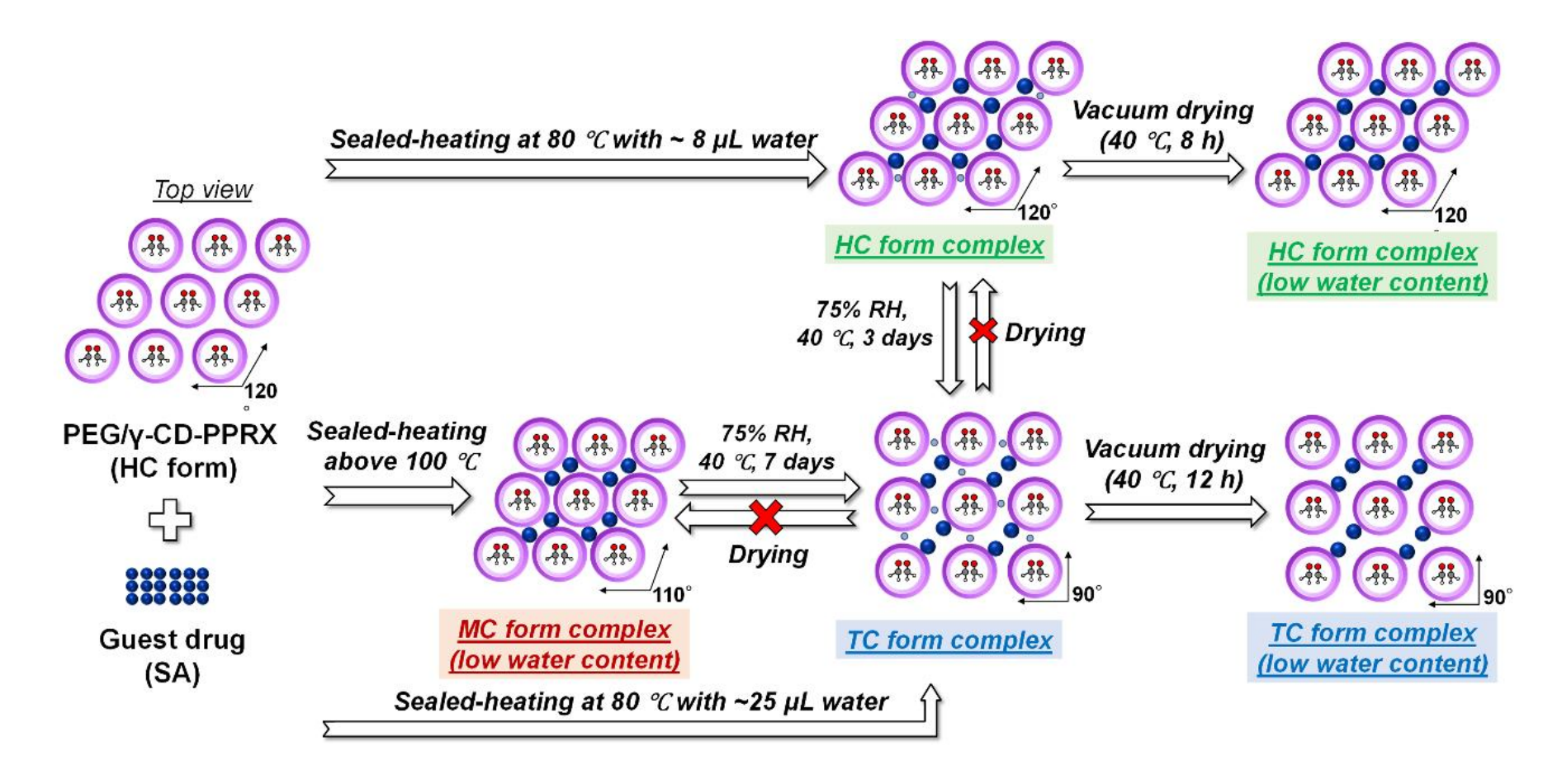


Figure 12. Schematic representation of structural changes in the polymorphic complexes of SA/(PEG/ γ -CD-PPRX) with respect to the sealed-heating conditions and water adsorption/desorption.

Encapsulation behavior of other guest drugs in the HC form complex

To rationalize the low temperature sealed-heating with a small amount of water for preparing the HC form complex, complex formation with other guest drugs was evaluated. Figure 13 shows the changes in the PXRD patterns of the SH samples of PM of the guest drugs (PCT and NPX) and the HC form of (PEG/γ-CD-PPRX) at respective sealed-heating conditions. The PXRD patterns of SH samples with PCT and NPX prepared at the optimized sealedheating conditions (80 °C, 3 h with 8 µL water) showed the diffraction peaks of HC form along with strong residual peaks of the drugs, suggesting less encapsulation of the guest drug (Figure 13g-h). Thus, the duration of sealed-heating at 80 °C was increased from 3 to 9 h. The complexation of PCT and NPX was enhanced, but not complete, as indicated by the decrease in the peak intensity of the guest drugs in the corresponding PXRD patterns presented in Figure 13g-1. While the sealed-heating temperature was increased to 90 °C with a duration of 3–9 h, the residual drug peaks were still retained along with the HC form peaks in the PXRD patterns (Figure 13m-q). However, in the SH samples of NPX prepared at the sealed-heating temperature of 90 °C for 6 and 9 h, conversion to MC form structure was observed, reflected by the broadening of the HC form peaks and appearance of MC form peak in the PXRD patterns, respectively (Figure 13p, 13r).

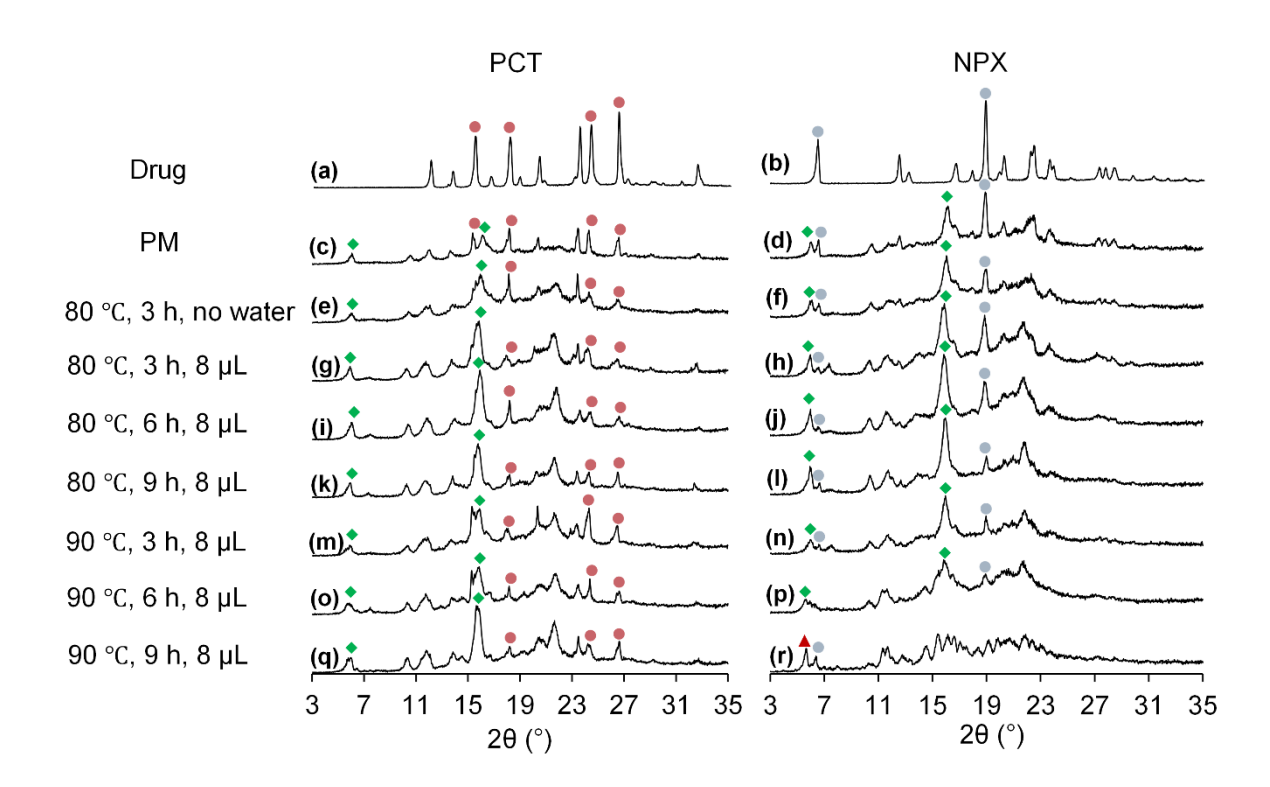


Figure 13. PXRD patterns of (a) PCT, (b) NPX, (c) PM of PEG/γ-CD-PPRX (HC form) and PCT (2:1), (d) PM of PEG/γ-CD-PPRX (HC form) and NPX (1:1), and (e-r) SH samples of (c) and (d) prepared at the indicated SH condition. The characteristic diffraction peaks are depicted by the following symbols, •; PCT •; NPX •; HC form, and ▲; MC form.

Figure 14 shows the changes in the PXRD patterns of the SH samples of PM of the guest drug (2-NA and PTZ) and the HC form of (PEG/γ-CD-PPRX) at respective sealed-heating conditions. Similar to PCT and NPX, the PXRD pattern of the SH sample prepared using 2-NA and PTZ as the guest drugs at the optimized sealed-heating condition (80 °C, 3 h with 8 μL water) exhibited diffraction peaks of residual drugs and HC form (Figure 14g-h). The changes in the PXRD pattern of the SH samples of 2-NA prepared at 80 °C with a duration from 3 to 9 h suggested that almost complete encapsulation of 2-NA was achieved, reflected by the almost disappearance of the diffraction peaks of the residual 2-NA and retention of the HC form peaks (Figure 14g, i, k). Further increasing the sealed-heating temperature to 100 °C in the case of 2-NA, complete encapsulation could be achieved within 3 h, as suggested by the presence of the HC form peaks and no residual 2-NA peaks (Figure 14m). On the other

hand, the PXRD patterns of the SH samples prepared with PTZ with an increased sealed-heating duration from 3 to 9 h at 80 °C revealed incomplete encapsulation owing to the presence of diffraction peaks of residual PTZ (Figure 7h, j, l). Complete encapsulation could not be achieved in the case of PTZ, even upon increasing the sealed-heating temperature to 100 °C (Figure 14n). Furthermore, it can be suggested that the complexation of 2-NA was higher than PTZ as the decrease of the peak intensity of 2-NA was significantly higher as compared to PTZ. From Figures 13 and 14, it can be inferred that the encapsulation behavior and efficiency could be dependent on the guest drug properties.

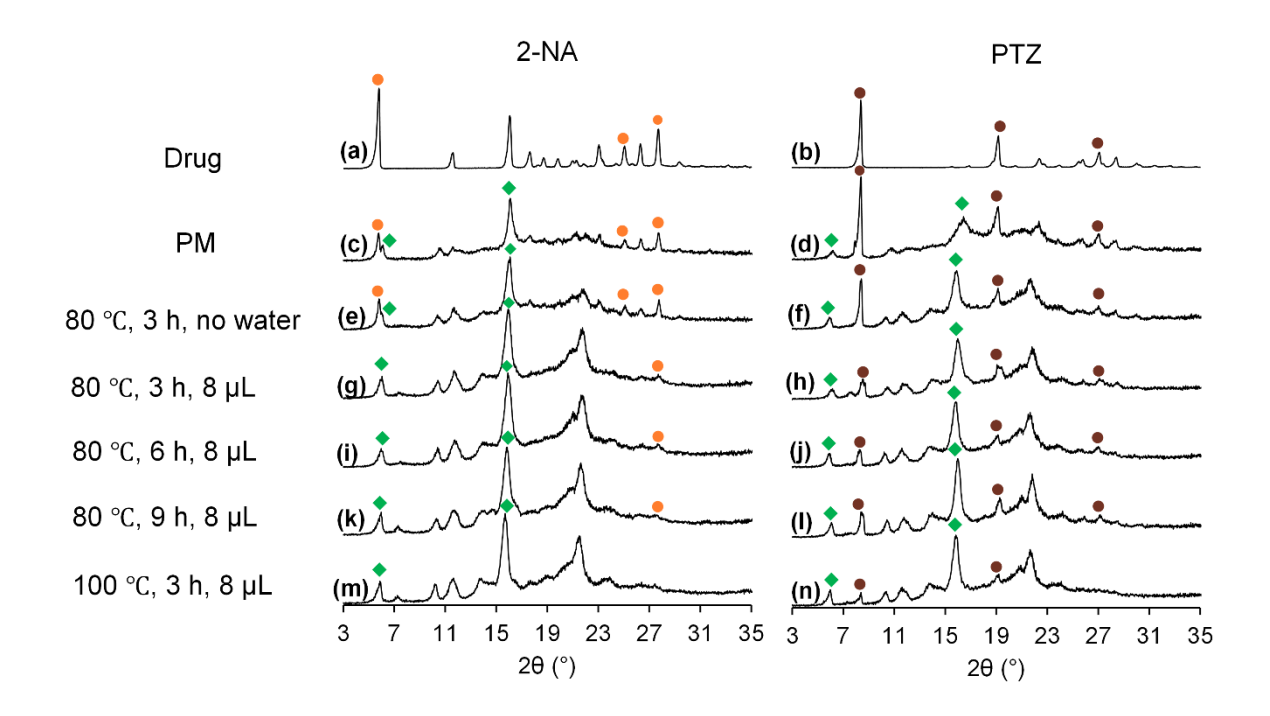


Figure 14. PXRD patterns of (a) 2-NA, (b) PTZ, (c) PM of PEG/γ-CD-PPRX (HC form) and 2- NA (1:1), (d) PM of PEG/γ-CD-PPRX (HC form) and PTZ (1:1), and (e-n) SH samples of (c) and (d) prepared at the indicated SH conditions. The characteristic diffraction peaks are depicted by the following symbols, •; 2-NA, •; PTZ, and •; HC form.

Determination of encapsulation efficiency of guest drugs by solution-state ¹H NMR

To clarify the difference in encapsulation efficiency of the guest drugs interpreted from the PXRD patterns, the amount of encapsulated drug (PCT, NPX, 2-NA, and PTZ) was evaluated by measuring solution state ¹H NMR spectra. Prior to measuring, the non-encapsulated drug in the SH sample was eluted by washing it with diethyl ether or acetone. The encapsulated amount of SH samples of NPX prepared at 90 °C for 6-9 h was not determined because of the partial transformation to the MC form structure as shown in Figures 13p and 13r. Figures 15 and 16 show representative ¹H NMR spectra of the SH samples of PCT, NPX, 2-NA, and PTZ obtained after washing. The integration value of the 'Ha' peak in PCT, the 'Hh' peak in NPX, the 'Hb' peak in 2-NA, and the 'He' peak in PTZ with respect to the H1 peak of γ-CD (8.00, containing 8 equivalent protons) were determined. From the obtained integration value, the percentage of encapsulated guest drug or encapsulation efficiency was calculated and plotted against the respective sealed-heating condition in Figure 17. The encapsulation efficiency was found to be different among PCT, NPX, 2-NA, and PTZ at respective sealedheating temperatures. For SH samples prepared at the sealed-heating condition of 80 °C, 3 h, with 8 µL water, the encapsulation efficiency of PCT, NPX, 2-NA, and PTZ was 23%, 24%, 68%, and 45%, respectively. The encapsulation efficiency of all guest drugs gradually increased with sealed-heating duration at the respective temperatures. In addition, with an increase in sealed-heating temperature, a significant increase in the encapsulation efficiency of the guest drugs of about 4-24% was observed. In the case of the SH sample of 2-NA, prepared at 100 °C for 3 h, the encapsulated amount reached 90% which is close to the initial ratio of 1:1 in the PM (Figure 17b). Thus, 2-NA was encapsulated in a stoichiometric ratio of 1:1 in the HC form complex.

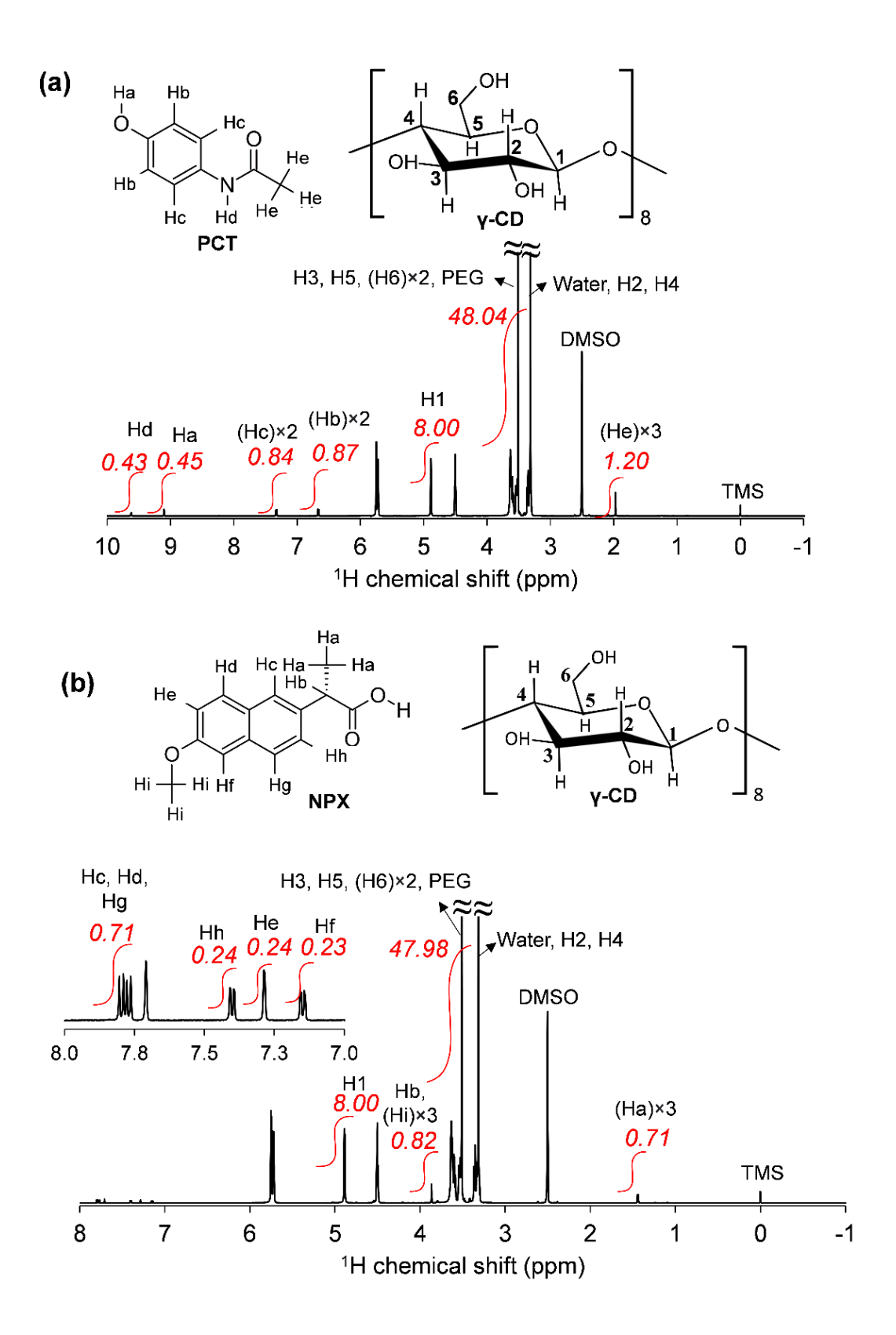


Figure 15. ¹H NMR spectra of washed (a) PCT, and (b) NPX SH samples prepared at a sealed-heating condition of 80 °C for 3 h with 8 μ L water in DMSO- d_6 .

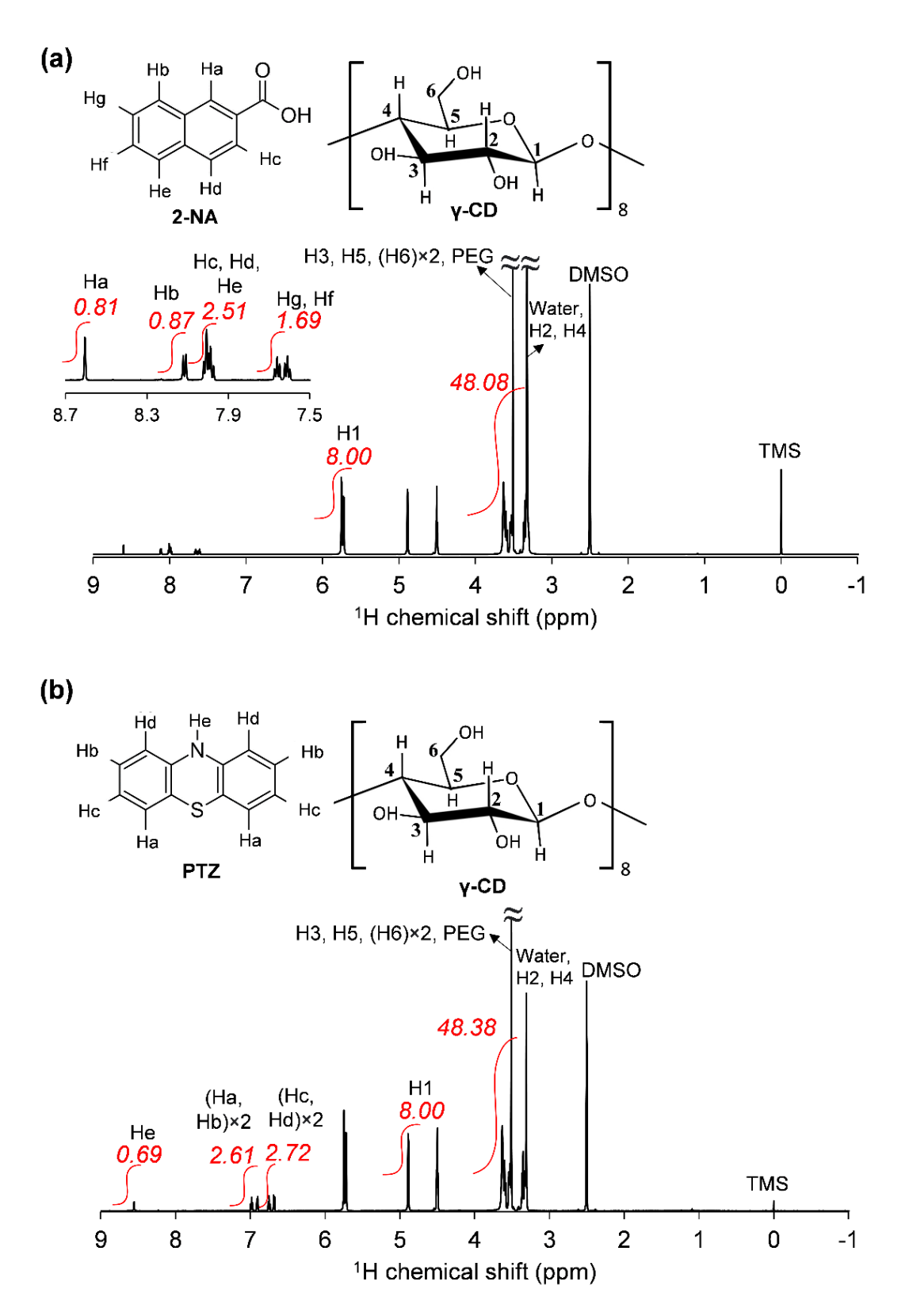


Figure 16. ¹H NMR spectra of washed (a) 2-NA, and (b) PTZ SH samples prepared at a sealed-heating condition of 100 °C for 3 h with 8 μL water in DMSO-*d*₆.

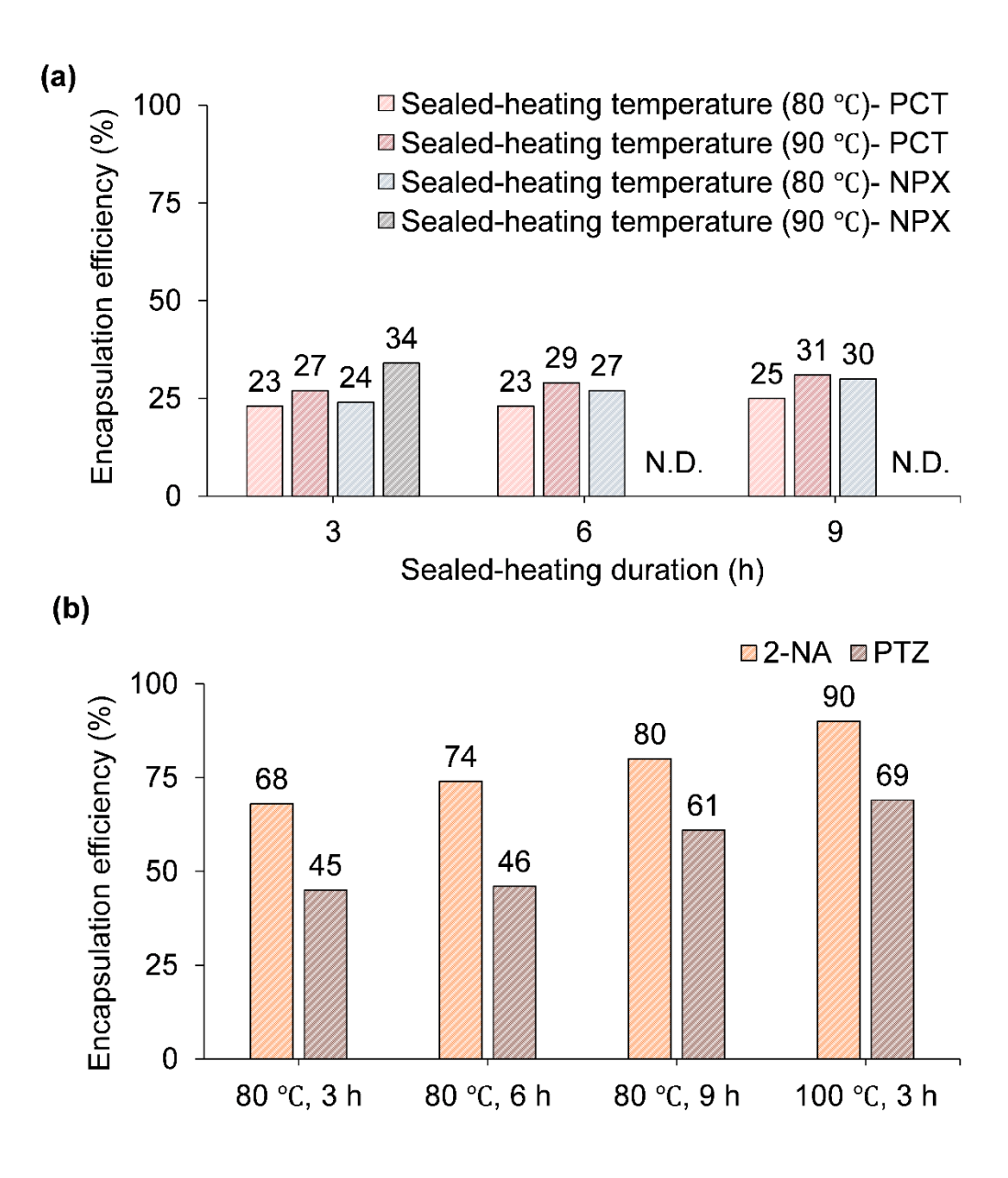


Figure 17. (a) Encapsulation efficiency (%) of PCT and NPX in the SH samples prepared at 80 °C and 90 °C for 3-9 h and (b) encapsulation efficiency (%) of 2-NA and PTZ in the SH samples prepared at 80 °C for 3-9 h and 100 °C for 3 h. The amount of water used in the SH samples is 8 μL. (N.D., not determined)

In the sealed-heating method, encapsulation of the guest molecule is facilitated by its vaporized/gas phase. For analyzing the effect of the vapor pressure of the guest drug on its encapsulation efficiency, SH samples with an excess amount of drug were prepared at the same sealed-heating conditions. The encapsulation efficiency of the guest drug remained the same in the SH samples prepared with an excess amount of drug as that of the SH samples prepared with the initial fixed amount of drug (Figure 18). This could be attributed to the fact that the vaporized amount of the guest drug is not dependent on the initial amount. Hence, the increase in the encapsulation efficiency of the guest drug with temperature is due to the increased vapor pressure of the drug with increasing temperature.

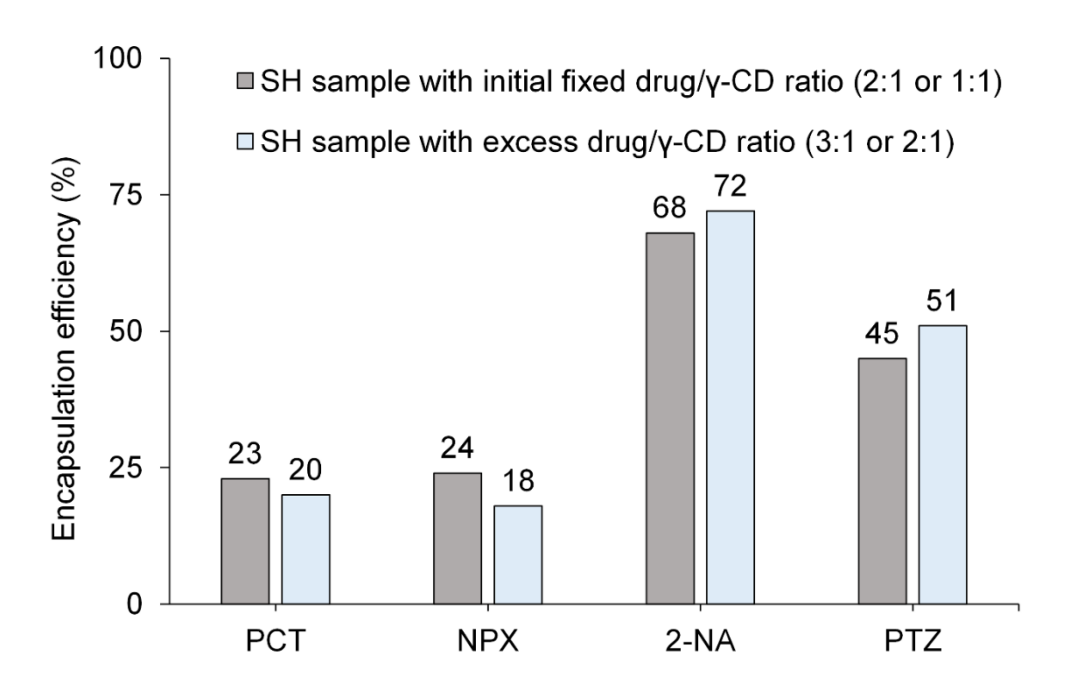


Figure 18. Comparison of encapsulation efficiency (%) in SH samples prepared at the optimized sealed-heating condition (80 °C, 3 h, 8 μL water) with the initial fixed and excess drug/γ-CD ratio. The initial fixed drug/γ-CD ratio for preparing SH samples was 2:1 in the case of PCT and 1:1 in the case of NPX, 2-NA, and PTZ. The drug/γ-CD ratio for preparing SH samples with an excess amount of drug was 3:1 in the case of PCT and 2:1 in the case of NPX, 2-NA, and PTZ.

Discussion on the correlation between encapsulation efficiency and guest drug properties

Previous studies have reported the MC form complex preparation with the same guest drugs used in this study and discussed the factors influencing the complexation behavior.⁴¹ The complexation behavior was not affected by the guest properties, such as molecular weight and polarity. 41 Whereas the stoichiometry of the guest to the host in the complex was found to be determined by the maximum cross-sectional area (CSA) of the drug. 41 Guest drugs, namely, SA, SAM, and PCT with a maximum CSA of 40-55 Å² formed the MC form complex in a 2:1 drug/γ-CD ratio. ^{38, 41} On the other hand, guest drugs, such as 2-NA, PTZ, and NPX, with a maximum CSA of 60–75 Å² formed the MC form complex in a 1:1 drug/y-CD ratio.⁴¹ In the present study, the guest drugs, SA and SAM formed the HC form complex in a 2:1 drug/y-CD ratio, while 2-NA formed the HC form complex in a 1:1 drug/ γ -CD ratio. From this result, it can be speculated that the intermolecular space size is approximately similar for the MC form and HC form structure of PEG/γ-CD-PPRX. Judging from this speculation, the difference in the extent of encapsulation of PCT, NPX, and PTZ in the HC form structure from the expected ratio could be associated with the guest drug properties rather than the host size. Further, guest drug properties such as vapor pressure and molecular size were considered to investigate the difference in encapsulation efficiency of the guest drug molecule. Vapor pressure is considered an important determining factor in the sealed-heating method as the encapsulation of the guest drug molecule is facilitated by the vaporized/gas phase. 65-67

The vapor pressure of the guest drugs at sealed-heating temperatures of 80–100 °C is listed in Table 1. Figure 19 illustrates the correlation plot between the vapor pressure of the guest drug and its maximum encapsulation efficiency at the respective sealed-heating temperatures. It was obvious that the encapsulation efficiency of the guest drug could be correlated to its vapor pressure at the corresponding sealed-heating temperature. The complete encapsulation

of SA and SAM in the HC form structure could be achieved at a low sealed-heating temperature owing to its relatively high vapor pressure. The encapsulation efficiency of PCT, NPX, 2-NA, and PTZ in the SH sample prepared at 80 °C was 25%, 30%, 80%, and 61%, respectively. The vapor pressure of PCT, NPX, 2-NA, and PTZ at 80 °C is 0.005 Pa, 0.019 Pa, 0.067 Pa, and 0.083 Pa, respectively. However, a few discrepancies in the correlation can be observed. For instance, at sealed-heating temperatures of 80 °C and 100 °C, the encapsulation efficiency of 2-NA (shown by the orange circle and square) was 80% and 90%, respectively. On the other hand, the encapsulation efficiency of PTZ at the sealed-heating temperature of 80 °C and 100 °C (shown by the brown circle and square) was 61% and 69%, respectively. However, the vapor pressure of PTZ was higher than 2-NA at 80 °C and was similar at 100 °C. Additionally, 2-NA and NPX had comparable vapor pressure at 80 °C and 90 °C (shown by the orange circle and gray triangle, respectively), yet a difference in the encapsulation efficiency of 2-NA and NPX can be observed.

It can be assumed that the encapsulation efficiency of the guest drugs was mainly governed by their vapor pressure but can be affected by other factors such as the host cavity size, guest size, or the complexation kinetics. The thermodynamics of complexation is defined by the binding constant which reflects the stability of the guest molecule inside the cavity, whereas the kinetics of complexation or the rate of association/dissociation reflects the extent of steric hindrance experienced by the guest molecule during entry/exit. Mârquez *et al.* highlighted that the binding constant between cucurbit[6]uril and various guests decreased with an increase in guest size, owing to the increased steric repulsion between the host walls and the guest during the ingression process.⁶⁸ In another study, Miskolczy *et al.* reported the effect of steric factors of protoberberine alkaloids on its kinetics to form an inclusion complex with cucurbit[7]uril. It was demonstrated that the rate of entry and exit of the guest alkaloids into the host cavity was kinetically favored by less bulky substituent groups.⁶⁹ So, the lack of

correlation between the encapsulation efficiency and vapor pressure in the case of NPX and PTZ can be explained by the increased molecular size of PTZ (maximum CSA of 68.4 Å²) and NPX (maximum CSA of 75.8 Å²) compared to 2-NA (maximum CSA of 58.7 Å²). As presented in Figure 17, in the case of NPX, 2-NA, and PTZ, the saturation state of complexation was not reached even after 9 h of sealed-heating, which could be due to the decrease in the complexation kinetics affected by its molecular size. The complete complexation of 2-NA could be achieved due to its significant vapor pressure and comparatively smaller size than NPX and PTZ. Thus, the increasing guest size could decrease the encapsulation kinetics resulting in reduced encapsulation efficiency of NPX and PTZ, despite the comparative vapor pressure.

An understanding of the complexation behavior of a guest drug in the PEG/γ-CD-PPRX structure would be helpful for the development of new strategies to control and enhance the encapsulation of the guest compound. The low temperature sealed-heating preparation condition of the HC form complex makes it a favorable host molecule for guest compounds prone to decomposition at high temperatures. So far, the host/guest complexation behavior of the solid host and gaseous guest compound has been mostly studied.^{70,71} From this study, new insights related to solid host/guest complexation systems were obtained and the encapsulation efficiency of the guest compound could be correlated with its vapor pressure and molecular size.

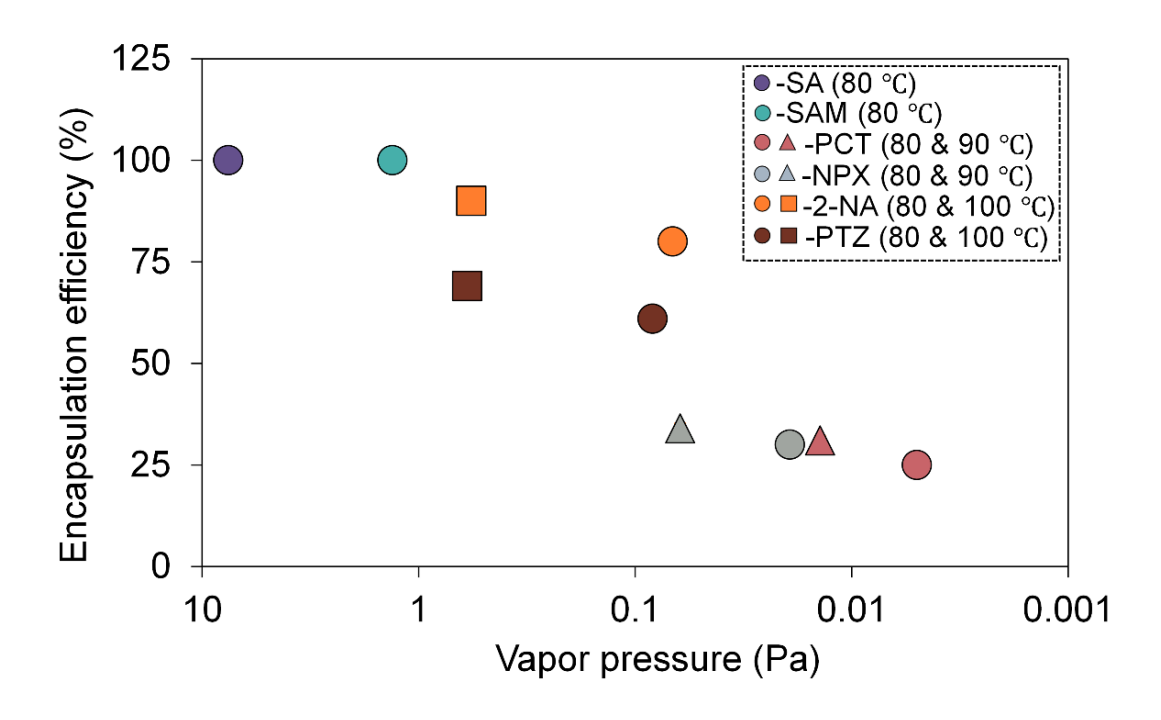


Figure 19. Relationship between the vapor pressure of the guest drug and its encapsulation efficiency (%) in the HC form complex. The circle, triangle, and square symbols indicate the vapor pressure and encapsulation efficiency of the guest drug at sealed-heating temperatures of 80 °C, 90 °C, and 100 °C, respectively.

<u>Part II</u> Evaluation of drug's sublimation rate and molecular mobility in three polymorphic complexes

Preparation of three polymorphic complexes with SA as the model drug

For evaluating the difference in the physical property, the three polymorphic forms of the drug/(PEG/γ-CD-PPRX) complex were prepared with SA as the model drug. The preparation scheme with structures of the three polymorphic forms of the SA/(PEG/γ-CD-PPRX) complex is shown in Figure 20. The successful preparation of the three polymorphic forms of the complex was confirmed by its PXRD patterns (Figure 21). The PXRD patterns showed the characteristic diffraction peaks of each form while the diffraction peaks of SA were absent, confirming the formation of the three polymorphic forms of the complex.

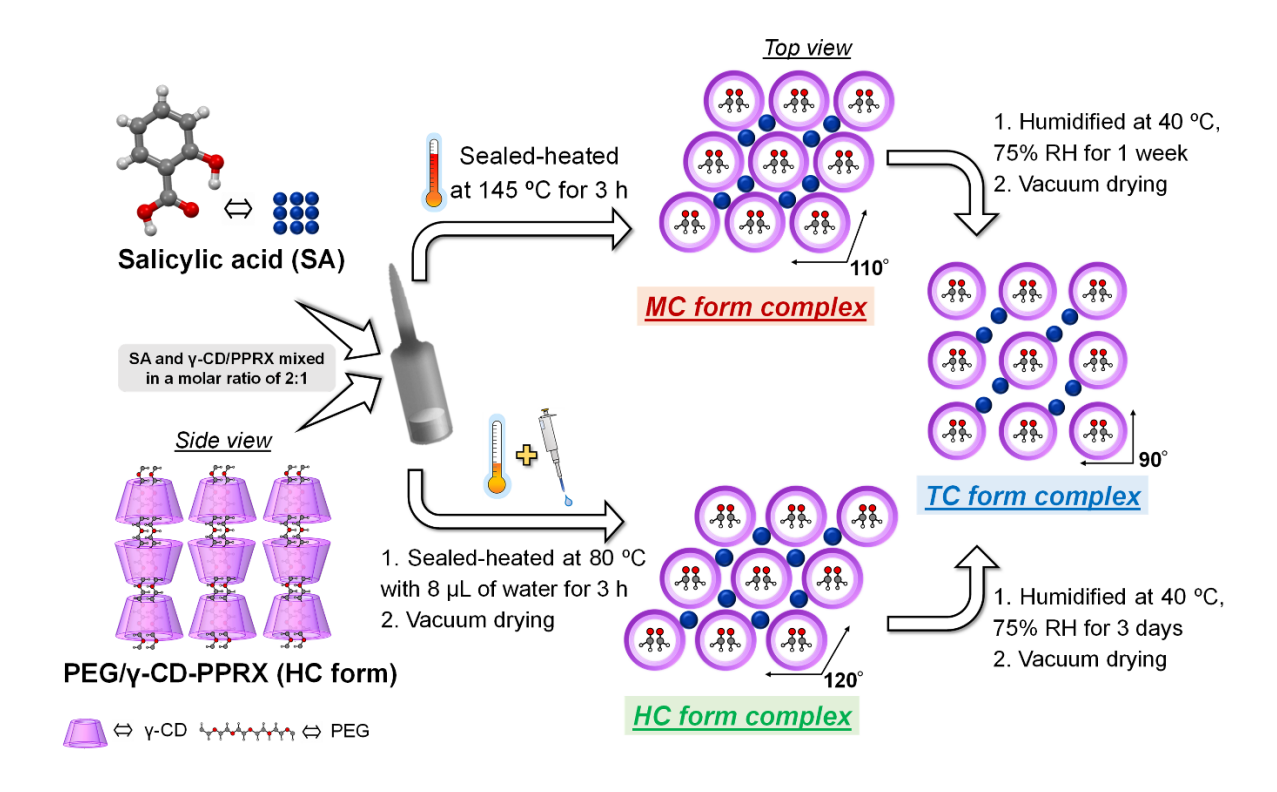


Figure 20. Schematic representation of the preparation of the three polymorphic forms of the SA/(PEG/γ-CD-PPRX) complex.

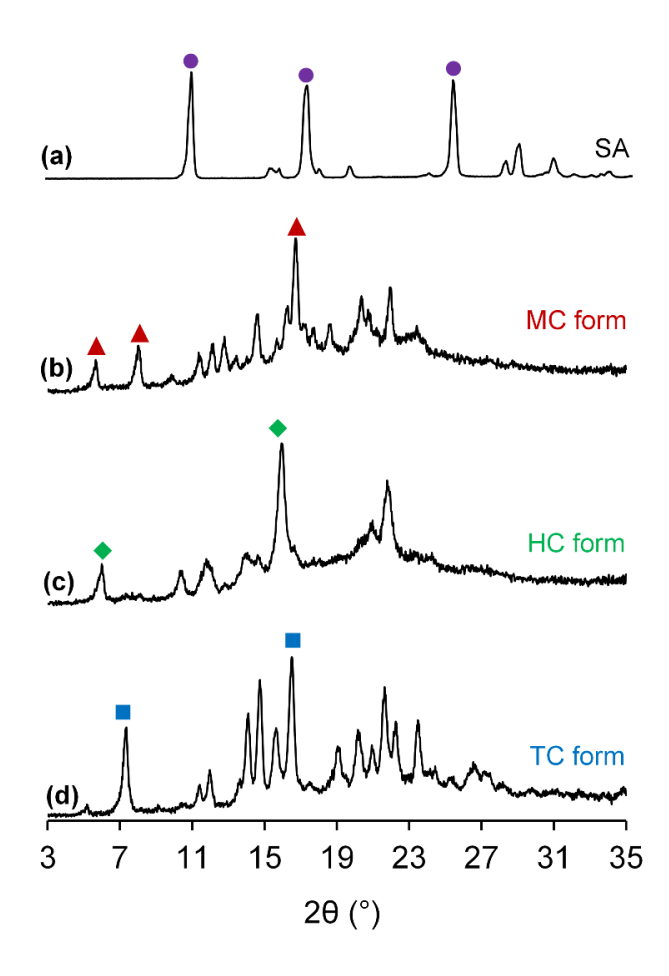


Figure 21. PXRD patterns of (a) SA, (b) MC form, (c) HC form, and (d) TC form of SA/(PEG/γ-CD-PPRX) complex. The characteristic diffraction peaks are represented by •; SA ▲; MC form •; HC form, and •; TC form.

Thermal stability of the three polymorphic complexes

The assessment of preparation conditions indicated that the sealed-heating temperature significantly influenced the conversion of the polymorphic forms of the SA/(PEG/γ-CD-PPRX) complex. Moreover, encapsulated SA in the complexes played a vital role in maintaining the stability of the complexes (Figure 12). Considering these factors, the thermal stability of the complexes was evaluated by VT-PXRD measurements. Preliminarily, the TG profiles of the complexes were measured and are presented in Figure 22. The TG profiles of the complexes showed two-step weight loss from 25/30–45 °C and 80–225/230 °C, respectively. The first weight loss in the range of 2–4% corresponds to the water in the complexes. The second weight loss of 14–16% was due to the SA sublimation. This weight loss corroborates with the theoretical weight % of SA (15.7%) in the complexes, indicating the complete release of SA until 230 °C. The thermal stability of the complexes was then examined by measuring VT-PXRD patterns at 30–230 °C, which are shown in Figure 23.

The PXRD patterns of the MC form complex remained unchanged from 30–230 °C. The PXRD patterns at 230 °C showed characteristic diffraction peaks of the MC form even after the complete release of SA, indicating high thermal stability at a high temperature (Figure 23a). On the other hand, with the removal of SA, the HC and TC form complex was converted to a disordered MC form structure at 130 and 170 °C, respectively (Figure 23b, c). The conversion to the MC form structure was indicated by the appearance of characteristic diffraction peaks of the MC form. However, the diffraction peaks were significantly broadened, suggesting the converted MC form structure is highly disordered but with the retention of the basic columnar structure. However, the manner of conversion in HC and TC form complex differed and the possible reasons have been discussed later. The thermal stability of the complexes increased in the order of HC form < TC form < MC form at a high

temperature. Furthermore, this also suggests that the sublimation tendency of SA in the complexes should be studied in the temperature range of 80-110 °C.

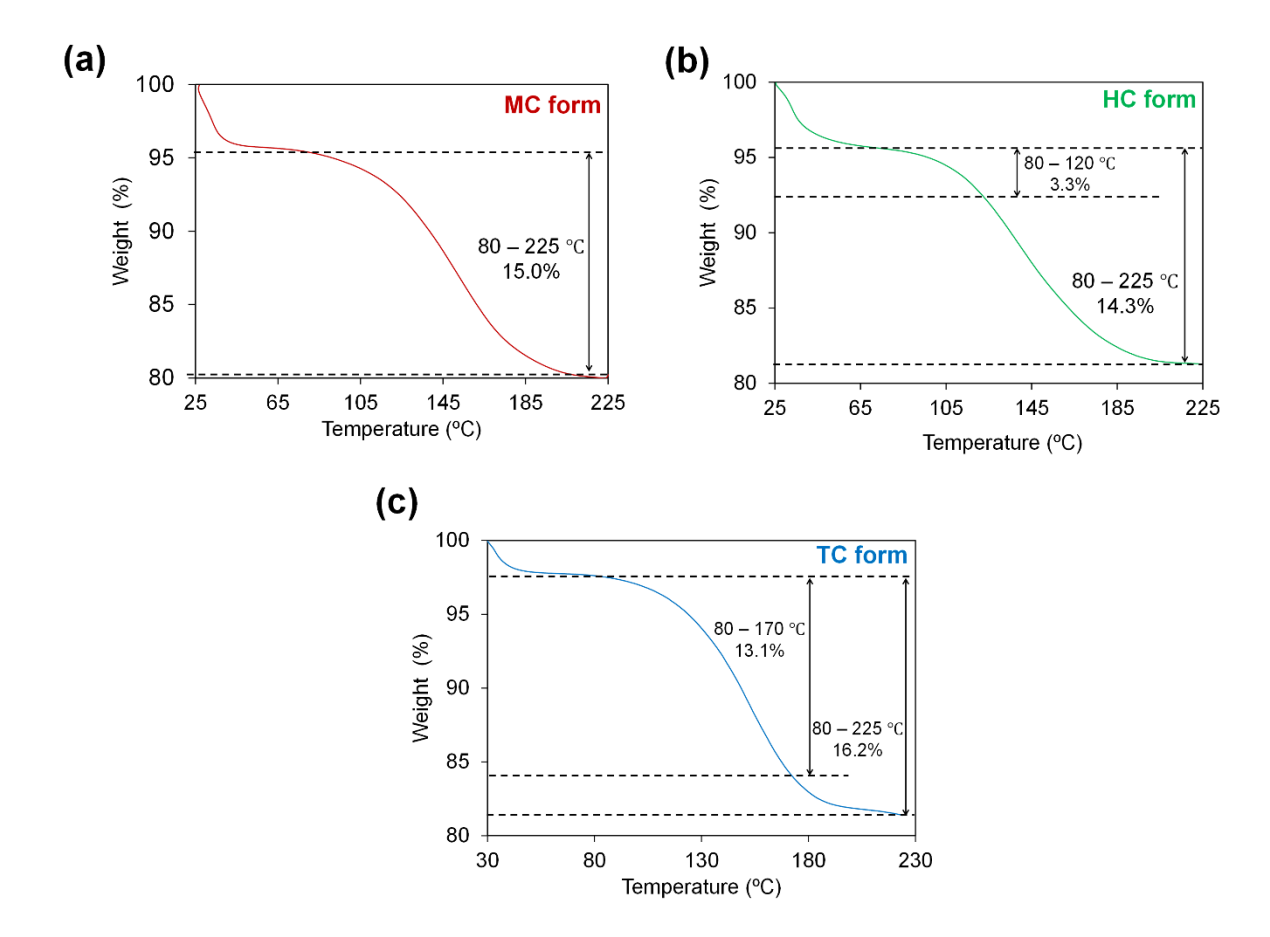


Figure 22. Weight loss curves of (a) MC form, (b) HC form, and (c) TC form complex measured at 25/30-225/230 °C with a heating rate of 0.5 °C/min.

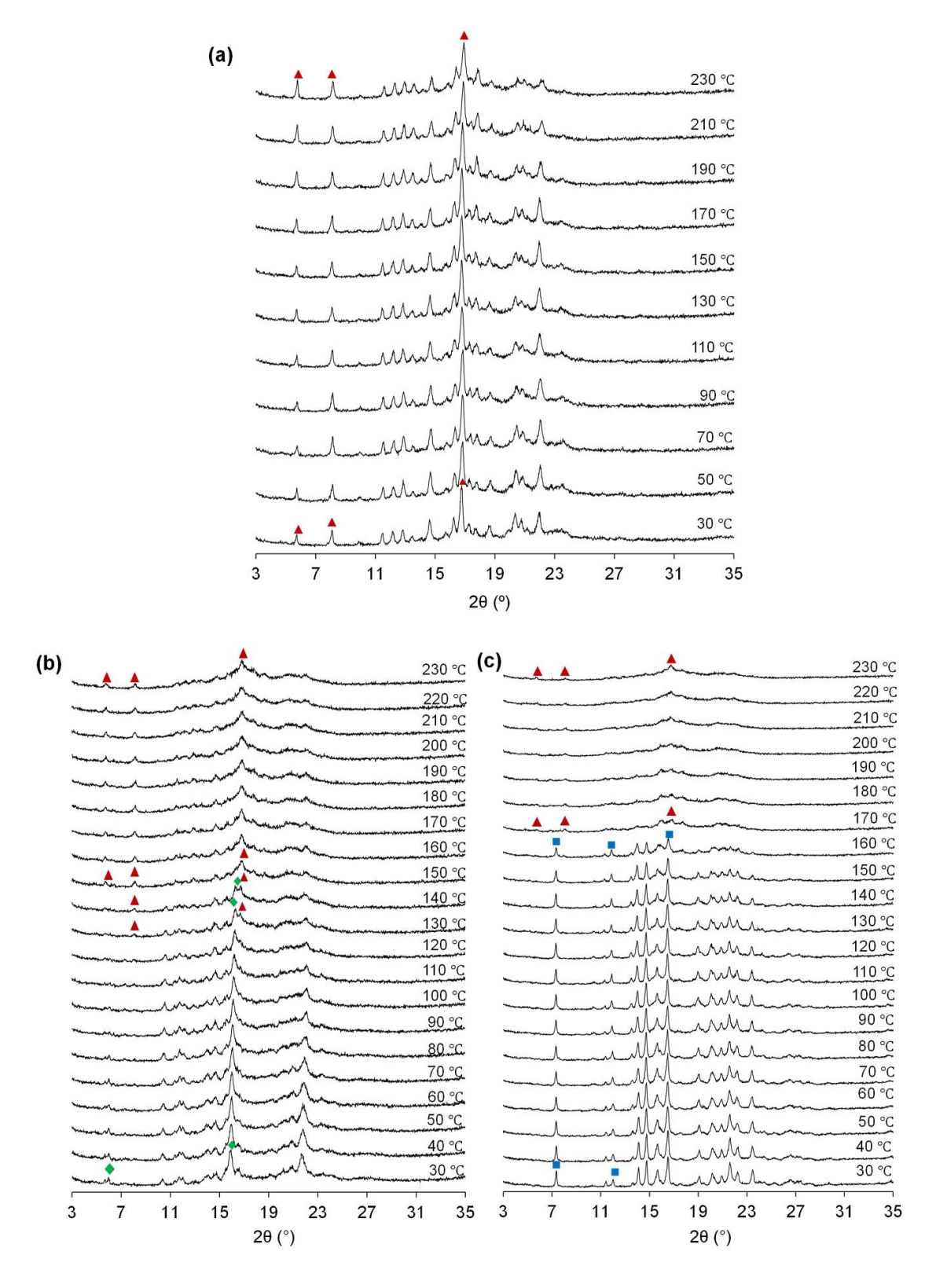


Figure 23. VT-PXRD patterns of (a) MC, (b) HC, and (c) TC form complex. The characteristic diffraction peaks are depicted by the following symbols, ■; TC form, ▲; MC form, and ♦; HC form.

Sublimation rate of SA from the polymorphic complexes

Investigation of the sublimation process of an API is crucial as it affects several industrial processes such as manufacturing, formulation development (drying process), and its stability during storage. APIs with high vapor pressure are susceptible to physical instability which compromises its potency and delivery. The change in physical stability of SA upon complexation was assessed by evaluating its sublimation rate from the crystalline state and complexes using TG under isothermal conditions. The isothermal TG was conducted at 80 °C as the sublimation of SA significantly increased above 76 °C. The isothermal time was set at 200-720 min. The representative isothermal weight loss curves of SA from its crystalline state, PM, and each polymorphic complex measured at 80 °C and 200 min are shown in Figure 24. The isothermal weight loss curve of SA in each complex and PM showed a two-step weight loss, the first occurring within 10 min and the second occurring from 10 to 200 min. This is typically observed for isothermal weight loss curves of hydrated salts or CD inclusion complexes. 53, 72 The first weight loss was in the range of 2–3%, corresponding to the amount of water in the complexes. Thus, the following weight loss from 10 to 200 min can be attributed to the sublimation of SA. The second weight loss due to the sublimation of SA was linear with respect to time, indicating that it follows an apparent zero-order kinetics. 72, 73 Furthermore, in the isothermal TG experiments conducted for 480–720 min, the weight loss attributed to SA sublimation followed the linear trend during the entire isothermal time, suggesting the maintenance of apparent zero-order kinetics (Figure 25). The sublimation rate was determined from the slope of the linear part of the profile by fitting a linear regression model, as shown in Figure 24a. In the isothermal weight loss curves of the complexes measured until 480 min, the sublimation rate of SA deviated at around 200 min and decreased slightly. In a particular experiment, the sublimation rate is dependent on the surface area of the solid. The decreased sublimation rate of SA after 200 min could be associated with a

decrease in surface area or entrapment sites of SA in the complexes. Furthermore, in the case of isothermal TG experiments conducted at 90 and 110 °C for 24 h, the HC form complex was converted to the MC form structure (data not shown). Thus, considering the stability and constant surface area, the sublimation parameters of SA in the complexes obtained at 80 °C until 200 min were analyzed for quantitative comparison.

The sublimation amount, percentage, and rate of SA from its crystalline state, PM, and each complex are presented in Table 2. The percentage of SA sublimated from its crystalline state, PM, MC, HC, and TC form complex was 4.8, 5.3, 1.7, 1.3, and 0.8, respectively. No difference was observed in the sublimation rate of SA from its crystalline state and PM (Figure 24f). Nevertheless, compared to crystalline SA, the sublimated amount and rate of SA from each complex were greatly reduced by complexation (Table 2, Figure 24f). Interestingly, the sublimation rate of SA was significantly different among polymorphic complexes, as shown in Figure 24f. It was in the order of MC form (0.50 μ g/min) > HC form (0.35 μ g/min) > TC form (0.22 μ g/min). Hence, the physical stability of SA was changed by the polymorphic forms of the complex at 80 °C and was in the order of TC form > HC form > MC form. This difference in the sublimation tendency of SA in the complexes should be affected by its molecular state as the macroscopic properties such as particle size and surface area were controlled at the same level.

Notably, the sublimation rate of SA is mostly controlled by the TC form complex, which is obtained by further humidifying the MC or HC form complex. The sublimation process of APIs is influenced by the crystal packing structure and thus differs between its polymorphic state. However, the influence of polymorphic host structure in controlling the sublimation rate of an encapsulated API has not been known yet. Thus, this result broadly implies that the desired physicochemical properties of API can be obtained by the precise selection of polymorphic host structures obtained through preparation design.

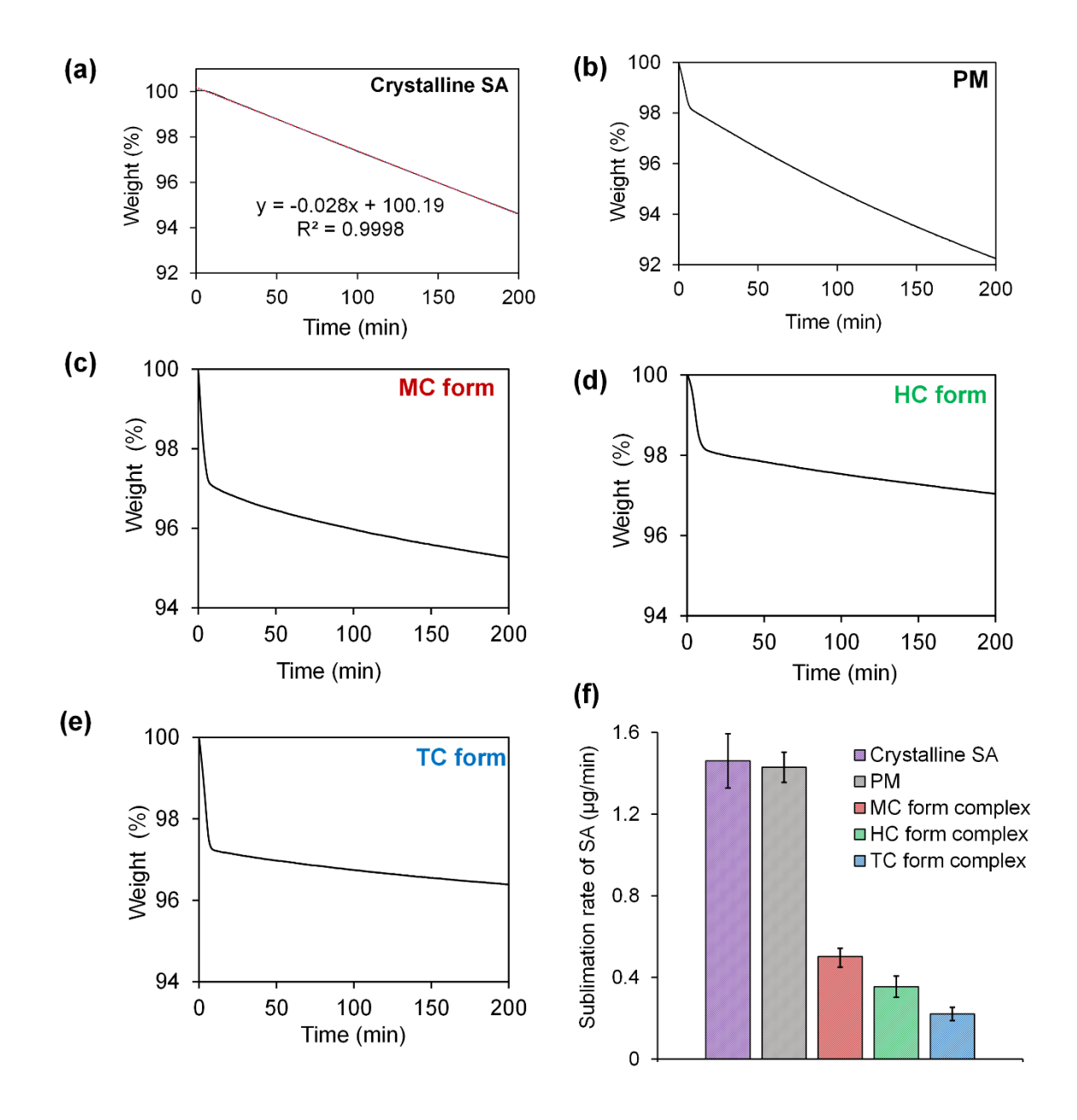


Figure 24. (a) Representative isothermal weight loss curves of SA from its crystalline state with linear regression model fitting, (b-e) representative isothermal weight loss curves of SA from the physical mixture (PM) and the three polymorphic complexes, and (f) comparison of sublimation rate of SA from its crystalline state, PM, MC, HC, and TC form of the complex. The sublimation rates are described as mean \pm S.D. (n = 3).

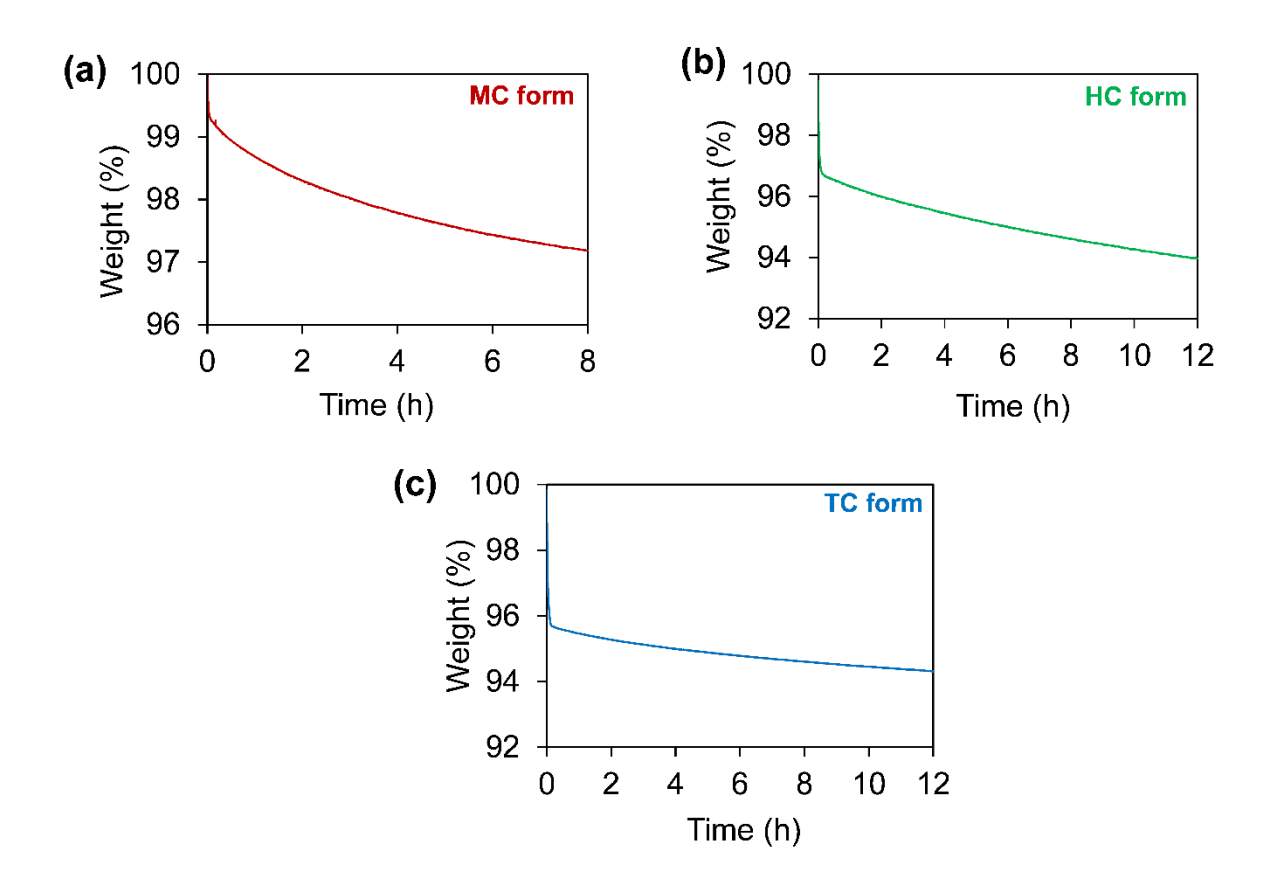


Figure 25. Isothermal weight loss curves of (a) MC form, (b) HC form, and (c) TC form complex measured at 80 °C for 8-12 h.

Table 2. Weight loss and sublimation rate of SA from its crystalline state, PM, MC form, HC form, and TC form of the complex determined from respective isothermal TG curves at 80 °C. The data are represented as mean \pm S.D. (n = 3).

Sample	Weight loss of water ^a (%)	Weight loss of SA ^b (μg)	Weight loss of SA ^b (%)	Sublimation rate of SA ^c (μg/min)
Crystalline SA	_	288.93 ± 20.43	4.77 ± 0.57	1.46 ± 0.13
PM	1.72 ± 0.12	281.98 ± 12.27	5.35 ± 0.46	1.43 ± 0.07
MC form	3.27 ± 0.63	104.68 ± 11.22	1.70 ± 0.16	0.50 ± 0.04
HC form	2.18 ± 0.29	69.56 ± 9.73	1.28 ± 0.20	0.35 ± 0.05
TC form	2.69 ± 0.79	45.35 ± 6.70	0.83 ± 0.10	0.22 ± 0.03

^a from 0 to 10 min;

^b from 10 to 200 min;

^c calculated from the slope of the linear regression line fitted from 30 to 150/200 min.

Molecular dynamics evaluation of the polymorphic complexes by ¹³C MAS measurements

To elucidate the underlying cause behind the different sublimation rates of SA, the molecular state of each complex was evaluated by ¹³C solid-state NMR spectroscopy. A combination of two pulse sequences, CP/MAS and PST/MAS techniques, were used to study the molecular state of the complexes. The CP/MAS method utilizes the heteronuclear ¹³C-¹H dipolar interaction for polarization transfer and enhances the ¹³C signals from rigid or low mobile regions. However, this cross-polarization build-up is mobility-dependent and ineffective in detecting the ¹³C signals from highly mobile regions. ⁷⁴ On the other hand, the PST/MAS method utilizes the nuclear Overhauser effect to detect the ¹³C signals by saturation of proton resonances. ⁷⁵ The ¹³C signals can be enhanced by the PST/MAS method irrespective of its mobility, depending on the recycle delay used. ⁸ Thus, the combined use of the CP/MAS and PST/MAS techniques can selectively distinguish the high and low-mobile regions in the complexes.

The CP/MAS and PST/MAS spectra of the complexes along with the CP/MAS spectrum of crystalline SA are shown in Figure 26. As per previous studies, the ¹³C signals at 62–104 ppm, 71 ppm, and 112–177 ppm are assigned to γ-CD, PEG, and SA, respectively. ^{42,76} Figures 27a and 27c show the expanded CP/MAS and PST/MAS spectra of SA and PEG in the complexes measured at a spin rate of 15 kHz. The ¹³C chemical shifts of SA signals in each complex were shifted compared to its crystalline state. In particular, the chemical shift of the carbonyl carbon of SA in each complex (denoted by 'a', Figure 27a) exhibited an up-field shift from 176 ppm to 172 ppm. The carboxylic acid group in SA forms a centrosymmetric intermolecular hydrogen-bonded dimer in its crystalline state and exhibits a ¹³C chemical shift at 176 ppm. ⁷⁶ Thus, the up-field shift of the carbonyl carbon of SA in each complex could be due to the conversion of the dimeric structure of SA into its monomeric form and the

subsequent formation of intermolecular interaction between the carbonyl carbon of SA and γ -CD.⁴² The ¹³C chemical shift of PEG in the complexes shifted up-field to 71 ppm compared to the reported ¹³C chemical shift of 72 ppm for neat PEG.⁷⁷ This up-field chemical shift could be due to the loss of intramolecular packing of the PEG chains and increased shielding by the CD cavity due to encapsulation in the PPRX structure.^{77, 78}

Furthermore, the ¹³C signals of SA and PEG in each complex were significantly enhanced in their respective PST/MAS spectra than its CP/MAS spectra, highlighting a reduction of the ¹³C-¹H dipolar interaction by the enhanced molecular motion of encapsulated SA and PEG (Figures 27a and 27c). The ¹³C linewidth is a function of chemical shift anisotropy and dipolar coupling. The appearance of spinning sidebands (SSBs) in a spectrum indicates incomplete averaging of chemical shift anisotropy.⁷⁹ For all the complexes, the SSBs of SA and PEG signals were absent even at a low spin rate of 5 kHz, whereas the SSBs of γ-CD could be observed (Figure 28). This suggests that the rapid molecular motion of the SA and PEG averaged the chemical shift anisotropy. Thus, the narrowing of the ¹³C linewidth of the SA and PEG signals could directly reflect its molecular mobility. In the PST/MAS spectra measured at 15 kHz, the ¹³C linewidth of SA and PEG signals in the complexes was in the order of TC form > HC form > MC form (Figures 27a and 27c). Hence, the molecular mobility of SA and PEG in the complexes could be in the order of MC form > HC form > TC form. The enhanced molecular mobility of PEG in the complexes agrees with the previous findings stating that the mobility of PEG or other polymers is enhanced when included in the CD cavity than in its bulk form due to the removal of the cooperative motion. 80, 81

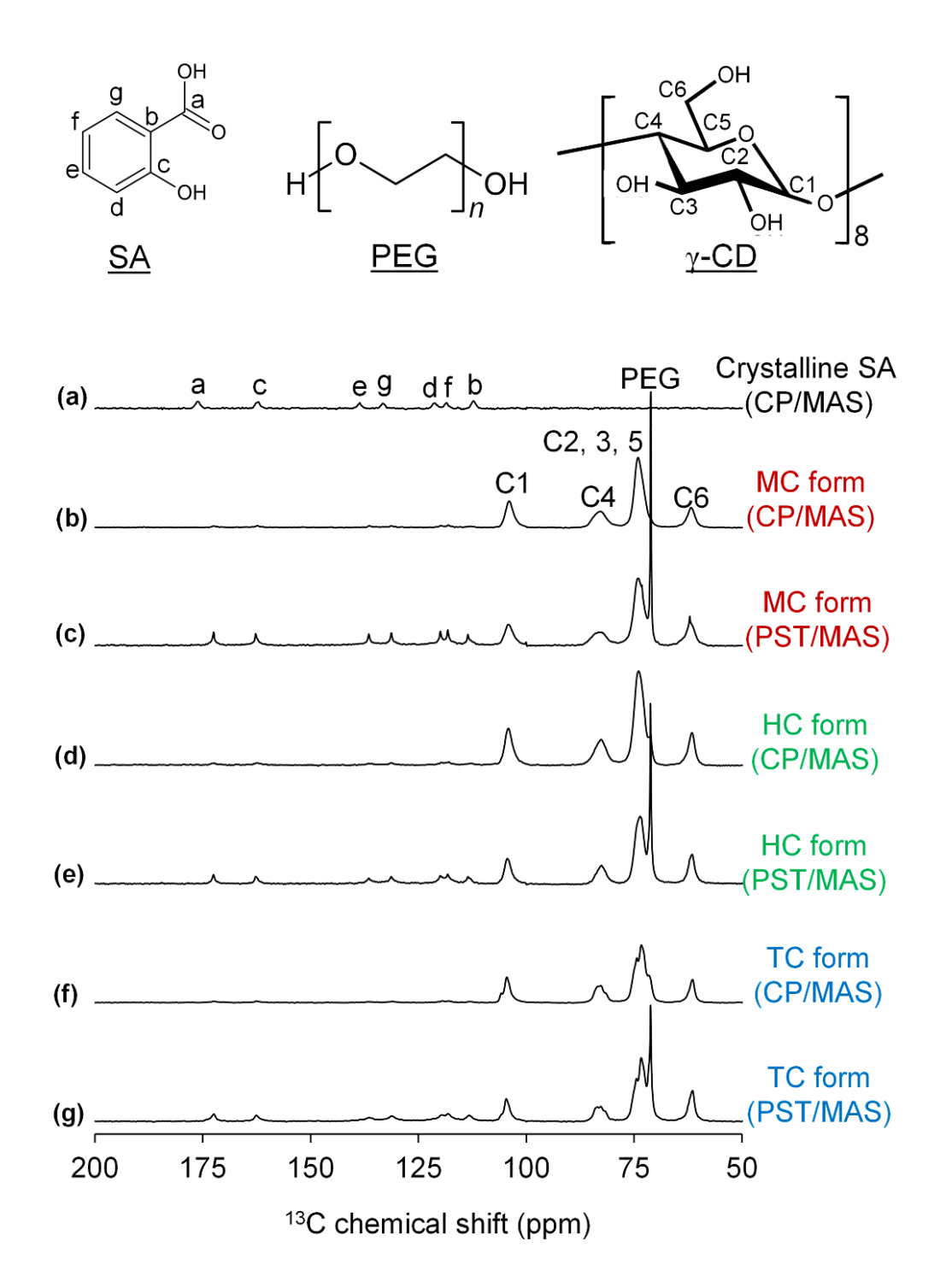


Figure 26. (a) 13 C CP/MAS spectrum of crystalline SA measured at 25 °C, (b, d, f) 13 C CP/MAS, and (c, e, g) 13 C PST/MAS spectra of the complexes measured at 50 °C, respectively. (Spin rate, v = 15 kHz)

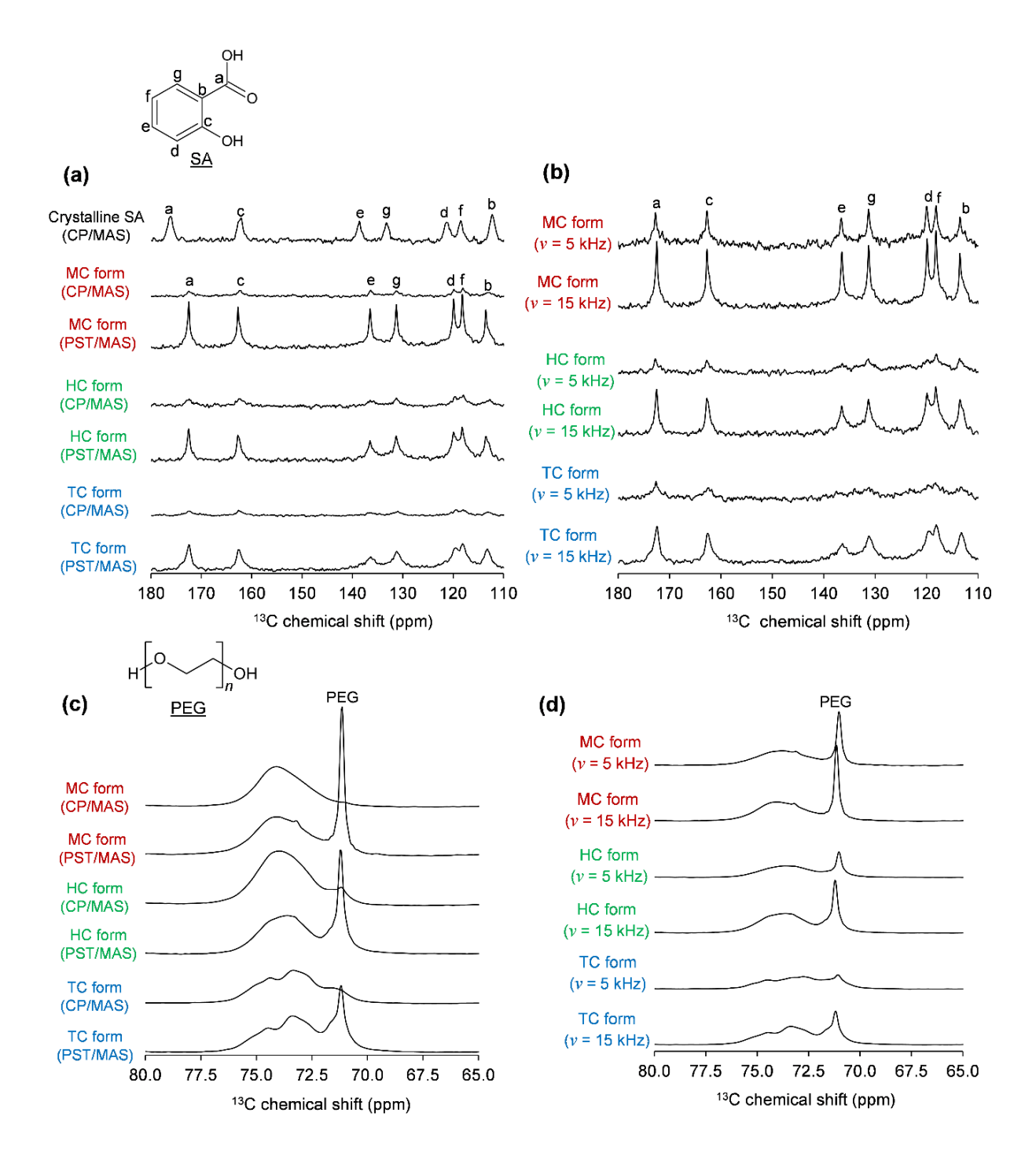


Figure 27. (a, c) 13 C CP/MAS and 13 C PST/MAS spectra of crystalline SA along with SA and PEG in the complexes measured at spin rate (v) = 15 kHz, and (b, d) 13 C PST/MAS spectra of SA and PEG in the complexes measured at v = 5 and 15 kHz. The 13 C CP/MAS spectrum of crystalline SA was measured at 25 °C, and the other spectra were measured at 50 °C. The spinning sidebands are not shown in the spectra measured at 5 kHz.

The molecular dynamics of SA and PEG in the complexes were further confirmed by analyzing the effect of spin rate on their ¹³C linewidths. Figures 27b and 27d show the PST/MAS spectra of SA and PEG in the complexes measured at the spin rates of 5 and 15 kHz. The technique of MAS suppresses the anisotropic interactions and dipolar coupling. The absence of SSBs of SA and PEG in the spectra measured at 5 kHz confirmed the motional averaging of the anisotropic interactions (Figure 28). At the reduced spin rate of 5 kHz, the ¹³C linewidths and intensity of the SA and PEG signals in each complex were broadened and reduced due to inefficient removal of dipolar coupling in the range of a few tens of kHz. In the PST/MAS spectra measured at 5 kHz, the ¹³C linewidths of the SA and PEG signals in the complex decreased in the order of TC form > HC form > MC form (Figures 27b and 27d), thus confirming the molecular mobility of SA and PEG is in the order of MC form > HC form > TC form. Additionally, this denotes that the dipolar coupling strength of SA and PEG was weakest in the MC form complex, which could be linked to its highest molecular mobility among the complexes.

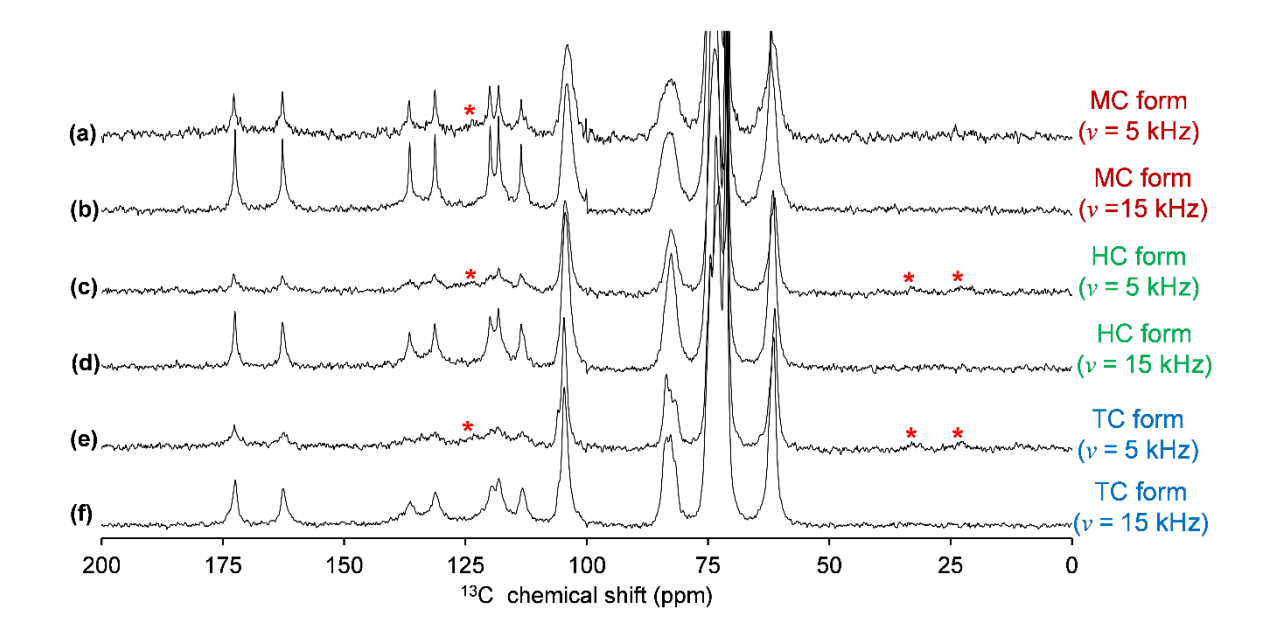


Figure 28. ¹³C PST/MAS spectra of the complexes measured at 50 °C with a spin rate of (a, c, e) 5 kHz and (b, d, f) 15 kHz, respectively. The spinning sidebands of γ -CD are shown by the asterisk symbol (*).

Figure 29a shows the 13 C CP/MAS and 13 C PST/MAS spectra of γ -CD in the complexes measured at a spin rate of 15 kHz. The 13 C signals at 104 ppm and 82 ppm correspond to the backbone carbons (C1 and C4) of γ -CD involved in the glycosidic linkage, while the 13 C signal at 61 ppm is from the side chain carbon. The 13 C signals of the backbone carbons are sensitive to the crystalline lattice structure and can reflect the overall motion of the CD. $^{82.84}$ The 13 C chemical shift of the C1 carbon in each polymorphic complex was different, although the difference was not larger than 1 ppm. The 13 C line shapes of the γ -CD carbons in the complexes were similar between the CP/MAS and PST/MAS spectra because of the crystalline state of the γ -CD (Figure 21). The 13 C signals of C1 and C4 carbons in the MC and HC form complex appeared broad and singlet (Figure 29a). On the other hand, the 13 C signals of C1 and C4 carbons in the TC form complex displayed multiple splitting exhibiting the different crystallographically inequivalent γ -CD glucose units in the asymmetric unit, thereby implying a highly crystalline structure. 85 The singlet and broader C1 and C4 signals in the

MC and HC form complex indicate a symmetrical yet more conformationally disordered structure. So This suggests that γ -CD in the MC and HC form complex is relatively more mobile than the TC form complex. Notably, in the MC form complex, there was a distinct difference in the 13C line shape of the C6 carbon between its CP/MAS and PST/MAS. In the PST/MAS spectrum, the C6 carbon resembled a combination of a sharp and broad component, whereas it resembled a single broad component in its CP/MAS spectrum (expanded region, Figure 29a). This suggests the co-existence of two γ -CD populations with a rigid and mobile phase in the MC form complex, exhibited by the broad and sharp components of the C6 carbon, respectively. Thus, it can be assessed that the molecular mobility of the γ -CD in the MC form complex is higher than the HC form complex owing to the presence of the mobile γ -CD population. Moreover, this enhanced side chain mobility can arise from the disruption of intermolecular hydrogen bonding between γ -CDs by the encapsulation of SA.

The molecular dynamics of γ -CD in the complexes were then analyzed by examining the SSBs and the effect of the spin rate on the 13 C signals. Due to the low signal-to-noise ratio of the PST/MAS spectra (Figure 28), the CP/MAS spectra measured at the spin rate of 5 kHz were analyzed for further comparison (Figure 30). The intensity of the SSB can be analyzed to extract information on the extent of anisotropic interactions and hence the structural rigidity. 87,88 The relative intensities of SSBs at 23 and 32 ppm of γ -CD in the complexes were in the order of TC form > HC form > MC form. This indicates the presence of larger anisotropic interactions or structural rigidity in the TC form complex compared to the HC and MC form complex. The lesser intense SSBs of MC and HC form complex could be associated with a partial motional averaging of the chemical shift anisotropy indicating higher molecular mobility than TC form complex. On comparing the 13 C signals of γ -CD in each complex measured at a spin rate from 5 to 15 kHz, no significant changes were observed, except for the 13 C signals of C6 carbon in the MC form complex (expanded region, Figure 29b). The

intensity of the sharp component of the C6 carbon was enhanced with an increased spin rate due to the reduction in dipolar coupling. Thus, based on the comparison of SSBs and 13 C line shapes of γ -CD signals, the molecular mobility of γ -CD in the complexes can be deduced to be in the order of MC form > HC form > TC form. The mobility of the γ -CD backbone carbons is in accordance with its side chain mobility in the complexes.

Overall, the information obtained from the PXRD patterns and 13 C solid-state NMR spectra of the complexes coincided. The PXRD patterns of the complexes displayed only diffraction peaks from the γ -CD packing structures showing the crystalline order. Adsorption of guest molecules in porous hosts such as mesoporous silica results in the loss of its original crystalline state and conversion to an amorphous state. $^{89,\,90}$ Thus, the disappearance of the SA and PEG diffraction peaks in the PXRD patterns of the complexes suggested the change in their molecular state to a glassy or supercooled state upon encapsulation, which is consistent with the solid-state NMR results.

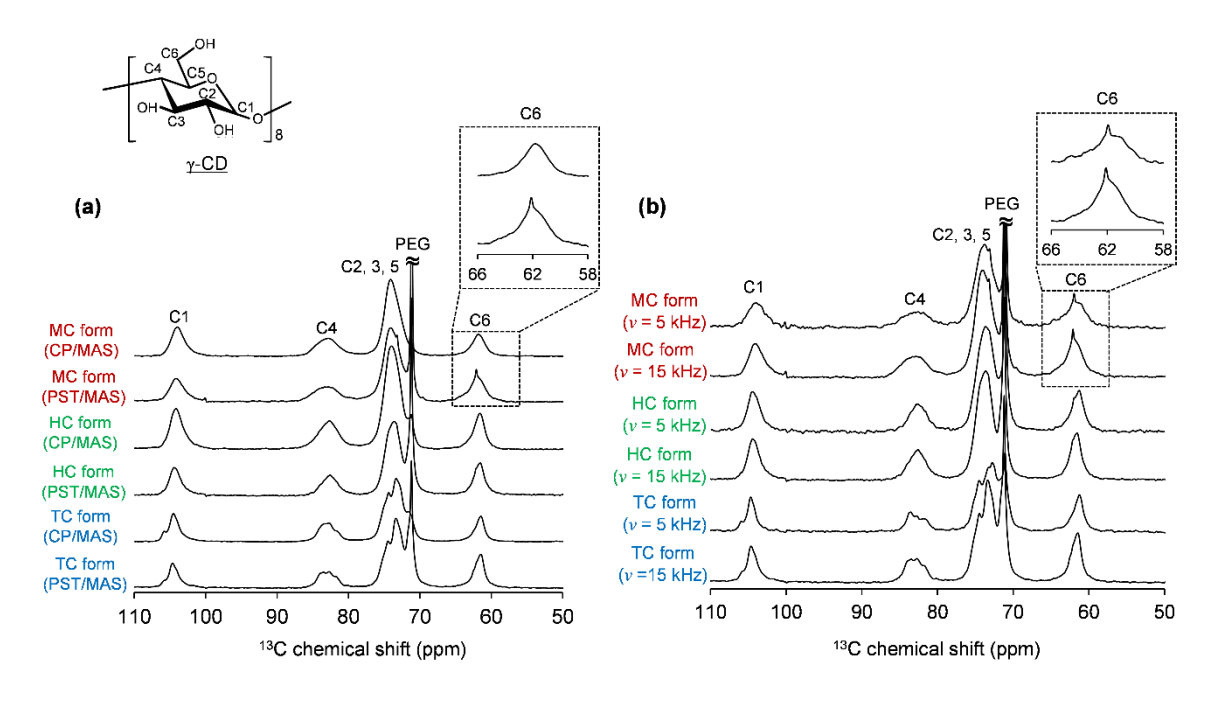


Figure 29. (a) 13 C CP/MAS and 13 C PST/MAS spectra of γ -CD in the complexes measured at v = 15 kHz, and (b) 13 C PST/MAS spectra of γ -CD in the complexes measured at v = 5 and 15 kHz. The spectra were measured at 50 °C.

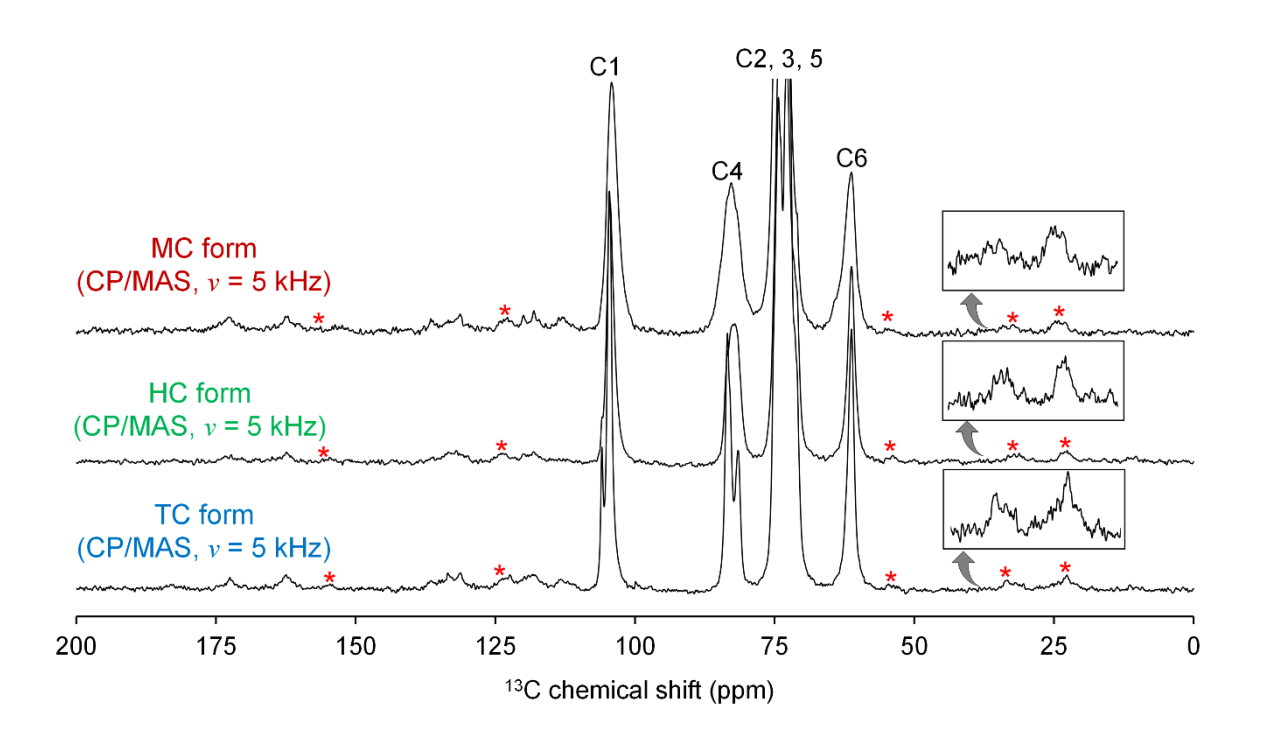


Figure 30. ¹³C CP/MAS spectra of the complexes measured at 50 °C, with a spin rate of 5 kHz. The spinning sidebands of γ-CD are shown by the asterisk symbols (*).

Temperature-dependent molecular dynamics of the polymorphic complexes

The influence of temperature on the molecular motions of SA, PEG, and γ -CD in each complex was further studied. Figure 31 shows the temperature-dependent ^{13}C PST/MAS spectra measured at 25, 50, and 70 °C with a spin rate of 15 kHz. The ^{13}C linewidths of the SA and PEG narrowed with increasing temperature. The ^{13}C linewidth narrowing of the SA and PEG in the complexes was in the order of MC form > HC form > TC form (Figures 31a-f). The ^{13}C linewidth narrowing with increased temperature is contributed by the enhanced molecular motion of the SA molecules and PEG chains with temperature and subsequent reduction of dipolar coupling. Due to their rigid crystalline nature, there was no significant difference in the ^{13}C line shapes of the backbone carbons of γ -CD in the complexes (Figures 31g-i). However, the sharp component of the C6 carbon in the MC form complex exhibited enhanced intensity with increasing temperature (Figure 31g). Additionally, a similar appearance of a sharp component of the C6 carbon (62 ppm) in the HC form complex was

observed at a temperature of 70 °C (expanded region, Figure 31h). This indicated the coexistence of two γ -CD populations in the HC form complex similar to the MC form complex. The sharp component associated with the mobile γ -CD population can be observed at the ambient temperature (25 °C) in the MC form complex, while it was observed for the HC form complex at an elevated temperature of 70 °C. This means that the molecular dynamics of the mobile γ -CD population in the MC form complex is higher than in the HC form complex. Thus, it can be confirmed that the molecular mobility of γ -CD in the complexes is in the order of MC form > HC form > TC form.

The ¹³C line shape of SA, which is sensitive to molecular dynamics, was studied for a detailed understanding. A closer examination revealed that the ¹³C line shape of SA in the complexes cannot be described as a typical Lorentzian shape. It resembled an asymmetrical line shape with a superimposition of a narrower/isotropic signal on top of a broader/anisotropic signal (Figures 31a-c). The two signals imply the presence of two dynamic states of SA, where the narrow and broad signals can be ascribed to free and bound SA, respectively. Moreover, it can be assumed that there is a rapid chemical exchange between the free and bound SA occurring faster than the NMR time scale, due to the absence of individual signals for each dynamic state. The temperature-dependent ¹³C PST/MAS spectra of SA in Figures 31a-c revealed that the intensity of the narrow signal increased while the linewidth of the broad signal decreased with increasing temperature in each complex, however, to a considerably different extent. This difference in the temperature-dependent ¹³C line shape of SA among the complexes could be linked to different free and bound SA populations resulting from its different exchange rates. In the MC form complex, the temperature-dependent increase of intensity of the isotropic/free SA and the linewidth decrease of the bound SA were comparatively higher than in the HC and TC form complex. This suggests that the exchange rate of SA molecules in the MC form complex was higher compared to the HC and TC form

complex. This exchange phenomenon is described as an adsorption/desorption process occurring at the milliseconds time scale. Thus, the molecular mobility order of SA in the complexes could be associated with the different adsorption/desorption rates between free and bound SA.

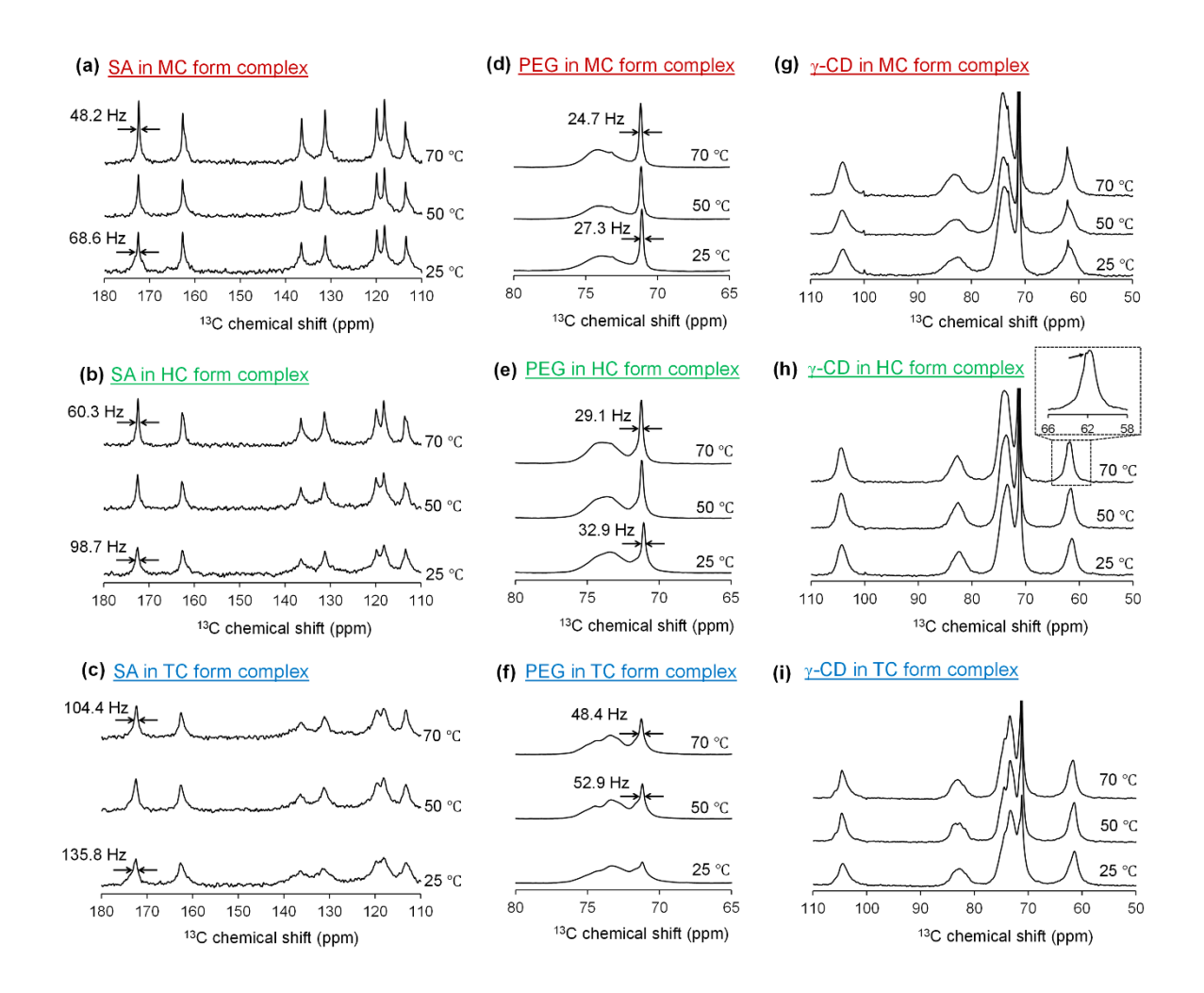


Figure 31. Temperature-dependent 13 C PST/MAS NMR spectra of SA, PEG, and γ -CD in (a, d, g) MC form, (b, e, h) HC form, and (c, f, i) TC form complex measured at 25, 50, and 70 °C, respectively. ($\nu = 15 \text{ kHz}$)

Molecular dynamics evaluation of the complexes by ¹H MAS measurement

The ¹H MAS spectra of the complexes were measured to examine the adsorption/desorption behavior of SA. Figures 32a and 32b show the full and expanded ¹H MAS spectra of the complexes measured at the ambient temperature (25 °C) with a spin rate of 15 kHz. A broad ¹H spectrum is typically obtained for rigid solids due to strong ¹H-¹H homonuclear dipolar coupling. Thus, obtaining the ¹H spectra of rigid solids is challenging and demands an ultrafast MAS rate of 40 kHz or higher to average the strong ¹H-¹H homonuclear dipolar coupling. Interestingly, the ¹H MAS spectra of the complexes exhibited well-resolved ¹H signals of SA and PEG at a moderately low spin rate of 15 kHz owing to the motional averaging of the ¹H-¹H homonuclear dipolar coupling. The ¹H signals at 3.5 ppm and 6.8–7.8 ppm were assigned to the PEG and phenyl ring (aromatic) protons of SA, respectively. The ¹H linewidth of the PEG signal in the complexes increased in the order of MC form < HC form < TC form, revealing that the molecular mobility of PEG in the complexes is in the order of MC form > HC form > TC form, as inferred from the ¹³C NMR spectra. Furthermore, the ¹H linewidth of the SA signal in the complexes also decreased in the order of TC form > HC form > MC form, suggesting that the adsorption/desorption rate of SA molecules was in the order of MC form > HC form > TC form. Surprisingly, the carboxyl proton of SA at around 11–12 ppm was absent in the ¹H MAS spectrum of the MC form and HC form complex, whereas it was broad and shifted to 11 ppm in the TC form complex (Figure 32b). This upfield shift as compared to the carboxyl proton of crystalline SA at 11.7 ppm further confirms that the carboxyl group of SA is the interaction site. ⁷⁶ On the other hand, the absence of the carboxyl proton signal in the MC and HC form complex implies a fast proton exchange between the COOH group and the hydroxyl proton of γ-CD and/or residual water at ambient temperature. However, the effect of water influencing the proton exchange can be ignored as the water content in the complexes was strictly controlled to a low percent of 2-3. Similar

fast carboxyl proton exchange has been observed for ibuprofen confined in mesoporous silica, which influenced the highly mobile behavior of ibuprofen and implied a weaker interaction between the ibuprofen and silica surface.^{7, 91} Thus, it can be suggested that SA is weakly interacted in the MC and HC form complex because of the proton exchange at the interaction site. In contrast, the broad COOH signal of SA in the TC form complex suggests relatively strong interaction, resulting in slower adsorption/desorption between free and bound SA.

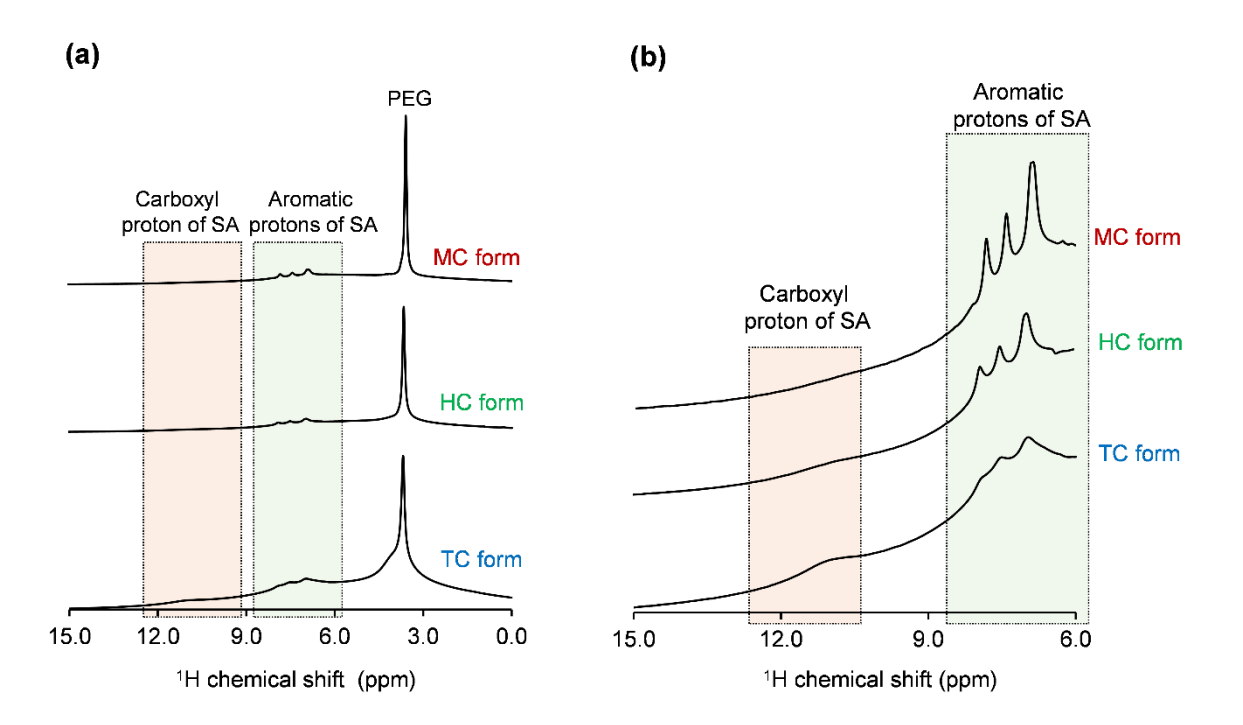


Figure 32. (a) ¹H MAS spectra of the complexes measured at the ambient temperature of 25 °C with a spin rate of 15 kHz, and (b) expanded ¹H MAS spectra (a) in the region of 6–15 ppm.

Quantitative assessment of molecular dynamics of SA and PEG in the polymorphic complexes by 13 C- T_1 measurement

The molecular dynamics of the SA and PEG in the complexes was quantitatively determined by measuring the $^{13}\text{C-}T_1$ in the temperature range of 25–70 °C. The $^{13}\text{C-}T_1$ values are sensitive to motion in the MHz region. The $^{13}\text{C-}T_1$ values provide molecular dynamic information at a localized level and reflect the average motion over a larger molecular domain. 92 For measuring the $^{13}\text{C-}T_1$, complexes were prepared with ^{13}C isotopically labeled SA at the carbonyl carbon. The ^{13}C labeled SA was used at a level of 15 wt.%. The selective isotopic enrichment enhanced the sensitivity of the carbonyl carbon, which is the interaction site. Figures 33a-c show the ^{13}C saturation recovery spectra of the complexes in the temperature range of 25–70 °C. Considering the relaxation time anisotropy, the relaxation of SA molecules can be contributed by SA molecules undergoing adsorption/desorption and those immobilized with γ -CD. The $^{13}\text{C-}T_1$ analysis showed a monoexponential recovery of magnetization, suggesting the presence of only one component of SA. Thus, the $^{13}\text{C-}T_1$ mostly reflected an effective value of SA molecules undergoing adsorption/desorption, which could be because of the presence of only a small fraction of SA in the immobilized state, and most SA molecules are involved in the adsorption/desorption process.

The obtained $^{13}\text{C-}T_1$ of the carbonyl carbon of SA and PEG in each complex as a function of inverse temperature are shown in Figures 33d and 33e. In the case of SA in the MC form complex, the $^{13}\text{C-}T_1$ values increased with increasing temperature, suggesting that it lies on the extremely narrowing regime of the T_1^{C} minimum and undergoing liquid-like isotropic motion (Figure 33d).^{88, 93} On the other hand, the $^{13}\text{C-}T_1$ value of SA in HC and TC form complex decreased with increasing temperature, suggesting it lies on the slow motional side of the T_1^{C} minimum (Figure 33d).^{88, 93} On comparing the $^{13}\text{C-}T_1$ values of SA in the HC and TC form complex, the $^{13}\text{C-}T_1$ value was higher in the TC form than the HC form. Thus, it can

be suggested that the molecular mobility of the SA in the complexes is in the order of MC form >> HC form > TC form. As presented in Figure 33e, the $^{13}\text{C-}T_1$ values of PEG in the complexes increased with increasing temperature, indicating that it is on the extremely narrowing regime of the T_1^{C} minimum and exhibiting nearly isotropic motion. The $^{13}\text{C-}T_1$ value of PEG in the complexes increased in the order of MC form >> HC form > TC form, inferring that the molecular mobility of PEG is in the same order. The quantitative mobility determination of SA and PEG is consistent with the inferences drawn from the $^{13}\text{C NMR}$ spectra. Furthermore, it can be suggested that the molecular mobility of SA correlates to the mobility of PEG in the complexes. This will be discussed in detail in the later section.

It is evident that temperature influences the dynamic process of SA. The temperaturedependent ¹³C chemical shift is sensitive to interaction strength and can provide additional information about the interaction strength of SA in the complexes (Figures 33a-c). In Figures 33f and 33g, the 13 C chemical shift (13 C δ) of the carboxyl carbon of SA and PEG are plotted as a function of temperature. The 13 C δ_{COOH} of SA in each complex shifted up-field with increasing temperature which suggests the weakening of interaction between SA and γ -CD. Moreover, the 13 C δ_{COOH} showed linear dependency with temperature. The magnitude of the temperature coefficient ($\Delta\delta_{COOH}/\Delta T$) of SA in the complexes was in the order of MC form $(-4.9 \times 10^{-3} \text{ ppm} \cdot \text{K}^{-1}) > \text{HC form } (-3.0 \times 10^{-3} \text{ ppm} \cdot \text{K}^{-1}) > \text{TC form } (-2.7 \times 10^{-3} \text{ ppm} \cdot \text{K}^{-1}).$ The smallest temperature coefficient in the TC form complex implies that SA is relatively strongly bonded among the complexes and corroborates with the ¹H MAS spectrum. Thus, the interaction strength of SA in the complexes is in the order of TC form > HC form > MC form. On the other hand, the order of 13 C δ_{COOH} value of SA in the complexes is rather opposite to the explanation of interaction strength suggested by the temperature coefficient. The ¹³C δ_{COOH} is primarily influenced by the local environment and cannot necessarily reflect the interaction strength. However, this order difference may be explained by the proximity of SA molecules with γ -CD in the intermolecular spaces and shielding by the γ -CDs. The order of 13 C δ_{COOH} at 25 °C reveals that SA in TC form is most shielded, followed by HC and MC form complex, denoting that SA in TC form complex is in a comparatively higher electron density environment than the others. The SA in TC form could be closer to γ -CDs than the HC and MC form complex, implying the presence of a relatively higher population of bound SA.

In the case of PEG, 13 C δ_{CH_2} shifted downfield with increasing temperature. However, a linear dependency was observed only in the MC and HC form complex. The polyoxyethylene chain (also known as PEG) in the nanotubes constructed with α -CD adopts a more extended structure comprising of trans conformation with a small population of gauche conformation and its molecular motion was facilitated by trans-gauche conformational transitions as revealed by 2 H NMR spectra. 80 The trans conformer of PEG has a higher or downfield chemical shift than the gauche conformer and is more favorable at higher temperatures. 94 Hence, the temperature-dependent downfield shift of PEG can be attributed to the gauchetrans conformational transition with increasing temperature. The linear dependency of 13 C δ_{CH_2} in MC and HC form complex could have been obtained due to the faster molecular motion of PEG than TC form complex. The PEG in the TC form complex exhibited a downfield shift starting at 50 $^{\circ}$ C, which implies the molecular motion of PEG was comparatively restricted at a lower temperature than the HC and MC form complex. The inconsistent order of 13 C δ_{CH_2} in the complexes could be associated with a different proportion of the trans and gauche population of PEG in the polymorphic complexes.

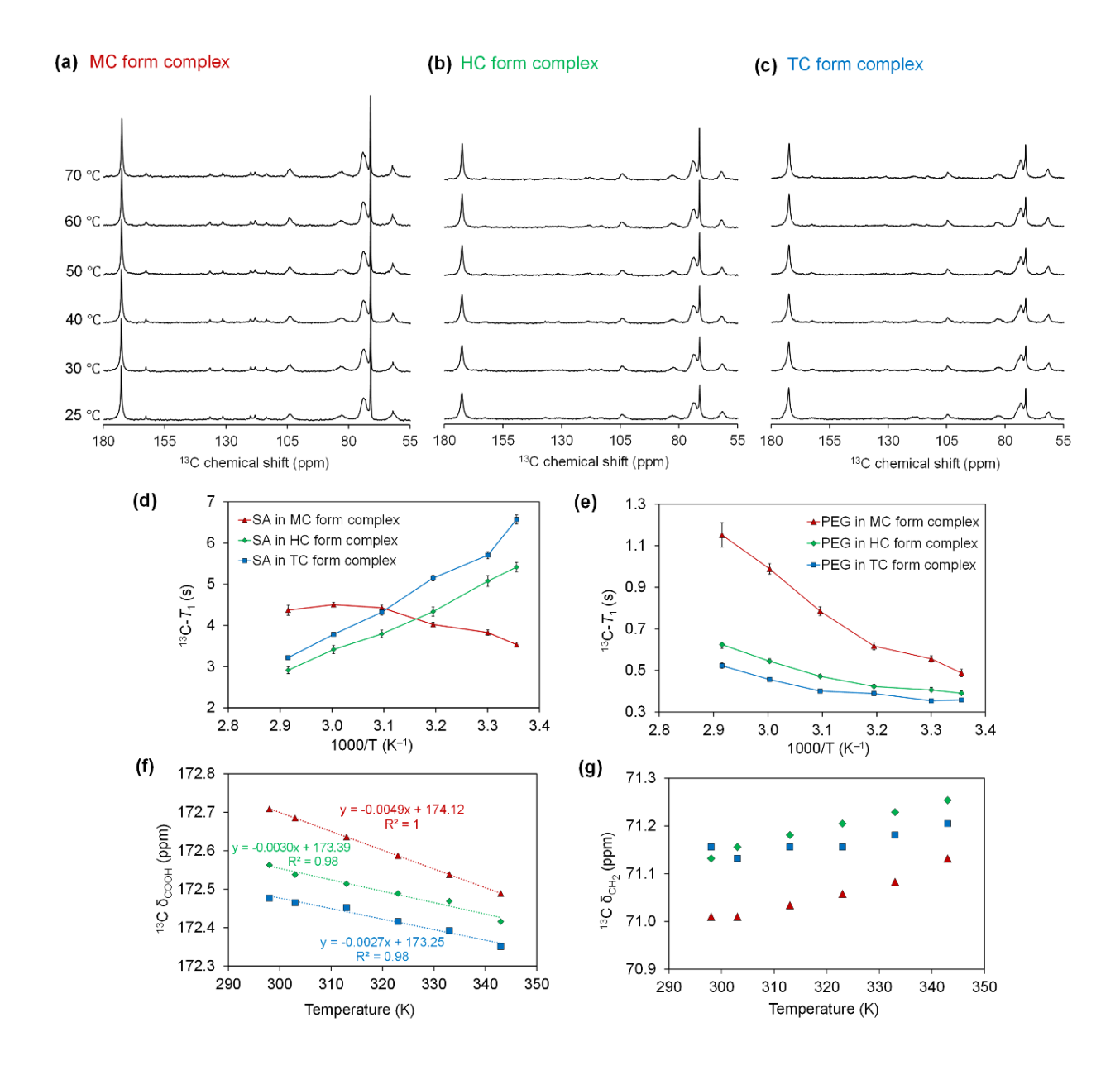


Figure 33. (a-c) 13 C saturation recovery spectra of the complexes measured at 25-70 °C with a spin rate of 15 kHz, and (d,e) 13 C- T_1 , (f,g) temperature-dependent 13 C chemical shift (13 C δ) of SA (COOH group) and PEG (CH₂) in the complexes determined from spectra in (a-c). Error bars in (d, e) indicate the standard errors of the fitting.

Discussion on the correlation between molecular mobility of SA and its sublimation rate

The ¹³C and ¹H NMR spectra revealed that the order of SA mobility in the complexes is MC form >> HC form > TC form, which coincided with the order of its sublimation. Mobility of a guest compound encapsulated in a host structure such as CD, or mesoporous silica can be affected by factors such as cavity size or pore diameter, pore matrix, host/guest interactions, and so on.⁷⁻¹² Generally, an increase in the cavity or pore size of the host compound has a direct effect on the molecular mobility of the guest compound. However, the mobility of SA could not be correlated to the host intermolecular space size, which is in the order of TC form > MC form ≥ HC form. From the obtained molecular dynamics information of SA, it can be suggested that the difference in molecular mobility was related to its adsorption/desorption process and is schematically represented in Figure 34. The SA molecules in the complexes are involved in an adsorption/desorption process, which is influenced by the proton exchange at the interaction site and the interaction strength of SA. The interaction strength of SA was highest in the TC form complex followed by the HC and MC form complex, which implied that the adsorption/desorption rates between free and bound SA in the complexes were in the order of MC form > HC form > TC form. The different adsorption/desorption rates of SA could result in different relative populations of free SA in the complexes and be attributed to the sublimation rate.

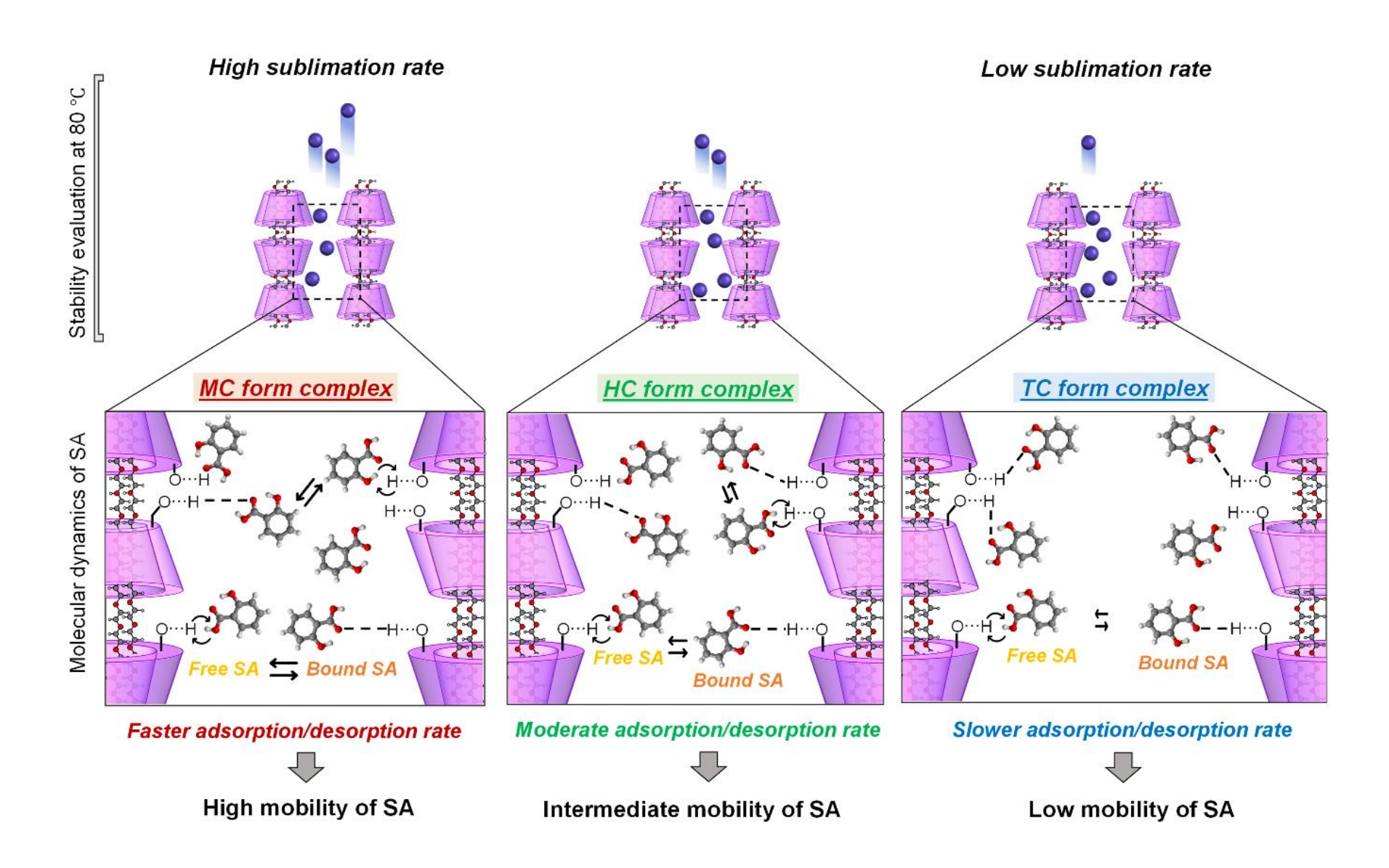


Figure 34. Schematic representation of the molecular motion of encapsulated SA in the complexes and its correlation with sublimation rate.

Discussion on the influence of SA dynamics on the molecular motion of γ -CD and PEG in the complexes

The 13 C line shape and relaxation time analysis indicated that the mobility of γ -CD and PEG in the complexes increased in the order of MC form >> HC form > TC form which coincided with the mobility order of SA. It can be assumed that the molecular dynamics of the host structure component (γ-CD and PEG) were influenced by the guest dynamics (SA). Lu *et al.* studied the structure and molecular dynamics of PPRX structure formed between α - and γ -CD and polycaprolactone (PCL).81 The PCL chains in the CD cavity exhibited faster relaxation time due to the removal of cooperative interchain interactions. Moreover, the ¹³C- T_1 of the CDs was reduced compared to its bulk state, indicating enhanced CD mobility facilitated by the fast guest-driven dynamics of the PCL chains. Additionally, it has been noted that modifications of the intermolecular interaction between the CD units in a PPRX structure can impact the mobility of the CD and polymer. Tang et al. investigated the effect of chemical modification of the hydroxyl functional groups of CDs by hydroxypropyl groups in a polyrotaxane on molecular dynamics of CD and PEG by several solid-state NMR techniques. 95 The mobility of the CD and PEG is strongly affected as the modification led to the suppression of the hydrogen bonding interactions between the CD molecules in the polyrotaxane structure. Previously, we have reported that encapsulation of drug molecules in the intermolecular spaces of the PEG/γ-CD-PPRX structure enhanced the molecular mobility of PEG owing to the altered interaction between γ-CD and PEG.⁴²

To investigate the effect of the dynamics of SA on the mobility of PEG and γ -CD in the complexes, the 13 C PST/MAS spectra of the PEG/ γ -CD-PPRX (HC form) were compared to the HC form complex (Figure 35). The change in molecular dynamics of γ -CD and PEG due to the encapsulation of SA is reflected by the change of 13 C linewidth and intensity (Figure 35c, d). The 13 C chemical shift of PEG in the PEG/ γ -CD-PPRX shifted from 71.67 ppm to

71.23 ppm in the complex. This slight up-field shift of PEG could be due to the alteration of van der Waals interaction between the PEG and γ -CD cavity upon encapsulation of SA in the intermolecular spaces. Furthermore, the 13 C linewidth of PEG and the backbone carbon (C1) of γ -CD was narrowed in the HC form complex compared to its host structure, indicating the enhanced mobility of PEG and γ -CD due to the complexation. Thus, it can be confirmed that the molecular dynamics of encapsulated SA influenced the molecular mobility of γ -CD and PEG. The fast guest-driven dynamics can explain the correlation of the molecular mobility of γ -CD and PEG with that of SA in the complexes.

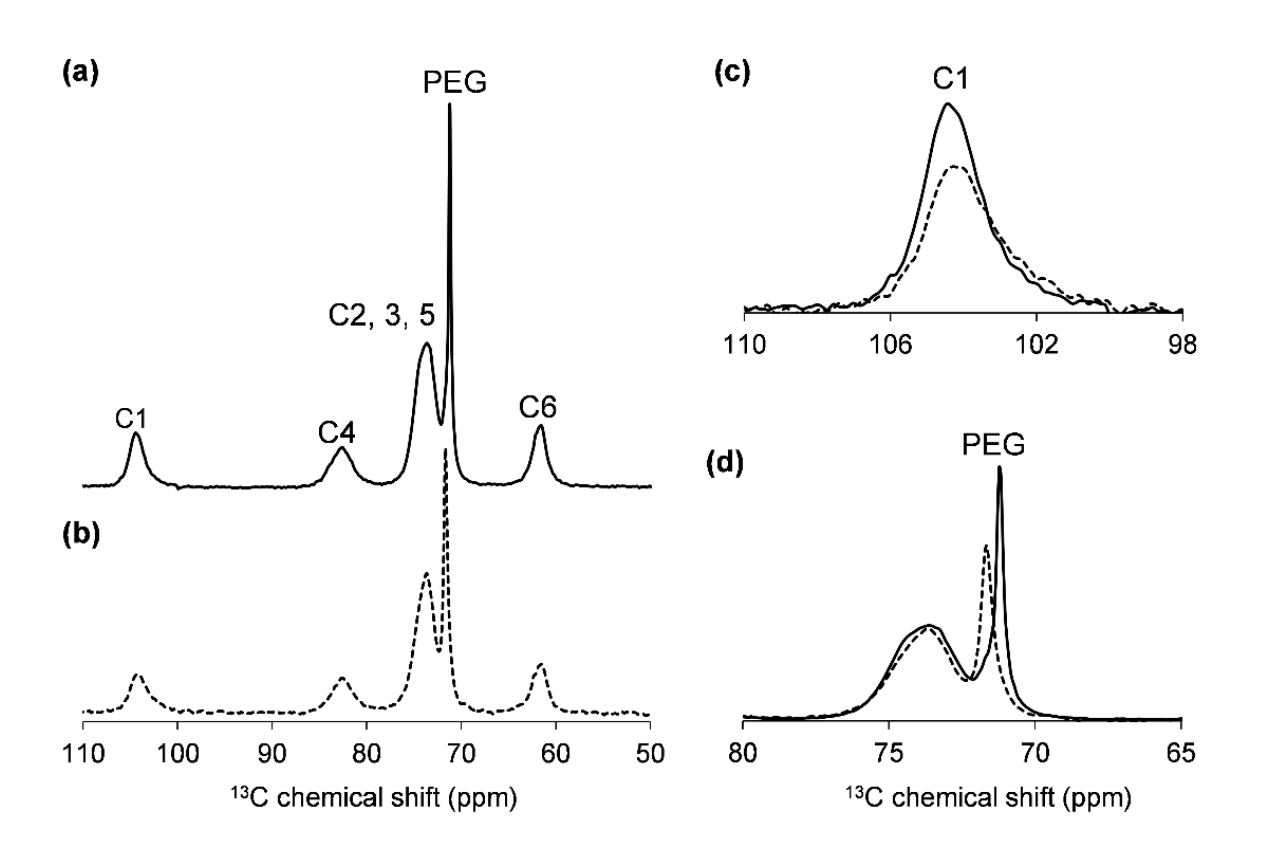


Figure 35. ¹³C PST/MAS NMR spectra of HC form of (a) SA/(PEG/ γ -CD-PPRX) complex (solid line), and (b) PEG/ γ -CD-PPRX (dotted line) measured at 50 °C, and (c, d) overlay spectra of (a, b) of the backbone carbons (C1), and PEG, respectively. (ν = 15 kHz).

To understand the influence of γ -CD mobility on the mobility of PEG, the differences in the crystal structure of γ -CD in the complexes were analyzed. Initially, the temperature-induced structural changes of the complexes observed in the VT-PXRD patterns were analyzed (Figure 23). It was revealed that the MC form complex exhibited high thermal stability at high temperatures. On the other hand, at higher temperatures, the HC and TC form complex was converted to a disordered MC form structure. Previously, we have reported that the HC form structure is converted to the MC form upon encapsulation of the guest molecule at higher temperatures. Thus, the conversion to the MC form structure at a higher temperature can be expected. Furthermore, this conversion was gradual in the HC form complex, while it was abrupt in the TC form complex. In the HC form complex, the characteristic peaks were broadened at 110 and 120 °C, and the MC form peaks started appearing at 130 °C, indicating a decrease in crystallinity followed by the conversion to the MC form structure. The weight loss of SA in the temperature range of 80–120 °C was only 3% (Figure 22b). The remaining SA molecules could have facilitated the conversion to the MC form structure. In the TC form complex, the intensity of the characteristic peaks decreased at 160 °C and the MC form peaks appeared at 170 °C. The TC form complex has a loosely packed columnar structure. At 170 °C, about 13% of SA was released by sublimation, which could have resulted in the collapse of the TC form complex to the closely packed MC form structure (Figure 22c). This suggests that the SA molecules mainly contributed to the maintenance of the columnar structure in the TC form complex and further corroborates that SA strongly interacted with γ -CDs in the TC form complex. On the other hand, the high thermal stability of the MC form complex implies that SA is relatively less interacted with γ -CDs and the columnar structure is mostly maintained through interactions between γ-CDs even at high temperatures. The crystal structural information about γ-CDs in the complex obtained from the VT-PXRD patterns corroborated with the solid-state NMR results.

The solid-state NMR results indicated that the γ -CD in MC form complex is composed of rigid and mobile populations. The presence of mobile γ -CD populations in the MC form complex can reduce the restricted cavity space and increase the uncovered region of PEG which could enhance its isotropic motion in the MC form complex (Figure 36). 80, 95 On the other hand, γ -CD in the TC form complex exhibited high crystalline order which could have been contributed by the strongly interacted SA. The high crystalline order in the TC form complex limits the mobility of PEG to the restricted cavity space of γ -CDs (Figure 36). Overall, the existing hydrogen-bond networks and the new interactions between γ -CD and SA in the crystal structure of γ -CD in the complexes determined the mobility of γ -CD and influenced the mobility of PEG in the complexes.

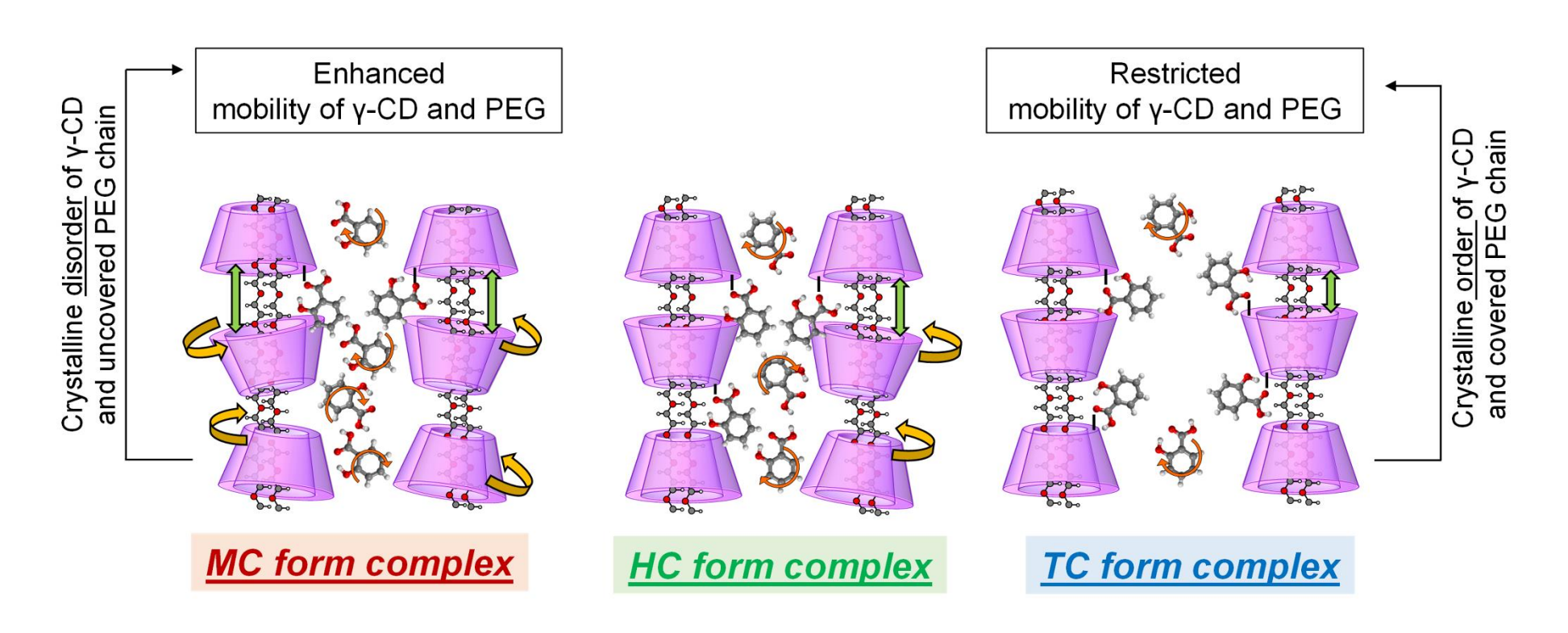


Figure 36. Schematic representation of the influence of SA dynamics on the mobility of γ -CD and PEG in the complexes.

CONCLUSIONS

This study explored the effect of encapsulation on the molecular dynamics and physical stability of an encapsulated drug in the polymorphic forms of a drug/(PEG/γ-CD-PPRX) complex. In the first part of the study, the sealed-heating preparation conditions to obtain an unexpected polymorphic form of the drug/(PEG/γ-CD-PPRX) complex, which is the hexagonal columnar (HC) form, were investigated. The screening study with six guest drugs (SA, SAM, PCT, 2-NA, PTZ, and NPX) to prepare the HC form complex with various sealedheating conditions enabled the understanding of the factors governing the complexation behavior and encapsulation efficiency of the guest drug. A low sealed-heating temperature of 80–100 °C with a small amount of water was necessary to stabilize the crystalline packing of the HC form and incorporate guest drugs in the intermolecular spaces to prepare the HC form complex. The guest drugs, SA and SAM formed HC form complex in a stoichiometric ratio of drug/γ-CD as 2:1, while 2-NA formed HC form complex in a stoichiometric ratio of drug/γ-CD as 1:1. The size-dependent stoichiometric complexation was consistent with the prior research. The correlation plot between the vapor pressure and encapsulation efficiency of the guest drug in the HC form complex revealed that the encapsulation efficiency was determined by the vapor pressure and molecular size of the guest drug.

In the second part of the study, the physical stability of SA encapsulated in three polymorphic forms of the SA/(PEG/ γ -CD-PPRX) complex was evaluated by analyzing its sublimation tendency. The sublimation rate of SA was controlled by the polymorphic complex and was in the order of MC form > HC form > TC form. Variable temperature 13 C solid-state NMR spectra in conjunction with T_1 measurement were employed to evaluate the molecular dynamics of the complexes. The 13 C and 1 H solid-state NMR results clarified that the encapsulated SA was in the monomeric form and formed a new intermolecular interaction with the γ -CD. Furthermore, the encapsulated SA showed liquid-like isotropic motion inside

the spaces and underwent fast chemical exchange between two dynamic states of SA which are free and bound SA. The molecular mobility of SA in the complexes was in the order of MC form > HC form > TC form, which was attributed to the difference in their exchange or adsorption/desorption rate. This process was further influenced by the carboxyl proton exchange of SA at the interaction site and its interaction strength. The different adsorption/desorption rates of the SA contributed to the relative population of free SA in the complexes, resulting in different sublimation rates. Moreover, the molecular mobility of γ -CD and PEG in the complexes was also in the order of MC form > HC form > TC form. This increased mobility order of PEG and γ-CD could be correlated to the molecular mobility of SA, demonstrating fast-guest-driven dynamics. The solid-state NMR and VT-PXRD results indicated that the mobility of γ-CD was governed by the existing hydrogen-bond networks and the new interactions between γ-CD and SA and the crystal structure of the complex influenced the mobility of PEG. The detailed molecular level investigation of the polymorphic forms drug/(PEG/γ-CD-PPRX) complex allowed a better understanding of the host-guest dynamics and its impact on the physical properties of the guest molecule. This is the first report on the stability improvement of an API through complexation in polymorphic supramolecular host structures.

FUTURE PERSPECTIVES

The present result combined with the previous findings on the ability of PEG/γ-CD-PPRX to encapsulate APIs with varying molecular size, and hydrophobicity, demonstrated that CD-based PPRX complexes can be a potential drug delivery system. Exploiting polymorphism in CD-based PPRX complexes can enhance and rationally control the physicochemical properties, such as dissolution and stability, of the encapsulated drug. The multicomponent supramolecular complex of drug/(PEG/γ-CD-PPRX) provides numerous possibilities for designing novel CD-based PPRX complexes with different CDs, different polymers, or varying the molecular weight of polymers. A thorough examination of the modified physical properties of the encapsulated polymer chain and drug in conjunction with molecular-level studies can reveal interesting applications of CD-based PPRX complexes.

The unique supramolecular structure of CD-based PPRX or polyrotaxanes has been employed to fabricate diverse 2D nanomaterials, including nanosheets and biomaterials for gene delivery, ligand binding, and tissue engineering. 96-98 The molecular-level information about the multicomponent CD-based PPRX complex in this study would contribute to the design and application of supramolecular nanomaterials and biomaterials. In addition, stimuli-responsive drug delivery systems that release the encapsulated API in response to stimuli like pH, temperature, or enzyme concentration can be developed using CD-based polyrotaxanes. Investigating the mechanism, kinetics, and their correlation with the molecular state adds an intriguing dimension to the study. CD-based PPRX can also form supramolecular hydrogels which are particularly attractive due to their biocompatibility, thixotropic nature, and reversible thermo-responsiveness. Researchers have explored the potential of these hydrogels for drug delivery applications. However, structural, and molecular-level studies to correlate the structural, rheological, and physicochemical properties remain unexplored. Undoubtedly, the CD-based PPRX complexes can be a promising candidate for smart drug delivery systems.

REFERENCES

- (1) Simões, S. M.; Rey-Rico, A.; Concheiro, A.; Alvarez-Lorenzo, C. Supramolecular cyclodextrin-based drug nanocarriers. *Chem. Commun.* **2015**, *51*, 6275-6289.
- (2) Wheate, N. J.; Limantoro, C. Cucurbit[n]urils as excipients in pharmaceutical dosage forms. *Supramol. Chem.* **2016**, *28*, 849-856.
- (3) Maleki, A.; Kettiger, H.; Schoubben, A.; Rosenholm, J. M.; Ambrogi, V.; Hamidi, M. Mesoporous silica materials: from physico-chemical properties to enhanced dissolution of poorly water-soluble drugs. *J. Control. Release* **2017**, *262*, 329-347.
- (4) Suresh, K.; Matzger, A. J. Enhanced drug delivery by dissolution of amorphous drug encapsulated in a water unstable metal—organic framework (MOF). *Angew. Chem. Int. Ed.* **2019**, *58*, 16790-16794.
- (5) Saji, V. S. Supramolecular organic nanotubes for drug delivery. *Mater. Today Adv.* **2022**, *14*, 100239.
- (6) Karoyo, A. H.; Sidhu, P. S.; Wilson, L. D.; Hazendonk, P.; Borisov, A. Counterion anchoring effect on the structure of the solid-state inclusion complexes of β-cyclodextrin and sodium perfluorooctanoate. *J. Phys. Chem. C* **2015**, *119*, 22225-22243.
- (7) Azaïs, T.; Tourné-Péteilh, C.; Aussenac, F.; Baccile, N.; Coelho, C.; Devoisselle, J.-M.; Babonneau, F. Solid-state NMR study of ibuprofen confined in MCM-41 material. *Chem. Mater.* **2006**, *18*, 6382-6390.
- (8) Liu, N.; Higashi, K.; Kikuchi, J.; Ando, S.; Kameta, N.; Ding, W.; Masuda, M.; Shimizu, T.; Ueda, K.; Yamamoto, K. Molecular-level understanding of the encapsulation and dissolution of poorly water-soluble ibuprofen by functionalized organic nanotubes using solid-state NMR spectroscopy. *J. Phys. Chem. B* **2016**, *120*, 4496-4507.
- (9) Figari, G.; Gonçalves, J. L.; Diogo, H. P.; Dionísio, M.; Farinha, J. P.; Viciosa, M. T. Understanding fenofibrate release from bare and modified mesoporous silica nanoparticles. *Pharmaceutics* **2023**, *15*, 1624.
- (10) Souza, B. E.; Rudić, S.; Titov, K.; Babal, A. S.; Taylor, J. D.; Tan, J.-C. Guest-host interactions of nanoconfined anti-cancer drug in metal-organic framework exposed by terahertz dynamics. *Chem. Commun.* **2019**, *55*, 3868-3871.
- (11) Knapik, J.; Wojnarowska, Z.; Grzybowska, K.; Jurkiewicz, K.; Stankiewicz, A.; Paluch, M. Stabilization of the amorphous ezetimibe drug by confining its dimension. *Mol. Pharmaceutics* **2016**, *13*, 1308-1316.

- (12) d'Orey, P.; Cordeiro, T.; Lourenço, M. A.; Matos, I.; Danède, F.; Sotomayor, J. C.; Fonseca, I. M.; Ferreira, P.; Correia, N. T.; Dionísio, M. How molecular mobility, physical state, and drug distribution influence the naproxen release profile from different mesoporous silica matrices. *Mol. Pharmaceutics* **2021**, 898-914.
- (13) Matencio, A.; Navarro-Orcajada, S.; Garcia-Carmona, F.; López-Nicolás, J. M. Applications of cyclodextrins in food science. a review. *Trends Food Sci. Technol.* **2020**, *104*, 132-143.
- (14) Loftsson, T.; Duchene, D. Cyclodextrins and their pharmaceutical applications. *Int. J. Pharm.* **2007**, *329*, 1-11.
- (15) Arora, D.; Saneja, A.; Jaglan, S. Cyclodextrin-based delivery systems for dietary pharmaceuticals. *Environ. Chem. Lett.* **2019**, *17*, 1263-1270.
- (16) Schneiderman, E.; Stalcup, A. M. Cyclodextrins: a versatile tool in separation science. *J. Chromatogr. B Biomed. Appl.* **2000**, 745, 83-102.
- (17) Marinescu, L.; Bols, M. Cyclodextrins as supramolecular organo-catalysts. *Curr. Org. Chem.* **2010**, *14*, 1380-1398.
- (18) dos Passos Menezes, P.; de Araújo Andrade, T.; Frank, L. A.; Trindade, G. d. G. G.; Trindade, I. A. S.; Serafini, M. R.; Guterres, S. S.; de Souza Araújo, A. A. Advances of nanosystems containing cyclodextrins and their applications in pharmaceuticals. *Int. J. Pharm.* **2019**, *559*, 312-328.
- (19) Brewster, M. E.; Loftsson, T. Cyclodextrins as pharmaceutical solubilizers. *Adv. Drug Deliv. Rev.* **2007**, *59*, 645-666.
- (20) Saokham, P.; Muankaew, C.; Jansook, P.; Loftsson, T. Solubility of cyclodextrins and drug/cyclodextrin complexes. *Molecules* **2018**, *23*, 1161.
- (21) Aiassa, V.; Garnero, C.; Zoppi, A.; Longhi, M. R. Cyclodextrins and their derivatives as drug stability modifiers. *Pharmaceuticals* **2023**, *16*, 1074.
- (22) Chay, S. K.; Keating, A. V.; James, C.; Aliev, A. E.; Haider, S.; Craig, D. Q. Evaluation of the taste-masking effects of (2-hydroxypropyl)-β-cyclodextrin on ranitidine hydrochloride; a combined biosensor, spectroscopic and molecular modelling assessment. *RSC Adv.* **2018**, *8*, 3564-3573.
- (23) Zhou, Y.; Feng, J.; Peng, H.; Guo, T.; Xiao, J.; Zhu, W.; Qian, W.; Zhang, J.; Wu, L. Allicin inclusions with α-cyclodextrin effectively masking its odor: preparation, characterization, and olfactory and gustatory evaluation. *J. Food Sci.* **2021**, *86*, 4026-4036.
- (24) Harada, A.; Takashima, Y.; Yamaguchi, H. Cyclodextrin-based supramolecular polymers. *Chem. Soc. Rev.* **2009**, *38*, 875-882.

- (25) Lo Nostro, P.; Lopes, J. R.; Cardelli, C. Formation of cyclodextrin-based polypseudorotaxanes: solvent effect and kinetic study. *Langmuir* **2001**, *17*, 4610-4615.
- (26) Wenz, G.; Han, B.-H.; Müller, A. Cyclodextrin rotaxanes and polyrotaxanes. *Chem. Rev.* **2006**, *106*, 782-817.
- (27) Higashi, T.; Motoyama, K.; Arima, H. Cyclodextrin-based polyrotaxanes and polypseudorotaxanes as drug delivery carriers. *J. Drug Deliv. Sci. Technol.* **2013**, *23*, 523-529.
- (28) Seki, T.; Abe, K.; Egawa, Y.; Miki, R.; Juni, K.; Seki, T. A pseudopolyrotaxane for glucose-responsive insulin release: The effect of binding ability and spatial arrangement of phenylboronic acid group. *Mol. Pharmaceutics* **2016**, *13*, 3807-3815.
- (29) Fang, G.; Wang, Q.; Yang, X.; Qian, Y.; Zhang, G.; Tang, B. γ-Cyclodextrin-based polypseudorotaxane hydrogels for ophthalmic delivery of flurbiprofen to treat anterior uveitis. *Carbohydr. Polym.* **2022**, *277*, 118889.
- (30) Ohshita, N.; Motoyama, K.; Iohara, D.; Hirayama, F.; Taharabaru, T.; Watabe, N.; Kawabata, Y.; Onodera, R.; Higashi, T. Polypseudorotaxane-based supramolecular hydrogels consisting of cyclodextrins and pluronics as stabilizing agents for antibody drugs. *Carbohydr. Polym.* **2021**, *256*, 117419.
- (31) Hunt, M. A.; Rusa, C. C.; Tonelli, A. E.; Balik, C. M. Structure and stability of columnar cyclomaltohexaose (α-cyclodextrin) hydrate. *Carbohydr. Res.* **2004**, *339*, 2805-2810.
- (32) Hunt, M. A.; Rusa, C. C.; Tonelli, A. E.; Balik, C. M. Structure and stability of columnar cyclomaltooctaose (γ-cyclodextrin) hydrate. *Carbohydr. Res.* **2005**, *340*, 1631-1637.
- (33) Harata, K. Crystal structure of γ-cyclodextrin at room temperature. *Chem. Lett.* **1984**, *13*, 641-644.
- (34) Harada, A.; Li, J.; Kamachi, M. Double-stranded inclusion complexes of cyclodextrin threaded on poly (ethylene glycol). *Nature* **1994**, *370*, 126-128.
- (35) Kawasaki, J.; Satou, D.; Takagaki, T.; Nemoto, T.; Kawaguchi, A. Structural features of inclusion complexes of γ-cyclodextrin with various polymers. *Polymer* **2007**, *48*, 1127-1138.
- (36) Kamitori, S.; Toyama, Y.; Matsuzaka, O. Crystal structures of cyclomaltohexaose (α-cyclodextrin) complexes with p-bromophenol and m-bromophenol. *Carbohydr. Res.* **2001**, *332*, 235-240.
- (37) Harata, K.; Uedaira, H.; Tanaka, J. The structure of the cyclodextrin complex. VI. The crystal structure of α-cyclodextrin-m-nitrophenol (1:2) complex. *Bull. Chem. Soc. Jpn.* **1978**, *51*, 1627-1634.

- (38) Higashi, K.; Ideura, S.; Waraya, H.; Moribe, K.; Yamamoto, K. Incorporation of salicylic acid molecules into the intermolecular spaces of γ-cyclodextrin-polypseudorotaxane. *Cryst. Growth Des.* **2009**, *9*, 4243-4246.
- (39) Park, J. S.; Jeong, S.; Chang, D. W.; Kim, J. P.; Kim, K.; Park, E.-K.; Song, K.-W. Lithium-induced supramolecular hydrogel. *Chem. Commun.* **2011**, *47*, 4736-4738.
- (40) Zhang, J.; Liu, C.; Hu, X.; Lv, Q.; Zhang, H.; Pi, B.; Yang, Z.; Lin, M. Supramolecular self-assembly of the γ-cyclodextrin and perfluorononanoic acid system in aqueous solution. *Soft Matter* **2021**, *17*, 1428-1436.
- (41) Higashi, K.; Waraya, H.; Lin, L. K.; Namiki, S.; Ogawa, M.; Limwikrant, W.; Yamamoto, K.; Moribe, K. Application of intermolecular spaces between polyethylene glycol/γ-cyclodextrin-polypseudorotaxanes as a host for various guest drugs. *Cryst. Growth Des.* **2014**, *14*, 2773-2781.
- (42) Ogawa, M.; Higashi, K.; Namiki, S.; Liu, N.; Ueda, K.; Limwikrant, W.; Yamamoto, K.; Moribe, K. Solid-phase mediated methodology to incorporate drug into intermolecular spaces of cyclodextrin columns in polyethylene glycol/cyclodextrin-polypseudorotaxanes by cogrinding and subsequent heating. *Cryst. Growth Des.* **2017**, *17*, 1055-1068.
- (43) Hilfiker, R.; Von Raumer, M. *Polymorphism in the pharmaceutical industry: solid form and drug development*; John Wiley & Sons, 2019.
- (44) Mezei, G.; Kampf, J. W.; Pecoraro, V. L. Temperature-, molar ratio-and counterion-effects on the crystal growth of bipyridinium-bis (alkylcarboxylic acid)—crown ether pseudorotaxanes. *New J. Chem.* **2007**, *31*, 439-446.
- (45) Orlando, T.; Salbego, P. R.; Taschetto, C. L.; Bonacorso, H. G.; Zanatta, N.; Hoerner, M.; Martins, M. A. Polymorphism in a rotaxane molecule: intra-and intermolecular understanding. *Cryst. Growth Des.* **2018**, *19*, 1021-1030.
- (46) Toropainen, T.; Heikkilä, T.; Leppänen, J.; Matilainen, L.; Velaga, S.; Jarho, P.; Carlfors, J.; Lehto, V.-P.; Järvinen, T.; Järvinen, K. Crystal structure changes of γ-cyclodextrin after the SEDS process in supercritical carbon dioxide affect the dissolution rate of complexed budesonide. *Pharm. Res.* **2007**, *24*, 1058-1066.
- (47) Hirotsu, T.; Higashi, T.; Motoyama, K.; Arima, H. Cyclodextrin-based sustained and controllable release system of insulin utilizing the combination system of self-assembly PEGylation and polypseudorotaxane formation. *Carbohydr. Polym.* **2017**, *164*, 42-48.
- (48) Klebeko, J.; Ossowicz-Rupniewska, P.; Świątek, E.; Szachnowska, J.; Janus, E.; Taneva, S. G.; Krachmarova, E.; Guncheva, M. Salicylic acid as ionic liquid formulation may have enhanced potency to treat some chronic skin diseases. *Molecules* **2021**, *27*, 216.

- (49) Vall, M.; Ferraz, N.; Cheung, O.; Strømme, M.; Zardán Gómez de la Torre, T. Exploring the use of amine modified mesoporous magnesium carbonate for the delivery of salicylic acid in topical formulations: in vitro cytotoxicity and drug release studies. *Molecules* **2019**, *24*, 1820.
- (50) SG, P.; Echanur, A. V.; Matadh, A. V.; Rangappa, S.; HN, S.; Murthy, R. N.; VS, R.; Ureña-Benavides, E. E.; Maibach, H.; Murthy, S. N. Sublimation of drugs from the site of application of topical products. *Mol. Pharmaceutics* **2023**, *20*, 2814–2821.
- (51) Alam, Q.; Ganeshpurkar, A.; Singh, S. K.; Krishnamurthy, S. Novel gastroprotective and thermostable cocrystal of dimethyl fumarate: its preparation, characterization, and in vitro and in vivo evaluation. *ACS Omega* **2023**, *8*, 26218-26230.
- (52) Zu, H.; Henry, R. F.; Zhang, G. G.; MacGillivray, L. R. Inhibiting sublimation of thymol by cocrystallization. *J. Pharm. Sci.* **2023**, *112*, 350-353.
- (53) Hu, S.; Wang, C.; He, X.; Sun, C. C. Reducing the sublimation tendency of ligustrazine through salt formation. *Cryst. Growth Des.* **2020**, *20*, 2057-2063.
- (54) Uyar, T.; Hunt, M. A.; Gracz, H. S.; Tonelli, A. E. Crystalline cyclodextrin inclusion compounds formed with aromatic guests: guest-dependent stoichiometries and hydration-sensitive crystal structures. *Cryst. Growth Des.* **2006**, *6*, 1113-1119.
- (55) Celebioglu, A.; Uyar, T. Fast dissolving oral drug delivery system based on electrospun nanofibrous webs of cyclodextrin/ibuprofen inclusion complex nanofibers. *Mol. Pharmaceutics* **2019**, *16*, 4387-4398.
- (56) Perlovich, G. L.; Volkova, T. V.; Bauer-Brandl, A. Towards an understanding of the molecular mechanism of solvation of drug molecules: A thermodynamic approach by crystal lattice energy, sublimation, and solubility exemplified by hydroxybenzoic acids. *J. Pharm. Sci.* **2006**, *95*, 1448-1458. DOI: https://doi.org/10.1002/jps.20611.
- (57) Manin, A. N.; Voronin, A. P.; Perlovich, G. L. Thermodynamic and structural aspects of hydroxybenzamide molecular crystals study. *Thermochim. Acta* **2013**, *551*, 57-61.
- (58) Perlovich, G.; Volkova, T. V.; Bauer-Brandl, A. Polymorphism of paracetamol: relative stability of the monoclinic and orthorhombic phase revisited by sublimation and solution calorimetry. *J. Therm. Anal. Calorim.* **2007**, *89*, 767-774.
- (59) Freitas, V. L.; Gomes, J. R.; da Silva, M. D. R. Structural, energetic and reactivity properties of phenoxazine and phenothiazine. *J. Chem. Thermodyn.* **2014**, *73*, 110-120.
- (60) Perlovich, G. L.; Kurkov, S. V.; Kinchin, A. N.; Bauer-Brandl, A. Thermodynamics of solutions III: comparison of the solvation of (+)-naproxen with other NSAIDs. *Eur. J. Pharm. Biopharm.* **2004**, *57*, 411-420.

- (61) Chickos, J. S.; Hillesheim, D. M.; Verevkin, S. P.; Roux, M. V.; Temprado, M.; Segura, M.; Notario, R.; Demasters, D. E.; Liebman, J. F. The energetics of the isomeric 1-and 2-naphthoic acids: context, quantum chemical calculations and thermochemical measurements. *Mol. Phys.* **2003**, *101*, 1311-1318.
- (62) Bolla, G.; Sanphui, P.; Nangia, A. Solubility advantage of tenoxicam phenolic cocrystals compared to salts. *Cryst. Growth Des.* **2013**, *13*, 1988-2003.
- (63) Jadrijević-Mladar Takač, M.; Vikić Topić, D.; Govorčinović, T. FT-IR and NMR spectroscopic studies of salicylic acid derivatives. I. gentisamide-a metabolite of salicylamide. *Acta Pharm.* **2004**, *54*, 163-176.
- (64) Tozuka, Y.; Oguchi, T.; Yamamoto, K. Adsorption and entrapment of salicylamide molecules into the mesoporous structure of folded sheets mesoporous material (FSM-16). *Pharm. Res.* **2003**, *20*, 926-930.
- (65) Nakai, Y.; Yamamoto, K.; Terada, K.; Watanabe, D. New methods for preparing cyclodextrin inclusion compounds. I. heating in a sealed container. *Chem. Pharm. Bull.* **1987**, *35*, 4609-4615.
- (66) Nakai, Y.; Yamamoto, K.; Terada, K.; Oguchi, T.; Saito, H.; Watanabe, D. New methods for preparing cyclodextrin inclusion compounds. II.: effects of heating temperature, water content and drug properties on the inclusion formation. *Chem. Pharm. Bull.* **1989**, *37*, 1055-1058.
- (67) Uchino, T.; Tozuka, Y.; Oguchi, T.; Yamamoto, K. Inclusion compound formation of amylose by sealed-heating with salicylic acid analogues. *J. Incl. Phenom. Macrocycl. Chem.* **2002**, *43*, 31-36.
- (68) Márquez, C.; Hudgins, R. R.; Nau, W. M. Mechanism of host–guest complexation by cucurbituril. *J. Am. Chem. Soc.* **2004**, *126*, 5806-5816.
- (69) Miskolczy, Z.; Biczók, L.; Lendvay, G. Substituent effect on the dynamics of the inclusion complex formation between protoberberine alkaloids and cucurbit[7]uril. *Phys. Chem. Chem. Phys.* **2018**, *20*, 15986-15994.
- (70) Ogoshi, T.; Saito, K.; Sueto, R.; Kojima, R.; Hamada, Y.; Akine, S.; Moeljadi, A. M. P.; Hirao, H.; Kakuta, T.; Yamagishi, T. a. Separation of linear and branched alkanes using host–guest complexation of cyclic and branched alkane vapors by crystal state pillar[6]arene. *Angew. Chem. Int. Ed.* **2018**, *57*, 1592-1595.
- (71) Ciobanu, A.; Landy, D.; Fourmentin, S. Complexation efficiency of cyclodextrins for volatile flavor compounds. *Food Res. Int.* **2013**, *53*, 110-114.

- (72) Ruz, V.; González, M. M.; Winant, D.; Rodríguez, Z.; Van den Mooter, G. Characterization of the sublimation and vapor pressure of 2-(2-Nitrovinyl) furan (G-0) using thermogravimetric analysis: effects of complexation with cyclodextrins. *Molecules* **2015**, *20*, 15175-15191.
- (73) Xie, M.; Ziemba, T. M.; Maurin, M. B. Sublimation characterization and vapor pressure estimation of an HIV nonnucleoside reverse transcriptase inhibitor using thermogravimetric analysis. *AAPS PharmSciTech* **2003**, *4*, 99-108.
- (74) Matlahov, I.; van der Wel, P. C. Hidden motions and motion-induced invisibility: dynamics-based spectral editing in solid-state NMR. *Methods* **2018**, *148*, 123-135.
- (75) Díez-Peña, E.; Quijada-Garrido, I.; Barrales-Rienda, J. M.; Wilhelm, M.; Spiess, H. W. NMR studies of the structure and dynamics of polymer gels based on N-isopropylacrylamide (NiPAAm) and methacrylic acid (MAA). *Macromol. Chem. Phys.* **2002**, *203*, 491-502.
- (76) Kong, X.; Shan, M.; Terskikh, V.; Hung, I.; Gan, Z.; Wu, G. Solid-state ¹⁷O NMR of pharmaceutical compounds: salicylic acid and aspirin. *J. Phys. Chem. B* **2013**, *117*, 9643-9654.
- (77) Ogoshi, T.; Sueto, R.; Yagyu, M.; Kojima, R.; Kakuta, T.; Yamagishi, T.-a.; Doitomi, K.; Tummanapelli, A. K.; Hirao, H.; Sakata, Y. Molecular weight fractionation by confinement of polymer in one-dimensional pillar[5]arene channels. *Nat. Commun.* **2019**, *10*, 479.
- (78) Spěváček, J.; Paternostre, L.; Damman, P.; Draye, A.; Dosiere, M. Solid state 13C NMR study of molecular complexes of poly (ethylene oxide) and hydroxybenzenes. *Macromolecules* **1998**, *31*, 3612-3616.
- (79) Nishiyama, Y.; Hou, G.; Agarwal, V.; Su, Y.; Ramamoorthy, A. Ultrafast magic angle spinning solid-state NMR spectroscopy: advances in methodology and applications. *Chem. Rev.* **2022**, *123*, 918-988.
- (80) Girardeau, T. E.; Leisen, J.; Beckham, H. W. Chain dynamics of poly (oxyethylene) in nanotubes of α-cyclodextrin by solid-state ²H NMR. *Macromol. Chem. Phys.* **2005**, *206*, 998-1005.
- (81) Lu, J.; Mirau, P. A.; Tonelli, A. E. Dynamics of isolated polycaprolactone chains in their inclusion complexes with cyclodextrins. *Macromolecules* **2001**, *34*, 3276-3284.
- (82) Tseng, W.-Y.; Chen, Y.-H.; Khairullin, I. I.; Cheng, S.; Hwang, L.-P. NMR study of solid C₆₀ (γ-cyclodextrin)₂. *Solid State Nucl. Magn. Reson.* **1997**, *8*, 219-229.
- (83) Cunha-Silva, L.; Teixeira-Dias, J. J. Solid state inclusion of the nonionic surfactant $C_{12}E_4$ in β-cyclodextrin, at various humidities: a combined raman and ^{13}C CP MAS NMR study. *J. Phys. Chem. B* **2002**, *106*, 3323-3328.

- (84) Castiglione, F.; Crupi, V.; Majolino, D.; Mele, A.; Panzeri, W.; Rossi, B.; Trotta, F.; Venuti, V. Vibrational dynamics and hydrogen bond properties of β-CD nanosponges: an FTIR-ATR, raman and solid-state NMR spectroscopic study. *J. Incl. Phenom. Macrocycl. Chem.* **2013**, *75*, 247-254.
- (85) Gidley, M. J.; Bociek, S. M. Carbon-13 CP/MAS NMR studies of amylose inclusion complexes, cyclodextrins, and the amorphous phase of starch granules: relationships between glycosidic linkage conformation and solid-state carbon-13 chemical shifts. *J. Am. Chem. Soc.* **1988**, *110*, 3820-3829.
- (86) Lu, J.; Mirau, P. A.; Shin, I. D.; Nojima, S.; Tonelli, A. E. Molecular Motions in the Supramolecular Complexes between Poly (ε -caprolactone)-Poly (ethylene oxide)-Poly (ε -caprolactone) and α -and γ -Cyclodextrins. *Macromol. Chem. Phys.* **2002**, *203*, 71-79.
- (87) Lee, Y. J.; Bingöl, B.; Murakhtina, T.; Sebastiani, D.; Meyer, W. H.; Wegner, G.; Spiess, H. W. High-resolution solid-state NMR studies of poly (vinyl phosphonic acid) proton-conducting polymer: molecular structure and proton dynamics. *J. Phys. Chem. B* **2007**, *111*, 9711-9721.
- (88) Deligey, F.; Bouguet-Bonnet, S.; Doudouh, A.; Marande, P.-L.; Schaniel, D.; Gansmüller, A. Bridging structural and dynamical models of a confined sodium nitroprusside complex. *J. Phys. Chem. C* **2018**, *122*, 21883-21890.
- (89) Qian, K. K.; Bogner, R. H. Application of mesoporous silicon dioxide and silicate in oral amorphous drug delivery systems. *J. Pharm. Sci.* **2012**, *101*, 444-463.
- (90) Nartowski, K. P.; Malhotra, D.; Hawarden, L. E.; Fabian, L.; Khimyak, Y. Z. Nanocrystallization of rare tolbutamide form V in mesoporous MCM-41 silica. *Mol. Pharmaceutics* **2018**, *15*, 4926-4932.
- (91) Azaïs, T.; Laurent, G.; Panesar, K.; Nossov, A.; Guenneau, F.; Sanfeliu Cano, C.; Tourné-Péteilh, C.; Devoisselle, J.-M.; Babonneau, F. Implication of water molecules at the silica-ibuprofen interface in silica-based drug delivery systems obtained through incipient wetness impregnation. *J. Phys. Chem. C* **2017**, *121*, 26833-26839.
- (92) Kono, H.; Nakamura, T.; Hashimoto, H.; Shimizu, Y. Characterization, molecular dynamics, and encapsulation ability of β-cyclodextrin polymers crosslinked by polyethylene glycol. *Carbohydr. Polym.* **2015**, *128*, 11-23.
- (93) Martini, F.; Borsacchi, S.; Spera, S.; Carbonera, C.; Cominetti, A.; Geppi, M. P3HT/PCBM photoactive materials for solar cells: morphology and dynamics by means of solid-state NMR. *J. Phys. Chem. C* **2013**, *117*, 131-139.

- (94) Bjoerling, M.; Karlstroem, G.; Linse, P. Conformational adaption of poly (ethylene oxide): a carbon-13 NMR study. *J. Phys. Chem.* **1991**, *95*, 6706-6709.
- (95) Tang, C.; Inomata, A.; Sakai, Y.; Yokoyama, H.; Miyoshi, T.; Ito, K. Effects of chemical modification on the molecular dynamics of complex polyrotaxanes investigated by solid-state NMR. *Macromolecules* **2013**, *46*, 6898-6907.
- (96) Li, J. J.; Zhao, F.; Li, J. Polyrotaxanes for applications in life science and biotechnology. *Appl. Microbiol. Biotechnol.* **2011**, *90*, 427-443.
- (97) Ooya, T.; Eguchi, M.; Yui, N. Supramolecular design for multivalent interaction: maltose mobility along polyrotaxane enhanced binding with concanavalin A. *J. Am. Chem. Soc.* **2003**, *125*, 13016-13017.
- (98) Uenuma, S.; Maeda, R.; Yokoyama, H.; Ito, K. Formation of isolated pseudo-polyrotaxane nanosheet consisting of α-cyclodextrin and poly (ethylene glycol). *Macromolecules* **2019**, *52*, 3881-3887.

ACKNOWLEDGEMENTS

I would like to express my sincere gratitude to the exceptional individuals who supported and guided me throughout this transformative journey, enabling me to successfully obtain my doctorate.

First and foremost, I want to extend my deepest gratitude and appreciation to my academic supervisor, Prof. Kunikazu Moribe, for his supervision, invaluable advice, and enduring support throughout my study at Chiba University, Japan. Without his understanding, encouragement, and kind cooperation, I believe that my research work would have never been successful. I am immensely grateful to Associate Professor Dr. Kenjirou Higashi, whose guidance, expertise, and unwavering support have been instrumental throughout this journey. He provided invaluable insights, challenged me to think critically, and encouraged me to push the boundaries of my research. I am extremely thankful to Assistant Professor Dr. Keisuke Ueda for his constructive feedback and thoughtful suggestions, which significantly contributed to the refinement of this thesis.

I wish to express my deep thanks to all my laboratory members of the Department of Pharmaceutical Technology for their kindness, help, and support all along with my study in Japan.

I express my thanks to MEXT, Ministry of Education, Culture, Sports, Science and Technology, Government of Japan, for providing me with financial assistance in the form of a fellowship.

I would like to thank Cyclochem Co., Ltd. (Japan) for kindly providing the γ -CD.

Lastly, I am grateful to my parents, family, and Subham Ranjan for their unwavering support and encouragement during my academic journey at Chiba University in Japan.

LIST OF PUBLICATIONS

This thesis is based on the following publications:

- Kundu, S.; Higashi, K.; Takamizawa, M.; Ueda, K.; Moribe, K.; Vapor-phase-mediated encapsulation of guest drug molecules in the hexagonal columnar form structure of polyethylene glycol/γ-cyclodextrin-polypseudorotaxane *Crystal Growth & Design*, 2023, 23 (8), 6119-6129.
- Kundu, S.; Higashi, K.; Takamizawa, M.; Ueda, K.; Limwikrant, W.; Yamamoto K.; Moribe, K.; Controlled sublimation rate of guest drug from polymorphic forms of a cyclodextrin-based polypseudorotaxane complex and its correlation with molecular dynamics as probed by solid-state NMR *Molecular Pharmaceutics*, DOI: https://doi.org/10.1021/acs.molpharmaceut.3c01148, 2024.

THESIS COMMITTEE

This thesis, conducted for the Degree of Doctoral of Philosophy (Pharmaceutical Sciences)											
was	examined	by	the	following	committee,	authorized	by	the	Graduate	School	of
Pharmaceutical Sciences, Chiba University, Japan.											

Professor Kousei Ito, Ph.D., Chairman

(Graduate School of Pharmaceutical Sciences, Chiba University)

Professor Noritaka Nishida, Ph.D.

(Graduate School of Pharmaceutical Sciences, Chiba University)

Professor Katsuhiko Yamamoto, Ph.D.

(Graduate School of Pharmaceutical Sciences, Chiba University)